Cytoplasmic and nuclear Sw-5b NLR act both independently and synergistically to dictate full host defense against tospovirus infection

Hongyu Chen[1, ¶], Xin Qian[1, ¶], Xiaojiao Chen[1, ¶], Tongqing Yang[1], Mingfeng Feng[1], Jing Chen[1], Ruixiang Cheng[1], Hao Hong[1], Ying Zheng[1], Yuzhen Mei[4], Danyu Shen[1], Yi Xu[1], Min Zhu[1], Xin Shun Ding[1] and Xiaorong Tao[1, *]

[1] Key Laboratory of Plant Immunity, Department of Plant Pathology, College of Plant Protection, Nanjing Agricultural University, Nanjing 210095, P. R. China.

[2] Huaiyin Institute of Agricultural Sciences of Xuhuai Region in Jiangsu，Huaian 223001, Jiangsu, P. R. China.

[3] College of Plant Protection, Yunnan Agricultural University, Kunming 650201, Yunnan, P. R. China.

[4] State Key Laboratory of Rice Biology, Institute of Biotechnology, Zhejiang University, Hanghzou 310029, P. R. China.

[¶] These authors contributed equally to this work.

Author for correspondence:

Xiaorong Tao

Tel: (+86)-25-84399027

Email: taoxiaorong@njau.edu.cn

RUNNING HEAD

Independent role of cytoplasmic and nuclear Sw-5b in immunity

Word Count: Main body of the text, 8136

Title 18, Summary 249, Keywords 8, Introduction 1286, Materials and Methods 1562, Results 3030, Discussion 1884, Acknowledgments 35, References 3687, Figure Legends 1103, Supporting Information Legends 786

9 Figures (Colors); Supporting information: 8 Supplemental Figures, 6 Supplemental Tables

Summary

- Plant intracellular nucleotide binding-leucine-rich repeat (NLR) receptors play critical roles in mediating host immunity to pathogen attack. We use tomato Sw-5b::tospovirus as a model system to study the specific role of the compartmentalized plant NLR in dictating host defense against virus at different infection steps.
- We demonstrated here that tomato NLR Sw-5b translocates to cytoplasm and nucleus, respectively, to play different roles in inducing host resistances against *Tomato spotted wilt tospovirus* (TSWV) infection. The cytoplasmic Sw-5b functions to induce a strong cell death response to inhibit TSWV replication. This host response is, however, insufficient to block viral intercellular and long-distance movement. The nucleus-localized Sw-5b triggers a host defense that weakly inhibits viral replication but strongly impedes virus intercellular and systemic movement. Furthermore, the cytoplasmic and nuclear Sw-5b act synergistically to dictate full host defense to TSWV infection.
- We further demonstrated that the extended N-terminal *Solanaceae* domain (SD) of Sw-5b plays critical roles in cytoplasm/nucleus partitioning. Sw-5b nucleotide-binding leucine-rich repeat (NB-LRR) controls its cytoplasm localization. Strikingly, the SD but not coil-coil (CC) domain is crucial for Sw-5b receptor to translocate from cytoplasm to nucleus to trigger the immunity. The SD was found to interact with importins. Silencing both importin α and β expression disrupted Sw-5b nucleus translocation and host immunity

against TSWV systemic infection.

- Collectively, our findings suggest that Sw-5b bifurcates disease resistances by cytoplasm/nucleus partitioning to block different infection steps of TSWV. The findings also identified a new regulatory role of extra domain of a plant NLR in mediating host innate immunity.

Keywords:

NLRs, Cytoplasm, Nuclear, Plant innate immunity, Tomato spotted wilt virus, Replication, Cell-to-cell movement and Long distance movement

Introduction

Plant innate immunity plays critical roles in host defense against pathogen invasions, and is triggered by cell-surface receptors or intracellular nucleotide-binding leucine-rich repeat (NLR) receptors (Soosaar *et al.*, 2005; Dodds & Rathjen, 2010; Cui *et al.*, 2015; Li *et al.*, 2015; Jones *et al.*, 2016; Kourelis & van der Hoorn, 2018; Kapos *et al.*, 2019; van Wersch, 2020). Plant intracellular NLRs are the largest classes of resistance proteins that function to detect pathogen effectors, and to activate host immunity upon pathogen attack (Caplan, J *et al.*, 2008; Takken & Goverse, 2012; Li *et al.*, 2015; Jones *et al.*, 2016; Kourelis & van der Hoorn, 2018; Kapos *et al.*, 2019). Plant NLRs typically contain an N-terminal domain, a central nucleotide-binding domain (NB), a nucleotide-binding adaptor (ARC domain shared by Apaf-1, certain resistance proteins, and CED-4), and a C-terminal leucine-rich repeat (LRR) domain (Ea & Jones, 1998; Jones *et al.*, 2016; Ma *et al.*, 2018; Wang *et al.*, 2019a; Wang *et al.*, 2019b; Ma *et al.*, 2020). Based on the differences among the N-terminal domains, plant NLRs can be further divided into two main categories, known as the coiled-coil NLR (refers to as CNL) category and the Toll/interleukin-1 receptor NLR (TNL) category (Meyers *et al.*, 2003; Collier & Moffett, 2009; Qi & Innes, 2013). The CC- or the TIR-domain-bearing NLRs have distinct genetic requirements and can regulate different functions in the downstream of defense signaling (Collier & Moffett, 2009; Qi & Innes, 2013; Horsefield *et al.*, 2019; Jubic *et*

114 *al.*, 2019; van Wersch & Li, 2019; Wan *et al.*, 2019).

115 In addition to classical domains, non-canonical domains were frequently found to
116 integrate into certain NLRs. The additional domain, called BED, was first found in 32
117 poplar NLR proteins (Germain & Seguin, 2011). This extra BED domain was also
118 found in nine rice NLRs (Das *et al.*, 2014). The RATX1/HMA domain in the rice
119 NLRs RGA5 and Pik‐1 was found to act as integrated decoys to detect the cognate
120 pathogen effectors (Kanzaki *et al.*, 2012; Cesari *et al.*, 2013; Cesari *et al.*, 2014). The
121 WRKY domain on Arabidopsis thaliana NLR RRS1 was further found to function as
122 an integrated decoy that recognizes the effectors AvrRps4 and PopP2 (Le Roux *et al.*,
123 2015; Sarris *et al.*, 2015). Genome-wide analyses of plant NLR receptors revealed
124 that about 3.5 % of the NLRs carried specific non-canonical domains (Cesari *et al.*,
125 2014; Kroj *et al.*, 2016; Sarris *et al.*, 2016), and some of these non-canonical domains
126 were shown to be targeted by pathogen effectors during pathogen infections (Sarris *et*
127 *al.*, 2016). However, molecular functions of most non-canonical domains in plant
128 NLRs remain largely unexplored.

129 Translocations of plant NLRs into proper subcellular compartments are critical for
130 the induction of innate immunity (Cui *et al.*, 2015; van Wersch, 2020). Multiple plant
131 NLRs and immune regulators, including tobacco N, Arabidopsis snc1, RRS1/RPS4,
132 barley MLA10, and Arabidopsis EDS1, NPR1, have been shown to accumulate in
133 both cytoplasm and nucleus, and for several nucleocytoplasmic NLRs accumulation
134 in nucleus is required for triggering host resistance to pathogen infections (Deslandes
135 *et al.*, 2003; Burch-Smith *et al.*, 2007; Shen *et al.*, 2007; Wirthmueller *et al.*, 2007;

136 Tasset *et al.*, 2010; Bai *et al.*, 2012; Inoue *et al.*, 2013; Padmanabhan *et al.*, 2013).
137 Wheat Sr33, a homolog of barley MLA10, however, was reported to accumulate in
138 cytoplasm to induce host resistance against stem rust pathogen (Cesari *et al.*, 2016).
139 For potato Rx, a balanced cytoplasm and nucleus accumulation of Rx is needed to
140 induce the host immunity (Slootweg *et al.*, 2010; Tameling *et al.*, 2010). Other studies
141 have shown that *Arabidopsis* Rpm1 (Gao *et al.*, 2011), RPS2 (Axtell & Staskawicz,
142 2003), RPS5 (Qi *et al.*, 2012), rice Pit (Takemoto *et al.*, 2012), and tomato Tm-2^2
143 (Chen *et al.*, 2017; Wang *et al.*, 2020) need to associate with plasma membrane in
144 order to trigger cell death and host immunity. Latest studies have shown that the
145 activated *Arabidopsis* ZAR1 can bind to cellular membrane, leading to a membrane
146 leakage followed by cell death and host immunity (Wang *et al.*, 2019a; Wang *et al.*,
147 2019b). Flax L6 and M have been shown to accumulate in both Golgi apparatus and
148 tonoplast, and these compartmentalized localizations are necessary for the induction
149 of host resistance (Kawano *et al.*, 2014). The re-distribution of potato R3a from
150 cytosol to endosomal compartments is crucial for the induction of host resistance to
151 *Phytophthora infestans* infection (Engelhardt *et al.*, 2012). Different plant NLRs have
152 diverse subcellular localizations for their proper functions. However, how the
153 compartmentalized plant NLRs specifically dictate defense signaling remains largely
154 unknown.

155 Tomato spotted wilt tospovirus (TSWV) is one of most destructive plant NSVs,
156 infecting more than 1000 plant species, and causes crop losses more than one billion
157 US dollars annually worldwide (Kormelink *et al.*, 2011; Scholthof *et al.*, 2011; Oliver

& Whitfield, 2016). Tomato NLR Sw-5b confers strong resistance to TSWV infection and has been widely used in tomato breeding projects to produce tospovirus resistant tomato cultivars (Brommonschenkel *et al.*, 2000; Spassova M I, 2001; Turina *et al.*, 2016; Zhu *et al.*, 2019). Upon recognition of TSWV movement protein, NSm, Sw-5b can trigger a hypersensitive response (HR), which typically associated with localized cell death (Lopez *et al.*, 2011; Hallwass *et al.*, 2014; Peiro *et al.*, 2014; De Oliveira *et al.*, 2016; Zhao *et al.*, 2016; Leastro *et al.*, 2017). Tospoviruses are divided into American and Euro-Asia type based on their geographic distribution and amino acid sequence identity of viral nucleocapsid protein. We have previously shown that Sw-5b can confer a broad-spectrum resistance to American type tospoviruses, including TSWV, through recognition of a conserved 21 amino acid PAMP-like region in the viral movement protein NSm (Zhu *et al.*, 2017). Sw-5b carries an extended N-terminal *Solanaceae* domain (SD), a CC domain, a NB-ARC domain, and a LRR domain (Brommonschenkel *et al.*, 2000; Spassova M I, 2001; Lukasik-Shreepaathy *et al.*, 2012). Similar SDs have also been found in the Mi-1.2, R8, Rpi-blb2, and Hero (Milligan *et al.*, 1998; Vos *et al.*, 1998; Ernst *et al.*, 2002; van der Vossen *et al.*, 2005; Lukasik-Shreepaathy *et al.*, 2012; Vossen *et al.*, 2016). More recently, Seong and others reported that the extended CNL has been evolved initially in the ancestor of *Asterids* and *Amaranthaceae*, predated the *Solanaceae* family (Seong *et al.*, 2020). In the presence of the extended N-terminal SD, Sw-5b is in an autoinhibited state through multilayered interactions between SD, CC, NB-ARC, and LRR domains (Chen *et al.*, 2016). For activation, the extra SD also recognizes NSm.

Sw-5b adopts a two-step NSm recognition strategy through SD and then LRR domain (Li *et al.*, 2019). This two-step recognition mechanism significantly enhances the sensitivity of the detection on TSWV NSm (Li *et al.*, 2019). Although Sw-5b is known to localize in both cytoplasm and nucleus (De Oliveira *et al.*, 2016), the biological roles of the cytoplasm- and the nucleus-accumulated Sw-5b in host immunity signaling are unknown.

In this study, we investigated the subcellular distribution pattern of Sw-5b and the functions of the compartmentalized Sw-5b in the induction of host immunity to TSWV infection. We determined here that cytoplasm- and nucleus-accumulated Sw-5b functions differently in inducing host defense response to inhibit multiple tospovirus infection steps. The cytoplasmic Sw-5b can induce a strong cell death response to suppress TSWV replication, whereas the nucleus-accumulated Sw-5b can induce a strong defense against viral intercellular movement and systemic infection. The combination of cytoplasmic and nuclear Sw-5b induces a synergistic and strong plant immunity against tospovirus infection. We also found that the extended SD functions as the key regulator for this critical intracellular translocation. The SD was also found to interact with importins α and β to mediate Sw-5b nucleus translocation, and to confer the full host immunity against tospovirus infection.

Materials and Methods

Plasmid construction

p2300S-YFP-Sw-5b was from a previously described source (Chen *et al.*, 2016).

Different domains of Sw-5b were PCR-amplified from p2300S-Sw-5b (Chen *et al.*, 2016) and cloned individually behind the *YFP* gene in the p2300S vector using a two-step overlap PCR procedure as described (Li *et al.*, 2019). All the primers used in this study are listed in Table S1.

To visualize the subcellular localization patterns of various fusion proteins, a SV40 T-Ag-derived nuclear localization signal (NLS, QPKKKRKVGG) (Lanford & Butel, 1984) or a PK1 nuclear export signal (NES, NELALKLAGLDINK) (Wen *et al.*, 1995) was fused to the N-terminus of YFP-Sw-5b or the C-terminus of NSm-YFP, as described (Kong *et al.*, 2017), to produce pNES-YFP-Sw-5b, pNLS-YFP-Sw-5b, pNSm-YFP-NES, and pNSm-YFP-NLS, respectively. In addition, YFP-Sw-5b and NSm-YFP were fused individually with a mutant NLS (nls, QPKKTRKVGG) or a mutant NES (nes, NELALKAAGADANK) to produce pnes-YFP-Sw-5b, pnls-YFP-Sw-5b, pNSm-YFP-nes, and pNSm-YFP-nls. The constructs were then transformed individually into *Agrobacterium tumefaciens* strain GV3101 cells.

Transient gene expression, stable plant transformation, and virus inoculation

Nicotiana benthamiana were grown in soil in pots inside a greenhouse maintained at 25°C and a 16 h light/8 h dark photoperiod. Six-to-eight week-old *N. benthamiana* plants were used for various assays. Transient gene expression assays were performed in *N. benthamiana* leaves through agro-infiltration using Agrobacterium cultures carrying specific expressing constructs as described previously (Feng *et al.*, 2016; Ma *et al.*, 2017). Transgenic *N. benthamiana* lines expressing YFP-Sw-5b or its

224 derivatives were made using constructs with a 35S promoter or a Sw-5b native
225 promoter via a standard leaf-disc transformation method (Chen *et al.*, 2016). The
226 resulting transgenic *N. benthamiana* lines were named as NES-YFP-Sw-5b,
227 NLS-YFP-Sw-5b, nes-YFP-Sw-5b, nls-YFP-Sw-5b, YFP-Sw-5b, and EV
228 (transformed with an empty vector), respectively. Inoculation of transgenic *N.*
229 *benthamiana* plants with TSWV was done by rubbing plant leaves with TSWV-YN
230 isolate-infected crude saps as described (Zhu *et al.*, 2017). TRV-mediated VIGS in *N.*
231 *benthamiana* plants was done as described (Ma *et al.*, 2015). The agro-infiltrated or
232 the virus-inoculated plants were growning inside a growth chamber maintained at
233 25/23 °C (day/night) with a 16/8 h light and dark photoperiod.
234
235 **Particle bombardment**
236 The particle bombardment is described (Feng et al., 2016). Briefly, 60 mg Tungsten
237 M-10 microcarrier (Bio-RAD) was placed into a 1.5 ml Eppendorf tube with 1 mL
238 70% ethanol. The tube was vortexes for 3 minutes, and then stood at room
239 temperature for 15 minutes. After centrifuge at low speed for 5 seconds, the
240 supernatant was removed and the pellet was rinsed with 70% ethanol for 3 times. One
241 mL 50% sterile glycerol solution was added and divided Tungsten M-10 microcarrier
242 into 50 µl. Five µg pRTL2-YFP, pRTL2-YFP-Sw-5b or pRTL2-YFP-Sw-5bD857V
243 plasmid DNA, 50 µl of 2.5 M CaCl2, and 20 µl of 0.1 M spermidine, respectively
244 were added and mixed with microcarrier. After centrifuge at low speed for 5 seconds
245 and the supernatant removed. The pellet was resuspended in 200 µl 70% ethanol and

246 centrifugation as described above. Use 48 µl of 100% ethanol to resuspend the
247 tungsten particle::plasmid DNA complexes, and load 15 48 µl mixture onto the center
248 of carrier (Bio-RAD), air dry, and use He/1000 particle transport system (BIO-RAD)
249 to bombard tomato leaves harvested from 3- or 4-week-old of Money Marker. The
250 bombarded leaves were incubated in Petri dishes for 24 hours at 25°C followed with
251 Confocal Microscope analysis.

252

253 **Trypan blue staining**

254 *N. benthamiana* leaves were harvested at 3 days post agro-infiltration (dpai) and
255 boiled for 5 min in a 1.15:1 (v/v) mixed ethanol and trypan blue staining solution (10
256 g phenol, 10 mL glycerol, 10 mL lactic acid, and 20 mg trypan blue in 10 mL distilled
257 water). The stained leaves were then de-stained in a chloral hydrate solution (2.5 g per
258 mL distilled water) as described (Bai *et al.*, 2012).

259

260 **Electrolyte leakage assay**

261 Electrolyte leakage assay was performed as previously described (Mittler *et al.*, 1999;
262 Zhu *et al.*, 2017) with slight modifications. Briefly, five leaf discs (9 mm in diameter
263 each) were taken from the agro-infiltrated leaves per treatment and at various dpai.
264 The harvested leaf discs from a specific treatment were floated on a 10 mL distilled
265 water for 3 h at room temperature (RT), and the conductivity of each bathing water
266 was measured (referred to as value A) using a Multiparameter Meter as instructed
267 (Mettler Toledo, Zurich, Switzerland). After the first measurement, the leaf discs were

268 returned to the bathing water and incubated at 95°C for 25 min. After cooling down to
269 RT, the conductivity of each bathing sample was measured again (referred to as value
270 B). The ion leakage was expressed as the ratio determined by value A/value B × 100.
271 The mean value and standard error of each treatment were calculated using the data
272 from three biological replicates per treatment at each sampling time point.
273
274 **Confocal laser scanning microscopy**
275 Tissue samples were collected from the leaves of transiently expressing YFP-Sw-5b
276 or one of the fusion proteins at 24–36 hours post agro-infiltration (hpai). The collected
277 tissue samples were mounted in water between a glass slide and a coverslip. Images
278 of individual samples were captured under a Carl Zeiss LSM 710 confocal laser
279 scanning microscope. YFP fusions were excited at 488 nm and the emission was
280 captured at 497–520 nm. The resulting images were further processed using the Zeiss
281 710 CLSM software followed by the Adobe Photoshop software (San Jose, CA,
282 USA).
283
284 **Nucleus and cytoplasm fractionations**
285 *N. benthamiana* leaf tissues (1 g per sample), representing a specific treatment, were
286 collected at 24 hpai, frozen in liquid nitrogen, ground to fine powders, and then
287 homogenized in 2 mL (per sample) extraction buffer 1 (20 mM Tris-HCl, pH 7.5, 20
288 mM KCl, 2.5 mM $MgCl_2$, 2 mM EDTA, 25% glycerol, 250 mM sucrose, 1×Protease
289 Inhibitor Cocktail, and 5 mM DTT). The resulting lysate was filtered through 30 μm

filters to remove debris, and the filtrate was centrifuged at 2,000 × *g* for 5 minutes to pellet nuclei. The supernatant from a sample was transferred into a new tube and centrifuged at 10,000 × *g* for 10 min. The resulting supernatant was used as the cytoplasm fraction. The nuclei containing pellet was resuspended in 5 mL extraction buffer 2 (20 mM Tris-HCl, pH 7.4, 25% glycerol, 2.5 mM MgCl2, and 0.2% Triton X-100), centrifuged for 10 min at 2,000 × *g* followed by 4-6 cycles of resuspension and centrifugation as described above. The resulting pellet was resuspended again in 500 μl extraction buffer 3 (20 mM Tris-HCl, pH 7.5, 0.25 M sucrose, 10 mM MgCl2, 0.5% Triton X-100, and 5 mM β-mercaptoethanol). The nuclei fraction was carefully layered on the top of 500 mL extraction buffer 4 (20 mM Tris-HCl, pH 7.5, 1.7 M sucrose, 10 mM MgCl2, 0.5% Triton X-100, 1×Protease Inhibitor Cocktail, and 5 mM β-mercaptoethanol), and then centrifuged at 16,000 × *g* for 1 h. The resulting pellet was resuspended in 500 μL extraction buffer 1 and stored at −80°C until use or used immediately for SDS-PAGE assays. All the processes were performed on ice or at 4°C. In this study, actin and histone H3 were used as the cytoplasmic and the nuclear markers, respectively.

Western blot, co-immunoprecipitation and mass spectrometry analysis

Western blot and co-immunoprecipitation assays were performed as described (Zhu *et al.*, 2017). Briefly, agro-infiltrated leaf samples (1 g per sample) were harvested and homogenized individually in pre-chilled mortars with pestles in 2 mL extraction buffer [10% (v/v) glycerol, 25 mM Tris, pH 7.5, 1 mM EDTA, 150 mM NaCl, 10 mM

312 DTT, 2% (w/v) polyvinylpolypyrrolidone, and 1 × protease inhibitor cocktail (Sigma,
313 Shanghai, China)]. Each crude slurry was transferred into a 2 mL Eppendorf tube, and
314 spun for 2 min at full speed in a refrigerated microcentrifuge. The supernatant was
315 transferred into a clean 1.5 mL Eppendorf tube and spun for 10 min at 4°C. For
316 Western blot assays, 50 μL supernatant from a sample was mixed with 150 μL
317 Laemmli buffer, boiled for 5 min, and analyzed in SDS-PAGE gels through
318 electrophoresis. For immunoprecipitation assays, 1 mL supernatant was mixed with
319 25 μL GFP-trap agarose beads (ChromoTek, Planegg-Martinsried, Germany),
320 incubated for 2 h at 4°C on an orbital shaker, and then pelleted through low speed
321 centrifugation. The blots were probed with a 1:2,500 (v/v) diluted anti-YFP antibody
322 or other specific antibodies followed a 1:10,000 (v/v) diluted horseradish peroxidase
323 (HRP)-conjugated goat anti-rabbit or a goat anti-mouse antibody (Sigma-Aldrich, St.
324 Louis, MO, USA). The detection signal was developed using the ECL substrate kit as
325 instructed (Thermo Scientific, Hudson, NH, USA).

326 For mass spectrometry analysis, the immunoprecipitation samples of YFP-SD
327 and SD without tag were processed by The Beijing Genomics Institute (BGI) for mass
328 spectrometry analysis. The immunoprecipitation samples of YFP-Sw-5b and Sw-5b
329 without tag were processed by Applied Protein Technology in Shanghai. Database
330 searches were performed using the Mascot search engine against *N. benthamiana*.
331 (https://solgenomics.net/organism/Nicotiana_benthamiana/genome).

332

333 **RT-PCR detection of TSWV infection**

Total RNA was extracted from TSWV-inoculated *N. benthamiana* plant leaves using an RNA Purification Kit (Tiangen Biotech, Beijing, China), and then treated with RNase-free DNase I (TaKaRa, Dalian, China). First-strand cDNA was synthesized using a TSWV-specific primer (S3 Table). PCR reactions were as follows: initial denaturation at 94°C for 2 min followed by 35 cycles of 94°C for 30 s, 52°C for 30 s, and 72°C for 1 min. The final extension was 72°C for 10 min. The resulting PCR products were visualized in 1.0% (w/v) agarose gels through electrophoresis.

Results

Determination of Sw-5b subcellular localization pattern

Expression of YFP-Sw-5b in *N. benthamiana* leaves resulted in a strong HR cell death as well as Sw-5b (Chen *et al.*, 2016; Zhu *et al.*, 2017). To investigate the subcellular localization pattern of Sw-5b, we transiently expressed YFP and YFP-Sw-5b in *N. benthamiana* leaves, respectively, through agro-infiltration. Confocal Microscopy results showed that the YFP-Sw-5b fusion accumulated in both cytoplasm and nucleus in *N. benthamiana* leaf cells (Fig. 1b, middle image). This subcellular localization pattern was similar to that of YFP (Fig. 1b, left image). When a D857V mutation, which keeps Sw-5b in an autoactivated state (Chen *et al.*, 2016), was introduced into Sw-5b to produce pYFP-Sw-5b^{D857V} and expressed in *N. benthamiana* leaves, the mutant YFP-Sw-5b^{D857V} fusion also accumulated in both cell cytoplasm and nucleus (Fig. 1b, right image). We also making a construct pNativePro::YFP-Sw-5b

355 expressing YFP-Sw-5b under native Sw-5b promoter. However, the expression of
356 YFP-Sw-5b by native Sw-5b promoter is too low to detect green fluorescence signal.
357 To investigate the subcellular localization pattern of Sw-5b in tomato leaf cells,
358 we transiently expressed YFP, YFP-Sw-5b, and YFP-Sw-5b^{D857V}, respectively,
359 through particle bombardment. Confocal Microscopy results showed that these three
360 proteins exhibited the same subcellular localization pattern as that in the *N.*
361 *benthamiana* leaf cells (Fig. 1c).
362 To further confirm the above results, we harvested *N. benthamiana* leaves
363 expressing YFP-Sw-5b or YFP-Sw-5b^{D857V} and analyzed by cytoplasm and nucleus
364 fractionation assay. Leaf samples agro-infiltrated with the empty vector (p2300S)
365 were also harvested and used as controls. Analyses of total protein, cytoplasm
366 fractions, and nucleus fractions from these harvested leaves using Western blot assays
367 showed that both YFP-Sw-5b and YFP-Sw-5b^{D857V} were accumulated in the
368 cytoplasm and nucleus (Fig. 1d).
369
370 **Sw-5b recognizes TSWV NSm in the cytoplasm**
371 TSWV NSm is known to reside in cytoplasm and plasmodesmata, but not in nucleus
372 (Kormelink *et al.*, 1994; Feng *et al.*, 2016). To determine where Sw-5b can recognize
373 TSWV NSm, we fused a NES, a nes, a NLS or a nls signal peptide to the C-terminus
374 of NSm-YFP to produce NSm-YFP-NES, NSm-YFP-nes, NSm-YFP-NLS, and
375 NSm-YFP-nls, respectively. Transient expressions of these fusions in *N. benthamiana*
376 leaves showed that NSm-YFP-NES accumulated exclusively in the cytoplasm, while

377 NSm-YFP-NLS accumulated in the nucleus (Fig. S1a). As expected, NSm-YFP-nes
378 and NSm-YFP-nls showed the same accumulation pattern as that of NSm-YFP (Fig.
379 S1a). When Sw-5b was co-expressed with one of the above four fusions in *N.*
380 *benthamiana* leaves through agro-infiltration, the leaf tissues co-expressing Sw-5b
381 and NSm-YFP-NES (Sw-5b + NSm-YFP-NES), Sw-5b and NSm-YFP-nes (Sw-5b +
382 NSm-YFP-nes), or Sw-5b and NSm-YFP-nls (Sw-5b + NSm-YFP-nls) developed a
383 strong HR cell death (Fig. S1b). In contrast, the leaf tissues co-expressing Sw-5b and
384 NSm-YFP-NLS (Sw-5b + NSm-YFP-NLS) did not. Western blot assays using a YFP
385 specific antibody confirmed that all the assayed proteins were expressed in the
386 infiltrated tissues (Fig. S1c), indicating that Sw-5b recognizes NSm in the cytoplasm.
387
388 **Sw-5b activity in cell death induction is enhanced in the cytoplasm but**
389 **suppressed in the nucleus**
390 To investigate the roles of the cytoplasmic and nuclear Sw-5b in the induction of cell
391 death and host immunity, we produced constructs to express YFP-Sw-5b,
392 NLS-YFP-Sw-5b, nls-YFP-Sw-5b, NES-YFP-Sw-5b, and nes-YFP-Sw-5b,
393 respectively, and then tested their abilities to elicit cell death and host immunity to
394 tospovirus infection. Transient expressions of these fusions in *N. benthamiana* leaves
395 showed that NES-YFP-Sw-5b accumulated exclusively in the cytoplasm, while
396 NLS-YFP-Sw-5b accumulated only in the nucleus (Fig. 2a). In addition,
397 nes-YFP-Sw-5b and nls-YFP-Sw-5b showed the same accumulation pattern as that
398 shown by YFP-Sw-5b. We then tested cell death induction through co-expressions of

399 NSm and YFP-Sw-5b (NSm + YFP-Sw-5b), NSm and NES-YFP-Sw-5b (NSm +
400 NES-YFP-Sw-5b), NSm and nes-YFP-Sw-5b (NSm + nes-YFP-Sw-5b), NSm and
401 NLS-YFP-Sw-5b (NSm + NLS-YFP-Sw-5b), or NSm and nls-YFP-Sw-5b (NSm +
402 nls-YFP-Sw-5b) in *N. benthamiana* leaves through agro-infiltration. Results of this
403 study showed that the NSm + NES-YFP-Sw-5b-induced cell death was stronger than
404 that induced by NSm + nes-YFP-Sw-5b or NSm + nls-YFP-Sw-5b co-expression (Fig.
405 2b). In addition, the cell death induced by NSm + NLS-YFP-Sw-5b co-expression
406 was suppressed (Fig. 2b). Western blot results showed that the stronger cell death
407 caused by NSm + NES-YFP-Sw-5b co-expression was not due to a greater
408 accumulation of NES-YFP-Sw-5b in the leaves (Fig. 2c). The ion leakage assay
409 results (Fig. 2d) agreed with the phenotype observation results, and indicated that
410 co-expression of NSm + NES-YFP-Sw-5b in leaves lead to a greater ion leakage
411 compared with that induced by the co-expression of NSm + nes-YFP-Sw-5b at 24 and
412 48 hours post agro-infiltration (hpai). The ion leakage caused by the co-expression of
413 NSm + NLS-YFP-Sw-5b was significantly weaker than that caused by the
414 co-expression of NSm + nls-YFP-Sw-5b (Fig. 2d).
415
416 **Cytoplasmic Sw-5b induces a strong host defense against tospovirus replication**
417 Virus infection in plant starts with virus replication in the initially infected cells
418 followed by spreading into adjacent cells for further infection. To monitor tospovirus
419 replication in plant cells, we recently developed a TSWV mini-replicon-based reverse
420 genetic system (Feng et al., 2020). In this study, co-expression of TSWV

421 mini-replicon $SR_{(+)eGFP}$, $L_{(+)opt}$ (with a codon usage optimized RdRp), VSRs and NSm
422 resulted in a cell-to-cell movement of $SR_{(+)eGFP}$. In contrast, co-expression of $SR_{(+)eGFP}$,
423 $L_{(+)opt}$, VSRs, and $NSm^{H93A\&H94A}$ mutant, a defective movement protein but can be
424 recognized by Sw-5b to cause a strong HR (Li *et al.*, 2009; Zhao *et al.*, 2016), in cells
425 resulted in the expression of $SR_{(+)eGFP}$ in only single cells (Fig. S2), thus dissecting the
426 viral replication from viral cell-to-cell movement. We then co-expressed $SR_{(+)eGFP}$,
427 $L_{(+)opt}$, VSRs, $NSm^{H93A\&H94A}$ mutant and one of the five proteins (i.e., Sw-5b,
428 NES-Sw-5b, nes-Sw-5b, NLS-Sw-5b, nls-Sw-5b) in *N. benthamiana* leaves. Leaves
429 co-expressing $SR_{(+)eGFP}$, $L_{(+)opt}$, VSRs, $NSm^{H93A\&H94A}$ mutant and p2300 (empty vector,
430 EV) were used as controls. The results showed that in the presence of Sw-5b or one of
431 its derivatives, the expression of $SR_{(+)eGFP}$ was strongly suppressed compared with
432 that expressed in the presence of EV (Fig. 3a). It is noteworthy that the expression of
433 $SR_{(+)eGFP}$ was less inhibited in the presence of NLS-Sw-5b (Fig. 3a). Western blot
434 result indicated that the GFP accumulation of $SR_{(+)eGFP}$ was strongly inhibited in the
435 presence of Sw-5b, NES-Sw-5b, nes-Sw-5b or nls-Sw-5b compared with that
436 expressed in the presence of NLS-Sw-5b or EV (Fig. 3b). This finding indicates that
437 the cytoplasmic Sw-5b can inhibit $SR_{(+)eGFP}$ expression, possibly through induction of
438 a host defense against TSWV replication.
439
440 **Sw-5b induces a host defense against viral NSm intercellular movement**
441 In our previous study, we used pmCherry-HDEL//NSm-GFP vector (Fig. 4a) to
442 investigate TSWV NSm cell-to-cell movement (Feng *et al.*, 2016). The expressed

443 mCherry-HDEL binds ER membrane in the initial cells but NSm-eGFP traffics
444 between cells. To investigate whether the Sw-5b-induced host defense can affect
445 TSWV NSm cell-to-cell movement, we co-expressed mCherry-HDEL, NSm-GFP,
446 and Sw-5b or mCherry-HDEL, NSm-GFP, and EV in *N. benthamiana* leaves through
447 agro-infiltration. Under the fluorescence microscope, both NSm-GFP and
448 mCherry-HDEL were found in single cells in the presence of Sw-5b. In the presence
449 of EV, however, NSm-GFP moved into multiple cells, while mCherry-HDEL
450 accumulated in the initial cells (Fig. 4b, upper two panels). The result suggested that
451 Sw-5b elicited a defense that strongly inhibited cell-to-cell movement of viral NSm.
452 To make sure this inhibition to viral NSm cell-to-cell movement is not caused by
453 overexpression of Sw-5b, we also used the NSm^{T120N} mutant, from the resistance -
454 breaking (RB) TSWV isolates, which cannot be recognized by Sw-5b (Zhao et al.,
455 2016). The assays showed that in the presence of either Sw-5b or EV, NSm^{T120N}-GFP
456 moved into multiple cells, while mCherry-HDEL retained in the initial cells (Fig S3a).
457

458 **Sw-5b in the nucleus but not in the cytoplasm triggers a defense against NSm**
459 **cell-to-cell movement**

460 To determine the effects of the cytoplasmic and nuclear Sw-5b on host defense against
461 TSWV NSm intercellular movement, we co-expressed mCherry-HDEL and
462 NSm-GFP with NES-Sw-5b, nes-Sw-5b, NLS-Sw-5b, or nls-Sw-5b in *N.*
463 *benthamiana* leaves via agro-infiltration. The results showed that in the presence of
464 NLS-Sw-5b, the cell-to-cell movement of NSm-GFP was inhibited (Fig. 4b). Similar

results were also obtained in the leaves co-expressing mCherry-HDEL and NSm-GFP with nls-YFP-Sw-5b or nes-YFP-Sw-5b (Fig S3b). In the presence of NES-YFP-Sw-5b, however, NSm-GFP did move into surrounding cells. (Fig. 4b). This finding indicates that the Sw-5b in the nucleus but not in the cytoplasm induced a host defense that inhibited TSWV NSm cell-to-cell movement.

Nuclear Sw-5b confers host immunity to TSWV systemic infection

To dissect the host immunity induced by the cytoplasmic and the nuclear Sw-5b, we generated transgenic *N. benthamiana* lines expressing YFP-Sw-5b, NES-YFP-Sw-5b, nes-YFP-Sw-5b, NLS-YFP-Sw-5b, and nls-YFP-Sw-5b, respectively (Tables S1 and S2). After inoculation of these transgenic lines with TSWV-YN isolate, the EV (control) transgenic plants developed typical viral symptoms including stunt, leaf curl and mosaic at 7 to 15 days post inoculation (dpi). The NES-YFP-Sw-5b transgenic plants developed a strong HR trailing in the systemic leaves by 7 to 15 days post inoculation (dpi) (Fig. 5a and Fig. S4a), suggesting that NES-YFP-Sw-5b transgenic plant did not block TSWV systemic infection and caused virus infection-related systemic HR. In contrast, no systemic virus infection symptoms were observed in the YFP-Sw-5b and the nes-YFP-Sw-5b transgenic plants. The RT-PCR agreed with the symptom observation results and showed that TSWV-YN genomic RNA was accumulated in the systemic leaves of the TSWV-YN-inoculated NES-YFP-Sw-5b or the EV transgenic plants, but not in the systemic leaves of the TSWV-YN-inoculated YFP-Sw-5b or nes-YFP-Sw-5b transgenic plants (Fig. 5c and Fig. S4b). Also in this

study, the TSWV-YN-inoculated NLS-YFP-Sw-5b or nls-YFP-Sw-5b transgenic plants did not show virus like symptoms in their systemic leaves by 7-15 dpi (Fig. 5a, and Fig. S4a). The RT-PCR result confirmed that TSWV-N genomic RNA had not accumulated in the systemic leaves of the NLS-YFP-Sw-5b or the nls-YFP-Sw-5b transgenic plants (Fig. 5c, and Fig. S4b), indicating that the nuclear Sw-5b is responsible for the host immunity against TSWV systemic infection.

The cytoplasmic and the nuclear Sw-5b act synergistically to confer a strong immunity to TSWV infection in *N. benthamiana*

To investigate whether cytoplasm-targeted and nucleus-targeted Sw-5b have joint effects on the defense against TSWV infection, we constructed a $M_{(-)opt}$-$pSR_{(+)eGFP}$ vector by inserting a cassette expressing optimized TSWV M genomic sequence (Feng *et al.*, 2020) into the $pSR_{(+)eGFP}$ mini-replicon to express NSm, N, and eGFP simultaneously in the same cells (Fig. 6a). The construct $M_{(-)opt}$-$pSR_{(+)eGFP}$ couples the functions for both viral replication and viral cell-to-cell movement, mimicking the virus infection in plant leaves. After co-expressing this vector, the $L_{(+)opt}$ and the EV in *N. benthamiana* leaves through agro-infiltration, the eGFP fluorescence was observed in many cells, due to the presence of the NSm movement protein and the $RdRp_{opt}$ (Fig. 6b, upper left image). When $M_{(-)opt}$-$SR_{(+)eGFP}$, $L_{(+)opt}$ and Sw-5b were co-expressed in *N. benthamiana* leaves, the eGFP fluorescence was hardly detected and some were observed only in single leaf cells (Fig. 6b upper right image, Fig. S5a and b). When $M_{(-)opt}$-$SR_{(+)eGFP}$, $L_{(+)opt}$ and NES-Sw-5b were co-expressed in *N. benthamiana* leaves,

509 the eGFP fluorescence was observed in clusters of a few cells (Fig. 6b, Fig. S5a),
510 indicating that limited cell-to-cell movement had occurred in these leaves (Fig. S5b).
511 When $M_{(-)opt}$-$SR_{(+)eGFP}$, $L_{(+)opt}$ and NLS-Sw-5b were co-expressed in leaves, a few of
512 eGFP fluorescence were detected but they were in single cells only. When leaves
513 co-expressing $M_{(-)opt}$-$SR_{(+)eGFP}$, $L_{(+)opt}$ and NES-Sw-5b + NLS-Sw-5b, the eGFP
514 fluorescence was also hardly detected and some were observed only in single leaf
515 cells. Western blot results showed that more eGFP had accumulated in the leaves
516 co-expressing $M_{(-)opt}$-$SR_{(+)eGFP}$, $L_{(+)opt}$, and EV, followed by the leaves co-expressing
517 $M_{(-)opt}$-$SR_{(+)eGFP}$, $L_{(+)opt}$, and NLS-Sw-5b, and then the leaves co-expressing
518 $M_{(-)opt}$-$SR_{(+)eGFP}$, $L_{(+)opt}$, and NES-Sw-5b. Much less eGFP had accumulated in the
519 leaves co-expressing $M_{(-)opt}$-$SR_{(+)eGFP}$, $L_{(+)opt}$, and NLS-Sw-5b + NES-Sw-5b, and in
520 the leaves co-expressing $M_{(-)opt}$-$SR_{(+)eGFP}$, $L_{(+)opt}$, and Sw-5b (Fig. 6c and d). The
521 accumulation of eGFP was lower in the leaves co-expressing NES-Sw-5b +
522 NLS-Sw-5b than that in the leaves co-expressing NES-Sw-5b or NLS-Sw-5b (Fig. 6c
523 and d), indicating that NES-Sw-5b and NLS-Sw-5b have additive role in mediating
524 host immunity against different TSWV infection steps.
525
526 **The Sw-5b NB-ARC-LRR control its cytoplasm localization whereas the**
527 **extended N-terminal SD domain is crucial for targeting Sw-5b into nucleus, and**
528 **for inducing host systemic immunity**
529 Sw-5b has an extended N-terminal SD domain, a CC domain, a NB-ARC domain, and
530 a C-terminal LRR domain (Chen *et al.*, 2016). To determine which domain(s) of

Sw-5b is/are responsible for nucleoplasm/nucleolus targeting and for plant immunity, we tested these domains using various deletion mutants and YFP fusion proteins (Fig. 7a). We reported previously that the Sw-5b NB-ARC-LRR region was able to induce HR cell death in plant in the presence of NSm (Chen *et al.*, 2016). In this study, we fused YFP to the N-terminus of NB-ARC-LRR (Fig. 7a). Transient expression of YFP-NB-ARC-LRR (112 kDa) in *N. benthamiana* leaf cells resulted in a localization of the fusion protein in cytoplasm exclusively (Fig. 7b).

A previous study had shown that the CC domain of potato NLR receptor Rx was required for targeting this protein to nucleus (Slootweg *et al.*, 2010). To determine the function of Sw-5b CC domain in intracellular trafficking, we inserted the CC domain between the YFP and NB-ARC-LRR to generate an YFP-CC-NB-ARC-LRR construct or fused the CC domain to YFP to produce an YFP-CC construct. Transient expression of these two fusion proteins individually in *N. benthamiana* leaves, and examined the leaves under a confocal microscope, we determined that the YFP-CC fusion protein accumulated in both cytoplasm and nucleus of the cells while the YFP-CC-NB-ARC-LRR fusion protein was in the cytoplasm only (Fig. 7b). This result indicated that addition of the CC domain to YFP-NB-ARC-LRR was not sufficient to traffic the fusion protein into the nucleus.

An extended N-terminal SD domain is known to be present at the upstream of the Sw-5b CC domain. In this study, we first generated an YFP-SD and an YFP-SD-CC constructs, and transiently expressed them individually in *N. benthamiana* leaf cells. Confocal Microscopy showed that both YFP-SD and YFP-SD-CC fusion proteins

553 accumulated in the cytoplasm and nucleus (Fig. 7b). We then inserted a SD between
554 the YFP and CC-NB-ARC-LRR to produce an YFP-SD-CC-NB-ARC-LRR
555 construction. Transient expression of this construct in *N. benthamiana* leaf cells
556 showed that this fusion protein accumulated in the cytoplasm and nucleus (Fig. 7b).

557 We next generated stable transgenic *N. benthamiana* plants expressing
558 YFP-NB-ARC-LRR, YFP-CC-NB-ARC-LRR and YFP-SD-CC-NB-ARC-LRR.
559 Upon inoculation transgenic *N. benthamiana* plants expressing YFP-NB-ARC-LRR
560 with TSWV, large HR foci were observed in the TSWV-inoculated leaves and later,
561 HR trailing was seen in the systemic leaves of most assayed plants (Fig. 7c; Table S2
562 and S3). RT-PCR results confirmed the presence of TSWV genomic RNA in these
563 systemic leaves (Fig. S6b). We also inoculate *N. benthamiana* plants expressing
564 YFP-CC-NB-ARC-LRR with TSWV. By 7 dpi, no systemic resistance to TSWV
565 infection was observed in these plants (Fig. 6a and B, Table S4). RT-PCR results
566 showed that systemic infection of TSWV did occur in the TSWV-inoculated
567 YFP-CC-NB-ARC-LRR transgenic plants (Fig. S6b). In contrast, transgenic plants
568 expressing YFP-SD-CC-NB-ARC-LRR fusion exhibited a systemic immunity to
569 TSWV infection (Fig. 7c, Fig. S6b).

570 These data indicated that Sw-5b NB-ARC-LRR control its cytoplasm localization,
571 CC domain of Sw-5b alone was not sufficient to transport the NB-ARC-LRR into
572 nucleus and the extended SD domain is required for targeting Sw-5b to the nucleus,
573 and for inducing host immunity.

574

The extended SD domain interacted with *importin α1*, *α2* and *β*

To identify the cellular machinery needed for transporting Sw-5b into nucleus, we co-expressed YFP-SD and YFP-Sw-5b in *N. benthamiana* leaves followed by a co-immunoprecipitation (co-IP) and Mass Spectrometry. The results identified *N. benthamiana* importin α as one of candidate proteins interacted with YFP-SD and YFP-Sw-5b (Table S5 and S6). The co-IP and Mass Spectrometry also identified nuclear pore complex protein TPRb and nuclear pore complex protein Nup160a interacted with YFP-Sw-5b (Table S6). *Importins* play important roles in translocating proteins from cytoplasm into nucleus (Kanneganti *et al.*, 2007). We used BiFC analysis to confirm the interaction between YFP-SD with *N. benthamiana* importin homologs α1, α2 and *β*. The result showed that co-expression of cYFP-SD with nYFP-IMP α1, nYFP-IMP α2 or nYFP-IMP *β* produced a strong YFP fluorescence signal in nucleus. Co-expression of cYFP-Sw-5b with nYFP-IMP α1, nYFP-IMP α2 or nYFP-IMP *β* also detected a strong YFP fluorescence signal in nucleus (Fig. S7). In contrast, co-expression of controls cYFP-SD and nYFP, cYFP-Sw-5b and nYFP, cYFP and nYFP-IMP α1, cYFP and nYFP-IMP α2 or cYFP and nYFP-IMP *β* did not show fluorescence signal in *N. benthamiana* leaf cells (Fig. S7).

Silencing *importin α1*, *α2* and *β* expression abolished Sw-5b nucleus accumulation and host resistance to TSWV systemic infection

To determine the functions of importin α1, α2 and β in Sw-5b nucleus localization, we

597 silenced *importin α1, α2, β, α1* and *α2,* and *α1* and *α2* and *β* expressions, respectively,
598 in *N. benthamiana* leaves using a tobacco rattle virus (TRV)-based virus-induced gene
599 silencing (VIGS) vector, and then transiently expressed YFP-Sw-5b in these plants.
600 Analyses of these plants through RT-PCR using gene specific primers showed that
601 silencing of these *importin* genes in *N. benthamiana* leaves were successful (Fig.
602 S8a). However, silencing individual *importin* gene or both *importin α1* and *α2* was
603 not enough to block the nucleus accumulation of YFP-Sw-5b (Fig. 8a). In contrast,
604 after *importin α1*, *α2* and *β* were all silenced through VIGS, the nucleus accumulation
605 of YFP-Sw-5b was inhibited (Fig. 8a, the middle image in the bottom panel).

606 To investigate the effects of nuclear import defected Sw-5b on host immunity to
607 TSWV systemic infection, we silenced these *importin* genes in the Sw-5b transgenic
608 *N. benthamiana* plants as described above, and then inoculated them with TSWV. The
609 results showed that the plants silenced for *importin α1*, *α2*, and *β* gene, individually,
610 did not show TSWV systemic infection (Fig. 8b and Fig. S8b). In addition, the
611 transgenic plants silenced for both *importin α1* and *α2* genes also did not show
612 TSWV systemic infection (Fig. 8b and Fig. S8b). In contrast, after silencing *importin*
613 *α1*, *α2* and *β* together, the plants developed clear TSWV symptoms in systemic
614 leaves followed by HR (Fig. 8b, white arrow and Fig. S8b), indicating that the nucleus
615 accumulation of Sw-5b is indispensable for the induction of host immunity against
616 TSWV systemic infection.

617

618 **Discussion**

In this report, we provide evidence to show that the cytoplasm-accumulated and the nucleus-accumulated Sw-5b, a tomato immune receptor, play different roles in inducing host defense against TSWV infection in plant. The cytoplasmic Sw-5b functions to induce a strong cell death response to inhibit TSWV replication. This host response is, however, insufficient to block virus intercellular and long-distance movement. The nuclear-localized Sw-5b triggers a host defense that weakly inhibit viral replication but strongly inhibit tospovirus intercellular and systemic movement. These findings suggest that tomato Sw-5b NLR induces different types of defense responses by cytoplasm and nucleus partitioning to combat virus at different infection steps. Furthermore, the cytoplasmic and the nuclear Sw-5b act synergistically to confer a strong host immunity to TSWV infection in plant. We also demonstrated that the extra SD domain functioned as a critical intracellular translocation modulator, allowing Sw-5b receptor to translocate from cytoplasm to nucleus to trigger the immunity. The Sw-5b NB-LRR controls its cytoplasm localization. Unlike Rx CC domain, Sw-5b CC domain is not sufficient to translocate NB-LRR into nucleus. Strikingly, the SD is crucial for Sw-5b to translocate from cytoplasm for nucleus. This SD-mediated receptor translocation is dependent on importins α and β.

Successful virus infection in plant requires several steps including viral replication in the initially infected cells followed by cell-to-cell and long-distance movement (Heinlein, 2015; Wang, 2015). After entering into plant cells, virus first encode multiple proteins needed for its replication. Once the initial replication is established, virus will encode specific protein(s), known as movement proteins (MPs), to traffic

641 viral genome or virions into adjacent cells through plasmodesmata in cell walls, and
642 then long-distantly into other parts of the plant to cause a systemic infection (Rao,
643 2002; Lucas, 2006; Taliansky *et al.*, 2008). To date, multiple plant NLRs, conferring
644 host resistance against plant viruses have been identified (Soosaar *et al.*, 2005; Meier
645 *et al.*, 2019), but how these plant NLRs induce host resistance against virus infection
646 remain largely unknown.

647 In this study, we have determined that the forced cytoplasm accumulation of
648 Sw-5b can induce a stronger cell death than that caused by the accumulation of Sw-5b
649 in both cytoplasm and nucleus. While, the cell death induced by the forced nucleus
650 accumulation of Sw-5b was significantly weakened. We then analyzed
651 Sw-5b-mediated immunity against TSWV replication using a TSWV mini-replicon
652 system and a movement defective NSm mutant. Our results showed that the forced
653 cytoplasm accumulation of Sw-5b can induce a strong host defense against virus
654 replication in cells. This finding implies that cytoplasm is one of the main source of
655 defense signaling against TSWV replication. The defense signaling generated in
656 nucleus can only induce a weak defense against TSWV replication. Therefore, the
657 nuclear localized Sw-5b is only partially responsible for the induction of host defense
658 against TSWV replication. It is also possible that this nuclear localized
659 Sw-5b-induced weak host response is caused by a trace of NLS-YFP-Sw-5b
660 maintained in the cytoplasm that maybe below the detection limit of Confocal
661 Microscope. It has been shown to accumulate in both cytoplasm and nucleus, and the
662 forced cytoplasm accumulation of Barley MLA10 enhance cell death signaling (Bai *et*

663 *al.*, 2012). We speculate that, for both MLA10 and Sw-5b, the cytoplasm
664 accumulation is crucial for the initiation and/or amplification of the cell death
665 signaling. The CC and the TIR domain of several plant NLRs have been shown to
666 trigger cell death (Swiderski *et al.*, 2009; Krasileva *et al.*, 2010; Bernoux *et al.*, 2011;
667 Collier *et al.*, 2011; Maekawa *et al.*, 2011; Bai *et al.*, 2012; Chen *et al.*, 2017; Wang
668 *et al.*, 2020). Analyses of the three dimensional structures of Arabidopsis ZAR1
669 resistosome have also shown that its CC domain can form pentamer structures that
670 was able to target into host cell membranes, leading to ion leakage and cell death
671 (Wang *et al.*, 2019a; Wang *et al.*, 2019b). We speculate that cell death likely cause the
672 toxicity on viral replicase or other proteins associated with virus replication in cells.

673 Plant virus encodes specific movement protein(s) to traffic viral genome between
674 cells and then leaves to cause systemic infection (Rao, 2002; Lucas, 2006; Taliansky
675 *et al.*, 2008). We reported previously that TSWV NSm alone can move between plant
676 cells (Feng *et al.*, 2016). In this study, we investigated the effect of the
677 Sw-5b-mediated host defense on TSWV intercellular movement. Through this study,
678 we have determined that after the recognition of NSm, Sw-5b receptor induced a
679 strong reaction to block NSm intercellular trafficking. Previous reports have some
680 indications on the role of plant NLRs in viral movement. Nevertheless it has no direct
681 evidence showing that plant NLRs induce resistance against viral movement. Deom
682 and colleagues had shown that the 9.4-kDa fluorescein isothiocyanate-labeled dextran
683 was unable to move between cells in the transgenic tobacco *N* leaves expressing
684 tobacco mosaic virus (TMV) movement protein at 24°C, an HR-permissive

685 temperature (Deom *et al.*, 1991). However, that study did not involve a TMV Avr
686 protein. In a different report, TMV-GFP showed a limited cell-to-cell movement in
687 leaves of tobacco cv. Sumsan NN at 33°C, an HR-nonpermissive temperature (Canto
688 & Palukaitis, 2002). Li and colleagues found that after treatment of SMV-inoculated
689 Jidou 7 resistant plants with a callose synthase inhibitor, the plants showed enlarged
690 HR lesions (Li *et al.*, 2012). The soybean *Rsv3* induced extreme resistance. However,
691 after this extremely resistant soybean line was treated with a callose synthase inhibitor,
692 the plants developed HR lesions upon SMV-G5H inoculation (Seo *et al.*, 2014). These
693 reports indicate that plant NLRs likely involves the defense against viral movement.
694 Here we provide the direct evidence that Sw-5b NLR can induce a strong defense
695 response to impede NSm intercellular trafficking. More importantly, we have
696 determined that the induction of host immunity to TSWV intercellular movement
697 requires the accumulation of Sw-5b in nucleus. Although the cytoplasmic Sw-5b can
698 induce a strong cell death response, it cannot prevent TSWV NSm cell-to-cell
699 movement. Consequently, we propose that nucleus is a key compartment to generate
700 defense signaling to block TSWV cell-to-cell movement.

701 In this study, although the NES-YFP-Sw-5b transgenic *N. benthamiana* plants
702 showed an HR, they were unable to stop TSWV systemic infection. We also showed
703 that Sw-5b YFP-NB-ARC-LRR (112 kDa) accumulates in cytoplasm exclusively (Fig.
704 7b), however, transgenic *N. benthamiana* plants expressing YFP-NB-ARC-LRR show
705 strong systemic HR trailing caused by TSWV infection. Based on these findings, we
706 conclude that HR cell death alone is not sufficient to block TSWV long-distance

707 movement. In our study, the NLS-YFP-Sw-5b transgenic plants were resistant to
708 TSWV systemic infection. After silencing the expressions of *importin α1*, *α2* and *β*
709 simultaneously to inhibit the nucleus accumulation of Sw-5b, however, the resistance
710 to TSWV systemic infection was abolished. These findings indicate that the
711 Sw-5b-mediated resistance signaling against viral systemic infection is generated in
712 nucleus. Some plant NLRs are known to interact with specific transcription factors in
713 nucleus upon recognition of pathogen effectors (Cui *et al.*, 2015; Kapos *et al.*, 2019).
714 The immune regulator EDS1 has also been shown to accumulate in nucleus to
715 reprogram RNA transcription (Garcia *et al.*, 2010; Heidrich *et al.*, 2011; Cui *et al.*,
716 2015; Lapin *et al.*, 2020). How Sw-5b regulates host immunity in nucleus requires
717 further investigations.

718 Several plant immune receptors and immune regulators, including, e.g. potato Rx
719 (Slootweg *et al.*, 2010; Tameling *et al.*, 2010), tobacco N (Burch-Smith *et al.*, 2007;
720 Caplan, JL *et al.*, 2008), barley MLA10 (Shen *et al.*, 2007), Arabidopsis
721 RRS1-R/RPS4, and snc1 (Deslandes *et al.*, 2003; Wirthmueller *et al.*, 2007; Cheng *et*
722 *al.*, 2009), as well as Arabidopsis NPR1 (Katagiri & Tsuda, 2010), and EDS1 (Lapin
723 *et al.*, 2020) have been found to be nucleocytoplasmic. For some of them, nuclear
724 accumulation of NLRs are required for the induction of plant immunity to pathogen
725 attacks. Moreover, the MLA10-YFP-NES fusion was found to induce a strong cell
726 death response, but not a strong host resistance to powdery mildew fungus infection.
727 In contrast, the MLA10-YFP-NLS fusion inhibited its activity to induce a cell death
728 response, but caused a host immunity to this pathogen (Bai *et al.*, 2012). In many

729 plant-pathogen interactions, cell death responses can be uncoupled from disease
730 resistance (Bendahmane *et al.*, 1999; Gassmann, 2005; Coll *et al.*, 2010; Heidrich *et*
731 *al.*, 2011). This separation raises questions about how host resistance prevents
732 pathogen invasion and what are the roles of cell death during pathogen infection. It is
733 unclear whether the MLA10-YFP-NES-induced cell death has some inhibitory effects
734 on powdery mildew fungus infection. In this study, we determined that cytoplasm-
735 and nuclear-accumulation of Sw-5b have different functions. The
736 cytoplasm-accumulated Sw-5b induces a strong defense against virus replication,
737 whereas the nuclear-accumulated Sw-5b induced an inhibition of virus cell-to-cell and
738 long distance movement. Both cytoplasmic and nuclear Sw-5b are needed to confer a
739 synergistic and full defense against tospovirus infection.

740 We have also determined that Sw-5b NB-ARC-LRR and SD domains are
741 important to regulate the proper subcellular localization of Sw-5b and the proper
742 nucleoplasmic distribution of Sw-5b is needed to elicit full immune responses to
743 inhibit different TSWV infection steps. Sw-5b NB-ARC-LRR controls its cytoplasm
744 localization. The CC domain of the Sw-5b is not sufficient to target the receptor into
745 nuclear. Importantly, the extended SD of Sw-5b is absolutely required for the nucleus
746 translocation. Because non-canonical domains are frequently found in other NLRs
747 and are quite diversified, our findings have broad implications to investigate the
748 potential new functions of non-canonical domains that integrated in the plant NLRs to
749 regulate the plant immunity against pathogen invasions.

750 Through co-IP, Mass Spectrometry and BiFC analysis, we found that the extended

751 SD domain and Sw-5b interacted with host importin machineries to translocate the
752 Sw-5b receptor from cytoplasm into nucleus to mediate local and systemic resistance
753 to tospovirus. Recent studies have shown that nuclearporin MOS3, MOS6 and nuclear
754 pore complex component MOS7/Nup88 proteins played important roles in regulating
755 Arabidopsis innate immunity (Palma *et al.*, 2005; Zhang & Li, 2005; Cheng *et al.*,
756 2009). We found that when *importin α1*, *importin α2* and *importin β* gene were all
757 silenced through VIGS, the nucleus targeting of Sw-5b were completely blocked, and
758 consequently, the Sw-5b-mediated systemic immunity to tospovirus infection was
759 compromised. Importin α and β are known to form a nucleus import complex.
760 Binding with importin β could activate importin α to form a binding surface for NLS
761 proteins (Stewart, 2007). Hence, disruption of either importin α or importin β would
762 block the nucleus import of NLS proteins. Because silencing *importin α* or
763 *importin β* gene expression through VIGS did not disrupt the nuclear targeting of
764 Sw-5b, we speculate that a non-canonical nuclear import pathway may take part in
765 importing Sw-5b into nucleus.

766 Based on the above results, we have created a working model for the Sw-5b
767 NLR-induced host resistance against TSWV replication, and intercellular and
768 long-distance movement in plant (Fig. 9). Upon recognition of NSm in cytoplasm,
769 Sw-5b switched from an autoinhibited state to an activated state. The activated Sw-5b
770 accumulated in cytoplasm and also translocate into nucleus via importins α and β .
771 The cytoplasm-accumulated and the nucleus-accumulated Sw-5b play different roles
772 in inducing host immunity against TSWV infection. The cytoplasmic Sw-5b functions

773 to induce a cell death response to inhibit TSWV replication, while the nuclear Sw-5b
774 functions to induce a weak host defense against TSWV replication, but a strong
775 defense against TSWV cell-to-cell and long-distance movement. The concerted
776 defense signaling generated in the cytoplasm and nucleus resulted in a strong host
777 resistance to tospovirus infection.
778
779
780 **Acknowledgments**
781 This work was supported by the National Natural Science Foundation of China
782 (31630062, 31925032 and 31870143), the Fundamental Research Funds for the
783 Central Universities (JCQY201904 and KYXK202012), Youth Science and
784 Technology Innovation Program to XT.
785
786 **Author contributions**
787 HC XQ, XC and XT, designed the research; HC, XQ and XC, TY, MF, JC, RC, HH,
788 YZ, YM, DS, YX, MZ performed the experiments; HC, XSD and XT interpreted the
789 result and wrote the paper.
790
791 **ORCID**
792 Hongyu Chen, 0000-0001-8142-0653
793 Yi Xu, 0000-0002-1913-4530
794 Min Zhu, 0000-0002-9354-4300

Xiaorong Tao, 0000-0003-1259-366X

Competing interests

The authors declare that nocompeting interests exist.

Data availability

All data produced in this study are presented in this manuscript or as the supporting files

References

Axtell MJ, Staskawicz BJ. 2003. Initiation of RPS2-specified disease resistance in Arabidopsis is coupled to the AvrRpt2-directed elimination of RIN4. *Cell* **112**(3): 369-377.

Bai S, Liu J, Chang C, Zhang L, Maekawa T, Wang Q, Xiao W, Liu Y, Chai J, Takken FL, Schulze-Lefert P, Shen QH. 2012. Structure-function analysis of barley NLR immune receptor MLA10 reveals its cell compartment specific activity in cell death and disease resistance. *PLoS Pathog* **8**(6): e1002752.

Bendahmane A, Kanyuka K, Baulcombe DC. 1999. The Rx gene from potato controls separate virus resistance and cell death responses. *Plant Cell* **11**(5): 781-792.

Bernoux M, Ve T, Williams S, Warren C, Hatters D, Valkov E, Zhang X, Ellis JG, Kobe B, Dodds PN. 2011. Structural and functional analysis of a plant resistance protein TIR domain reveals interfaces for self-association, signaling, and autoregulation. *Cell Host Microbe* **9**(3): 200-211.

Brommonschenkel SH, Frary A, Frary A, Tanksley SD. 2000. The broad-spectrum tospovirus resistance gene Sw-5 of tomato is a homolog of the root-knot nematode resistance gene Mi. *Mol Plant Microbe Interact* **13**(10): 1130-1138.

Burch-Smith TM, Schiff M, Caplan JL, Tsao J, Czymmek K, Dinesh-Kumar SP. 2007. A novel role for the TIR domain in association with pathogen-derived elicitors. *PLoS Biol* **5**(3): e68.

Canto T, Palukaitis P. 2002. Novel N gene-associated, temperature-independent resistance to the movement of tobacco mosaic virus vectors neutralized by a cucumber mosaic virus RNA1 transgene. *J Virol* **76**(24): 12908-12916.

Caplan J, Padmanabhan M, Dinesh-Kumar SP. 2008. Plant NB-LRR Immune Receptors: From Recognition to Transcriptional Reprogramming. *Cell Host Microbe* **3**(3): 126-135.

827 **Caplan JL, Mamillapalli P, Burch-Smith TM, Czymmek K, Dinesh-Kumar SP. 2008.**
828 Chloroplastic protein NRIP1 mediates innate immune receptor recognition of a viral effector.
829 *Cell* **132**(3): 449-462.
830 **Cesari S, Bernoux M, Moncuquet P, Kroj T, Dodds PN. 2014.** A novel conserved mechanism for
831 plant NLR protein pairs: the "integrated decoy" hypothesis. *Front Plant Sci* **5**: 606.
832 **Cesari S, Moore J, Chen C, Webb D, Periyannan S, Mago R, Bernoux M, Lagudah ES, Dodds**
833 **PN. 2016.** Cytosolic activation of cell death and stem rust resistance by cereal MLA-family
834 CC-NLR proteins. *Proc Natl Acad Sci U S A* **113**(36): 10204-10209.
835 **Cesari S, Thilliez G, Ribot C, Chalvon V, Michel C, Jauneau A, Rivas S, Alaux L, Kanzaki H,**
836 **Okuyama Y, Morel JB, Fournier E, Tharreau D, Terauchi R, Kroj T. 2013.** The rice
837 resistance protein pair RGA4/RGA5 recognizes the Magnaporthe oryzae effectors AVR-Pia
838 and AVR1-CO39 by direct binding. *Plant Cell* **25**(4): 1463-1481.
839 **Chen T, Liu D, Niu X, Wang J, Qian L, Han L, Liu N, Zhao J, Hong Y, Liu Y. 2017.** Antiviral
840 Resistance Protein Tm-2(2) Functions on the Plasma Membrane. *Plant Physiol* **173**(4):
841 2399-2410.
842 **Chen X, Zhu M, Jiang L, Zhao W, Li J, Wu J, Li C, Bai B, Lu G, Chen H, Moffett P, Tao X. 2016.**
843 A multilayered regulatory mechanism for the autoinhibition and activation of a plant
844 CC-NB-LRR resistance protein with an extra N-terminal domain. *New Phytol* **212**(1):
845 161-175.
846 **Cheng YT, Germain H, Wiermer M, Bi D, Xu F, Garcia AV, Wirthmueller L, Despres C, Parker**
847 **JE, Zhang Y, Li X. 2009.** Nuclear pore complex component MOS7/Nup88 is required for
848 innate immunity and nuclear accumulation of defense regulators in Arabidopsis. *Plant Cell*
849 **21**(8): 2503-2516.
850 **Coll NS, Vercammen D, Smidler A, Clover C, Van Breusegem F, Dangl JL, Epple P. 2010.**
851 Arabidopsis type I metacaspases control cell death. *Science* **330**(6009): 1393-1397.
852 **Collier SM, Hamel LP, Moffett P. 2011.** Cell death mediated by the N-terminal domains of a unique
853 and highly conserved class of NB-LRR protein. *Mol Plant Microbe Interact* **24**(8): 918-931.
854 **Collier SM, Moffett P. 2009.** NB-LRRs work a "bait and switch" on pathogens. *Trends Plant Sci*
855 **14**(10): 521-529.
856 **Cui H, Tsuda K, Parker JE. 2015.** Effector-triggered immunity: from pathogen perception to robust
857 defense. *Annu Rev Plant Biol* **66**: 487-511.
858 **Das B, Sengupta S, Prasad M, Ghose TK. 2014.** Genetic diversity of the conserved motifs of six
859 bacterial leaf blight resistance genes in a set of rice landraces. *BMC Genet* **15**: 82.
860 **De Oliveira AS, Koolhaas I, Boiteux LS, Caldararu OF, Petrescu AJ, Oliveira Resende R,**
861 **Kormelink R. 2016.** Cell death triggering and effector recognition by Sw-5 SD-CNL proteins
862 from resistant and susceptible tomato isolines to Tomato spotted wilt virus. *Mol Plant Pathol*
863 **17**(9): 1442-1454.
864 **Deom CM, Wolf S, Holt CA, Lucas WJ, Beachy RN. 1991.** Altered function of the tobacco mosaic
865 virus movement protein in a hypersensitive host. *Virology* **180**(1): 251-256.
866 **Deslandes L, Olivier J, Peeters N, Feng DX, Khounlotham M, Boucher C, Somssich I, Genin S,**
867 **Marco Y. 2003.** Physical interaction between RRS1-R, a protein conferring resistance to
868 bacterial wilt, and PopP2, a type III effector targeted to the plant nucleus. *Proc Natl Acad Sci*
869 *U S A* **100**(13): 8024-8029.
870 **Dodds PN, Rathjen JP. 2010.** Plant immunity: towards an integrated view of plant-pathogen

interactions. *Nat Rev Genet* **11**(8): 539-548.

Ea VDB, Jones JD. 1998. Plant disease-resistance proteins and the gene-for-gene concept. *Trends in Biochemical Sciences* **23**(12): 454-456(453).

Engelhardt S, Boevink PC, Armstrong MR, Ramos MB, Hein I, Birch PR. 2012. Relocalization of late blight resistance protein R3a to endosomal compartments is associated with effector recognition and required for the immune response. *Plant Cell* **24**(12): 5142-5158.

Ernst K, Kumar A, Kriseleit D, Kloos DU, Phillips MS, Ganal MW. 2002. The broad-spectrum potato cyst nematode resistance gene (Hero) from tomato is the only member of a large gene family of NBS-LRR genes with an unusual amino acid repeat in the LRR region. *Plant J* **31**(2): 127-136.

Feng M, Cheng R, Chen M, Guo R, Li L, Feng Z, Wu J, Xie L, Hong J, Zhang Z, Kormelink R, Tao X. 2020. Rescue of tomato spotted wilt virus entirely from complementary DNA clones. *Proc Natl Acad Sci U S A* **117**(2): 1181-1190.

Feng Z, Xue F, Xu M, Chen X, Zhao W, Garcia-Murria MJ, Mingarro I, Liu Y, Huang Y, Jiang L, Zhu M, Tao X. 2016. The ER-Membrane Transport System Is Critical for Intercellular Trafficking of the NSm Movement Protein and Tomato Spotted Wilt Tospovirus. *PLoS Pathog* **12**(2): e1005443.

Gao Z, Chung EH, Eitas TK, Dangl JL. 2011. Plant intracellular innate immune receptor Resistance to Pseudomonas syringae pv. maculicola 1 (RPM1) is activated at, and functions on, the plasma membrane. *Proc Natl Acad Sci U S A* **108**(18): 7619-7624.

Garcia AV, Blanvillain-Baufume S, Huibers RP, Wiermer M, Li G, Gobbato E, Rietz S, Parker JE. 2010. Balanced nuclear and cytoplasmic activities of EDS1 are required for a complete plant innate immune response. *PLoS Pathog* **6**: e1000970.

Gassmann W. 2005. Natural variation in the Arabidopsis response to the avirulence gene hopPsyA uncouples the hypersensitive response from disease resistance. *Mol Plant Microbe Interact* **18**(10): 1054-1060.

Germain H, Seguin A. 2011. Innate immunity: has poplar made its BED? *New Phytol* **189**(3): 678-687.

Hallwass M, de Oliveira AS, de Campos Dianese E, Lohuis D, Boiteux LS, Inoue-Nagata AK, Resende RO, Kormelink R. 2014. The Tomato spotted wilt virus cell-to-cell movement protein (NSM) triggers a hypersensitive response in Sw-5-containing resistant tomato lines and in Nicotiana benthamiana transformed with the functional Sw-5b resistance gene copy. *Mol Plant Pathol* **15**(9): 871-880.

Heidrich K, Wirthmueller L, Tasset C, Pouzet C, Deslandes L, Parker JE. 2011. Arabidopsis EDS1 connects pathogen effector recognition to cell compartment-specific immune responses. *Science* **334**(6061): 1401-1404.

Heinlein M. 2015. Plant virus replication and movement. *Virology* **479-480**: 657-671.

Horsefield S, Burdett H, Zhang X, Manik MK, Shi Y, Chen J, Qi T, Gilley J, Lai JS, Rank MX, Casey LW, Gu W, Ericsson DJ, Foley G, Hughes RO, Bosanac T, von Itzstein M, Rathjen JP, Nanson JD, Boden M, Dry IB, Williams SJ, Staskawicz BJ, Coleman MP, Ve T, Dodds PN, Kobe B. 2019. NAD(+) cleavage activity by animal and plant TIR domains in cell death pathways. *Science* **365**(6455): 793-799.

Inoue H, Hayashi N, Matsushita A, Xinqiong L, Nakayama A, Sugano S, Jiang CJ, Takatsuji H. 2013. Blast resistance of CC-NB-LRR protein Pb1 is mediated by WRKY45 through

protein-protein interaction. *Proc Natl Acad Sci U S A* **110**(23): 9577-9582.

Jones JD, Vance RE, Dangl JL. 2016. Intracellular innate immune surveillance devices in plants and animals. *Science* **354**(6316).

Jubic LM, Saile S, Furzer OJ, El Kasmi F, Dangl JL. 2019. Help wanted: helper NLRs and plant immune responses. *Curr Opin Plant Biol* **50**: 82-94.

Kanneganti TD, Bai X, Tsai CW, Win J, Meulia T, Goodin M, Kamoun S, Hogenhout SA. 2007. A functional genetic assay for nuclear trafficking in plants. *Plant J* **50**(1): 149-158.

Kanzaki H, Yoshida K, Saitoh H, Fujisaki K, Hirabuchi A, Alaux L, Fournier E, Tharreau D, Terauchi R. 2012. Arms race co-evolution of Magnaporthe oryzae AVR-Pik and rice Pik genes driven by their physical interactions. *Plant J* **72**(6): 894-907.

Kapos P, Devendrakumar KT, Li X. 2019. Plant NLRs: From discovery to application. *Plant Sci* **279**: 3-18.

Katagiri F, Tsuda K. 2010. Understanding the plant immune system. *Mol Plant Microbe Interact* **23**(12): 1531-1536.

Kawano Y, Fujiwara T, Yao A, Housen Y, Hayashi K, Shimamoto K. 2014. Palmitoylation-dependent membrane localization of the rice resistance protein pit is critical for the activation of the small GTPase OsRac1. *J Biol Chem* **289**(27): 19079-19088.

Kong L, Qiu X, Kang J, Wang Y, Chen H, Huang J, Qiu M, Zhao Y, Kong G, Ma Z, Wang Y, Ye W, Dong S, Ma W, Wang Y. 2017. A Phytophthora Effector Manipulates Host Histone Acetylation and Reprograms Defense Gene Expression to Promote Infection. *Curr Biol* **27**(7): 981-991.

Kormelink R, Garcia ML, Goodin M, Sasaya T, Haenni AL. 2011. Negative-strand RNA viruses: the plant-infecting counterparts. *Virus Res* **162**(1-2): 184-202.

Kormelink R, Storms M, Van Lent J, Peters D, Goldbach R. 1994. Expression and subcellular location of the NSM protein of tomato spotted wilt virus (TSWV), a putative viral movement protein. *Virology* **200**(1): 56-65.

Kourelis J, van der Hoorn RAL. 2018. Defended to the Nines: 25 Years of Resistance Gene Cloning Identifies Nine Mechanisms for R Protein Function. *Plant Cell* **30**(2): 285-299.

Krasileva KV, Dahlbeck D, Staskawicz BJ. 2010. Activation of an Arabidopsis resistance protein is specified by the in planta association of its leucine-rich repeat domain with the cognate oomycete effector. *Plant Cell* **22**(7): 2444-2458.

Kroj T, Chanclud E, Michel-Romiti C, Grand X, Morel JB. 2016. Integration of decoy domains derived from protein targets of pathogen effectors into plant immune receptors is widespread. *New Phytol* **210**(2): 618-626.

Lanford RE, Butel JS. 1984. Construction and characterization of an SV40 mutant defective in nuclear transport of T antigen. *Cell* **37**(3): 801-813.

Lapin D, Bhandari DD, Parker JE. 2020. Origins and Immunity Networking Functions of EDS1 Family Proteins. *Annu Rev Phytopathol* **58**: 253-276.

Le Roux C, Huet G, Jauneau A, Camborde L, Tremousaygue D, Kraut A, Zhou B, Levaillant M, Adachi H, Yoshioka H, Raffaele S, Berthome R, Coute Y, Parker JE, Deslandes L. 2015. A receptor pair with an integrated decoy converts pathogen disabling of transcription factors to immunity. *Cell* **161**(5): 1074-1088.

Leastro MO, Pallas V, Resende RO, Sanchez-Navarro JA. 2017. The functional analysis of distinct tospovirus movement proteins (NSM) reveals different capabilities in tubule formation,

cell-to-cell and systemic virus movement among the tospovirus species. *Virus Res* **227**: 57-68.

Li J, Huang H, Zhu M, Huang S, Zhang W, Dinesh-Kumar SP, Tao X. 2019. A Plant Immune Receptor Adopts a Two-Step Recognition Mechanism to Enhance Viral Effector Perception. *Mol Plant* **12**(2): 248-262.

Li W, Lewandowski DJ, Hilf ME, Adkins S. 2009. Identification of domains of the Tomato spotted wilt virus NSm protein involved in tubule formation, movement and symptomatology. *Virology* **390**(1): 110-121.

Li W, Zhao Y, Liu C, Yao G, Wu S, Hou C, Zhang M, Wang D. 2012. Callose deposition at plasmodesmata is a critical factor in restricting the cell-to-cell movement of Soybean mosaic virus. *Plant Cell Rep* **31**(5): 905-916.

Li X, Kapos P, Zhang Y. 2015. NLRs in plants. *Curr Opin Immunol* **32**: 114-121.

Lopez C, Aramburu J, Galipienso L, Soler S, Nuez F, Rubio L. 2011. Evolutionary analysis of tomato Sw-5 resistance-breaking isolates of Tomato spotted wilt virus. *J Gen Virol* **92**(Pt 1): 210-215.

Lucas WJ. 2006. Plant viral movement proteins: agents for cell-to-cell trafficking of viral genomes. *Virology* **344**(1): 169-184.

Lukasik-Shreepaathy E, Slootweg E, Richter H, Goverse A, Cornelissen BJ, Takken FL. 2012. Dual regulatory roles of the extended N terminus for activation of the tomato MI-1.2 resistance protein. *Mol Plant Microbe Interact* **25**(8): 1045-1057.

Ma S, Lapin D, Liu L, Sun Y, Song W, Zhang X, Logemann E, Yu D, Wang J, Jirschitzka J, Han Z, Schulze-Lefert P, Parker JE, Chai J. 2020. Direct pathogen-induced assembly of an NLR immune receptor complex to form a holoenzyme. *Science* **370**(6521).

Ma Y, Guo H, Hu L, Martinez PP, Moschou PN, Cevik V, Ding P, Duxbury Z, Sarris PF, Jones JDG. 2018. Distinct modes of derepression of an Arabidopsis immune receptor complex by two different bacterial effectors. *Proc Natl Acad Sci U S A* **115**(41): 10218-10227.

Ma Z, Song T, Zhu L, Ye W, Wang Y, Shao Y, Dong S, Zhang Z, Dou D, Zheng X, Tyler BM, Wang Y. 2015. A Phytophthora sojae Glycoside Hydrolase 12 Protein Is a Major Virulence Factor during Soybean Infection and Is Recognized as a PAMP. *Plant Cell* **27**(7): 2057-2072.

Ma Z, Zhu L, Song T, Wang Y, Zhang Q, Xia Y, Qiu M, Lin Y, Li H, Kong L, Fang Y, Ye W, Wang Y, Dong S, Zheng X, Tyler BM, Wang Y. 2017. A paralogous decoy protects Phytophthora sojae apoplastic effector PsXEG1 from a host inhibitor. *Science* **355**(6326): 710-714.

Maekawa T, Cheng W, Spiridon LN, Toller A, Lukasik E, Saijo Y, Liu P, Shen QH, Micluta MA, Somssich IE, Takken FLW, Petrescu AJ, Chai J, Schulze-Lefert P. 2011. Coiled-coil domain-dependent homodimerization of intracellular barley immune receptors defines a minimal functional module for triggering cell death. *Cell Host Microbe* **9**(3): 187-199.

Meier N, Hatch C, Nagalakshmi U, Dinesh-Kumar SP. 2019. Perspectives on intracellular perception of plant viruses. *Mol Plant Pathol* **20**(9): 1185-1190.

Meyers BC, Kozik A, Griego A, Kuang H, Michelmore RW. 2003. Genome-wide analysis of NBS-LRR-encoding genes in Arabidopsis. *Plant Cell* **15**(4): 809-834.

Milligan SB, Bodeau J, Yaghoobi J, Kaloshian I, Zabel P, Williamson VM. 1998. The root knot nematode resistance gene Mi from tomato is a member of the leucine zipper, nucleotide binding, leucine-rich repeat family of plant genes. *Plant Cell* **10**(8): 1307-1319.

Mittler R, Herr EH, Orvar BL, van Camp W, Willekens H, Inze D, Ellis BE. 1999. Transgenic

tobacco plants with reduced capability to detoxify reactive oxygen intermediates are hyperresponsive to pathogen infection. *Proc Natl Acad Sci U S A* **96**(24): 14165-14170.

Oliver JE, Whitfield AE. 2016. The Genus Tospovirus: Emerging Bunyaviruses that Threaten Food Security. *Annu Rev Virol* **3**(1): 101-124.

Padmanabhan MS, Ma S, Burch-Smith TM, Czymmek K, Huijser P, Dinesh-Kumar SP. 2013. Novel positive regulatory role for the SPL6 transcription factor in the N TIR-NB-LRR receptor-mediated plant innate immunity. *PLoS Pathog* **9**(3): e1003235.

Palma K, Zhang Y, Li X. 2005. An importin alpha homolog, MOS6, plays an important role in plant innate immunity. *Curr Biol* **15**(12): 1129-1135.

Peiro A, Canizares MC, Rubio L, Lopez C, Moriones E, Aramburu J, Sanchez-Navarro J. 2014. The movement protein (NSm) of Tomato spotted wilt virus is the avirulence determinant in the tomato Sw-5 gene-based resistance. *Mol Plant Pathol* **15**(8): 802-813.

Qi D, DeYoung BJ, Innes RW. 2012. Structure-function analysis of the coiled-coil and leucine-rich repeat domains of the RPS5 disease resistance protein. *Plant Physiol* **158**(4): 1819-1832.

Qi D, Innes RW. 2013. Recent Advances in Plant NLR Structure, Function, Localization, and Signaling. *Front Immunol* **4**: 348.

Rao ALNC, Y. G，Khan, J. A，Dijkstra, J. 2002. Molecular biology of plant virus movement. *Plant Viruses As Molecular Pathogens*.

Sarris PF, Cevik V, Dagdas G, Jones JD, Krasileva KV. 2016. Comparative analysis of plant immune receptor architectures uncovers host proteins likely targeted by pathogens. *BMC Biol* **14**: 8.

Sarris PF, Duxbury Z, Huh SU, Ma Y, Segonzac C, Sklenar J, Derbyshire P, Cevik V, Rallapalli G, Saucet SB, Wirthmueller L, Menke FL, Sohn KH, Jones JD. 2015. A Plant Immune Receptor Detects Pathogen Effectors that Target WRKY Transcription Factors. *Cell* **161**(5): 1089-1100.

Scholthof KB, Adkins S, Czosnek H, Palukaitis P, Jacquot E, Hohn T, Hohn B, Saunders K, Candresse T, Ahlquist P, Hemenway C, Foster GD. 2011. Top 10 plant viruses in molecular plant pathology. *Mol Plant Pathol* **12**(9): 938-954.

Seo JK, Kwon SJ, Cho WK, Choi HS, Kim KH. 2014. Type 2C protein phosphatase is a key regulator of antiviral extreme resistance limiting virus spread. *Sci Rep* **4**: 5905.

Seong K, Seo E, Witek K, Li M, Staskawicz B. 2020. Evolution of NLR resistance genes with noncanonical N-terminal domains in wild tomato species. *New Phytol* **227**(5): 1530-1543.

Shen QH, Saijo Y, Mauch S, Biskup C, Bieri S, Keller B, Seki H, Ulker B, Somssich IE, Schulze-Lefert P. 2007. Nuclear activity of MLA immune receptors links isolate-specific and basal disease-resistance responses. *Science* **315**(5815): 1098-1103.

Slootweg E, Roosien J, Spiridon LN, Petrescu AJ, Tameling W, Joosten M, Pomp R, van Schaik C, Dees R, Borst JW, Smant G, Schots A, Bakker J, Goverse A. 2010. Nucleocytoplasmic distribution is required for activation of resistance by the potato NB-LRR receptor Rx1 and is balanced by its functional domains. *Plant Cell* **22**(12): 4195-4215.

Soosaar JL, Burch-Smith TM, Dinesh-Kumar SP. 2005. Mechanisms of plant resistance to viruses. *Nat Rev Microbiol* **3**(10): 789-798.

Spassova M I PTW, Folkertsma R T, et al. 2001. The tomato gene Sw-5 is a member of the coiled coil, nucleotide binding, leucine-rich repeat class of plant resistance genes and confers resistance to TSWV in tobacco. *Molecular Breeding.* **7(2)**: 151.

Stewart M. 2007. Molecular mechanism of the nuclear protein import cycle. *Nat Rev Mol Cell Biol* **8**(3): 195-208.

Swiderski MR, Birker D, Jones JD. 2009. The TIR domain of TIR-NB-LRR resistance proteins is a signaling domain involved in cell death induction. *Mol Plant Microbe Interact* **22**(2): 157-165.

Takemoto D, Rafiqi M, Hurley U, Lawrence GJ, Bernoux M, Hardham AR, Ellis JG, Dodds PN, Jones DA. 2012. N-terminal motifs in some plant disease resistance proteins function in membrane attachment and contribute to disease resistance. *Mol Plant Microbe Interact* **25**(3): 379-392.

Takken FLW, Goverse A. 2012. How to build a pathogen detector: structural basis of NB-LRR function. *Current Opinion in Plant Biology* **15**(4): 375-384.

Taliansky M, Torrance L, Kalinina NO. 2008. Role of plant virus movement proteins. *Methods Mol Biol* **451**: 33-54.

Tameling WI, Nooijen C, Ludwig N, Boter M, Slootweg E, Goverse A, Shirasu K, Joosten MH. 2010. RanGAP2 mediates nucleocytoplasmic partitioning of the NB-LRR immune receptor Rx in the Solanaceae, thereby dictating Rx function. *Plant Cell* **22**(12): 4176-4194.

Tasset C, Bernoux M, Jauneau A, Pouzet C, Briere C, Kieffer-Jacquinod S, Rivas S, Marco Y, Deslandes L. 2010. Autoacetylation of the Ralstonia solanacearum effector PopP2 targets a lysine residue essential for RRS1-R-mediated immunity in Arabidopsis. *PLoS Pathog* **6**(11): e1001202.

Turina M, Kormelink R, Resende RO. 2016. Resistance to Tospoviruses in Vegetable Crops: Epidemiological and Molecular Aspects. *Annu Rev Phytopathol* **54**: 347-371.

van der Vossen EA, Gros J, Sikkema A, Muskens M, Wouters D, Wolters P, Pereira A, Allefs S. 2005. The Rpi-blb2 gene from Solanum bulbocastanum is an Mi-1 gene homolog conferring broad-spectrum late blight resistance in potato. *Plant J* **44**(2): 208-222.

van Wersch S, Li X. 2019. Stronger When Together: Clustering of Plant NLR Disease resistance Genes. *Trends Plant Sci* **24**(8): 688-699.

van Wersch S, Tian, L., Hoy, R., Li, X. . 2020. Plant NLRs: The whistleblowers of plant immunity. *Plant Commun*: doi: https://doi.org/10.1016/j.xplc.2019.100016.

Vos P, Simons G, Jesse T, Wijbrandi J, Heinen L, Hogers R, Frijters A, Groenendijk J, Diergaarde P, Reijans M, Fierens-Onstenk J, de Both M, Peleman J, Liharska T, Hontelez J, Zabeau M. 1998. The tomato Mi-1 gene confers resistance to both root-knot nematodes and potato aphids. *Nat Biotechnol* **16**(13): 1365-1369.

Vossen JH, van Arkel G, Bergervoet M, Jo KR, Jacobsen E, Visser RG. 2016. The Solanum demissum R8 late blight resistance gene is an Sw-5 homologue that has been deployed worldwide in late blight resistant varieties. *Theor Appl Genet* **129**(9): 1785-1796.

Wan L, Essuman K, Anderson RG, Sasaki Y, Monteiro F, Chung EH, Osborne Nishimura E, DiAntonio A, Milbrandt J, Dangl JL, Nishimura MT. 2019. TIR domains of plant immune receptors are NAD(+)-cleaving enzymes that promote cell death. *Science* **365**(6455): 799-803.

Wang A. 2015. Dissecting the molecular network of virus-plant interactions: the complex roles of host factors. *Annu Rev Phytopathol* **53**: 45-66.

Wang J, Chen T, Han M, Qian L, Li J, Wu M, Han T, Cao J, Nagalakshmi U, Rathjen JP, Hong Y, Liu Y. 2020. Plant NLR immune receptor Tm-22 activation requires NB-ARC domain-mediated self-association of CC domain. *PLoS Pathog* **16**(4): e1008475.

Wang J, Hu M, Wang J, Qi J, Han Z, Wang G, Qi Y, Wang HW, Zhou JM, Chai J. 2019a. Reconstitution and structure of a plant NLR resistosome conferring immunity. *Science* **364**(6435).

Wang J, Wang J, Hu M, Wu S, Qi J, Wang G, Han Z, Qi Y, Gao N, Wang HW, Zhou JM, Chai J. 2019b. Ligand-triggered allosteric ADP release primes a plant NLR complex. *Science* **364**(6435).

Wen W, Meinkoth JL, Tsien RY, Taylor SS. 1995. Identification of a signal for rapid export of proteins from the nucleus. *Cell* **82**(3): 463-473.

Wirthmueller L, Zhang Y, Jones JD, Parker JE. 2007. Nuclear accumulation of the Arabidopsis immune receptor RPS4 is necessary for triggering EDS1-dependent defense. *Curr Biol* **17**(23): 2023-2029.

Zhang Y, Li X. 2005. A putative nucleoporin 96 Is required for both basal defense and constitutive resistance responses mediated by suppressor of npr1-1,constitutive 1. *Plant Cell* **17**(4): 1306-1316.

Zhao W, Jiang L, Feng Z, Chen X, Huang Y, Xue F, Huang C, Liu Y, Li F, Liu Y, Tao X. 2016. Plasmodesmata targeting and intercellular trafficking of Tomato spotted wilt tospovirus movement protein NSm is independent of its function in HR induction. *J Gen Virol* **97**(8): 1990-1997.

Zhu M, Jiang L, Bai B, Zhao W, Chen X, Li J, Liu Y, Chen Z, Wang B, Wang C, Wu Q, Shen Q, Dinesh-Kumar SP, Tao X. 2017. The Intracellular Immune Receptor Sw-5b Confers Broad-Spectrum Resistance to Tospoviruses through Recognition of a Conserved 21-Amino Acid Viral Effector Epitope. *Plant Cell* **29**(9): 2214-2232.

Zhu M, van Grinsven IL, Kormelink R, Tao X. 2019. Paving the Way to Tospovirus Infection: Multilined Interplays with Plant Innate Immunity. *Annu Rev Phytopathol* **57**: 41-62.

FIGURE LEGENDS

Fig. 1. Subcellular localization of Sw-5b in *Nicotiana benthamiana* and tomato leaf cells. (a) Schematic diagrams of Sw-5b. (b) Subcellular localizations of free YFP (left), YFP-Sw-5b (middle) and autoactive YFP-Sw-5b^{D857V} mutant (right) in *N. benthamiana* leaf cells at 24 hours post agro-infiltration (hpi). (c) Subcellular localization of free YFP (left), YFP-Sw-5b (middle) and autoactive YFP-Sw-5b^{D857V} mutant (right) in tomato leaf cells at 24 hpi. N nucleus, and C cytoplasm inside the cell are indicated. Bar = 10 μm. (d) Nucleocytoplasmic partitioning analysis of YFP-Sw-5b and autoactive YFP-Sw-5b^{D857V}. Total lysate (T) from p2300S empty vector (EV), YFP-Sw-5b or YFP-Sw-5b^{D857V} expressing leaves were fractionated into cytoplasm and nucleus, and analyzed by immunoblots using antibodies against YFP. The actin and histone were used as a cytoplasm marker and nucleus marker, respectively, in the fractionation analysis. Ponceau S staining was also used as cytoplasm marker.

Fig. 2. Effect of Sw-5b subcellular localization pattern on HR induction. (a) Confocal images of *N. benthamiana* leaf cells transiently expressing NES-YFP-Sw-5b, nes-YFP-Sw-5b, NLS-YFP-Sw-5b or nls-YFP-Sw-5b fusion. The images were taken at 24–36 hpi. N nucleus and C cytoplasm (c). Bar = 10 μm. (b) Induction of HR in *N. benthamiana* leaf tissues co-expressing NSm and one of the five Sw-5b fusion proteins. The infiltrated *N. benthamiana* leaf was photographed at 3 dpi (left image). Induction of HR in the infiltrated tissues were visualized using a trypan blue staining

method (right image). (c) Immunoblot analysis of NES-YFP-Sw-5b, nes-YFP-Sw-5b, NLS-YFP-Sw-5b, and nls-YFP-Sw-5b expressions in the infiltrated *N. benthamiana* leaf tissues. These fusion proteins were enriched using the GFP-Trap beads prior to SDS-PAGE, and the blot was probed using an YFP specific antibody. Ponceau-S staining was used to estimate sample loadings. (d) Time course analysis of ion leakage in Nicotiana benthamiana leaves co-expressing NSm with one of the five Sw-5b fusion proteins. Measurements were performed at 4 h intervals starting from 24 to 48 hpi. Error bars (SEs) were calculated using the results from three biological replicates per treatment collected at each time point.

Fig. 3. The effect of cytoplasm- and nucleus-targeted Sw-5b on viral replication. (a) Schematic representation of binary constructs to express TSWV $SR_{(-)eGFP}$ mini-genome replicon, TSWV L RNA segment containing an optimized RdRp and $NSm^{H93A\&H94A}$ mutant that defected in viral movement. Minus sign (-) and 5′ to 3′ designation represent the negative (genomic)-strand of tospovirus RNA. 35S: a double 35S promoter; HH: hammerhead ribozyme; RZ: hepatitis delta virus (HDV) ribozyme; NOS: nopaline synthase terminator; 35S Ter: a 35S transcription terminator. (b) Accumulation of eGFP fluorescence in *N. benthamiana* leaves co-expressing p2300S empty vector (EV), Sw-5b, NES-Sw-5b, nes-Sw-5b, NLS-Sw-5b, or nls-Sw-5b with TSWV $SR_{(-)eGFP}$, L, and $NSm^{H93A\&H94A}$ at 4 days post infiltration (dpi) viewed with a fluorescence microscope. Bar represents 400 μm. (c) Immunoblot analysis of expression of eGFP proteins in leaves shown in panel (b) using specific

1163 antibodies against YFP. Ponceau S staining of rubisco large subunit is shown for
1164 protein loading control.
1165
1166 **Fig. 4.** Effect of subcellular localization of Sw-5b on cell-to-cell movement of NSm
1167 in leaf epidermis of *N. benthamiana.* (a) Schematic diagram of the binary construct to
1168 co-express mCherry-HDEL and NSm-GFP. (b) Cell-to-cell movement analysis of
1169 NSm-GFP in *N. benthamiana* leaves co-expressing p2300S empty vector (EV), Sw-5b,
1170 NES-Sw-5b, NLS-Sw-5b, or nls-Sw-5b with the construct harboring both
1171 mCherry-HDEL and NSm-GFP. *Agrobacterium* containing the construct to co-express
1172 mCherry-HDEL and NSm-GFP was diluted 500 times for expression in a single
1173 epidermal cell. All other *Agrobacterium* were infiltrated at the concentration of OD_{600}
1174 = 0.2. Bar, 50 μm.
1175
1176 **Fig. 5.** Analysis of cytoplasm- and nucleus-targeted Sw-5b-mediated host immunity
1177 to TSWV systemic infection. (a) TSWV systemic infection in transgenic *N.*
1178 *benthamiana* plants expressing NES-YFP-Sw-5b, nes-YFP-Sw-5b, NLS-YFP-Sw-5b,
1179 nls-YFP-Sw-5b, YFP-Sw-5b or p2300S empty vector (EV) driven by 35S promoter.
1180 TSWV-inoculated plants were photographed at 15 dpi. White arrow indicates the
1181 systemic leaves showing HR trailing. White arrowhead indicates the systemic leaves
1182 showing mosaic. (b) Immunoblot analysis of NES-YFP-Sw-5b, nes-YFP-Sw-5b,
1183 NLS-YFP-Sw-5b, nls-YFP-Sw-5b and YFP-Sw-5b expressions in different transgenic
1184 *N. benthamiana* plants. EV plants transformed with an empty vector and were used as

a negative control. (c) RT-PCR analysis of TSWV accumulation in the systemic leaves of different transgenic *N. benthamiana* plants at 15 dpi.

Fig. 6. Joint effects of cytoplasm- and nucleus-targeted Sw-5b on defenses against tospovirus infection in *Nicotiana benthamiana* leaves. (a) Schematic representation of binary constructs to express TSWV $SR_{(+)eGFP}$-$M_{(-)op}$ and TSWV L RNA segment containing an optimized RdRp. 35S: a double 35S promoter; HH: hammerhead ribozyme; RZ: hepatitis delta virus (HDV) ribozyme; NOS: nopaline synthase terminator. (b) Accumulation of eGFP fluorescence in *N. benthamiana* leaves co-expressing p2300S empty vector (EV), Sw-5b, NES-Sw-5b, NLS-Sw-5b, or NES-Sw-5b+NLS-Sw-5b with TSWV $SR_{(+)eGFP}$-$M_{(-)op}$ at 4 days post infiltration (dpi) viewed with a fluorescence microscope. Bar represents 400 μm. (c) Immunoblot analysis of expression of eGFP proteins in leaves shown in panel (b) using specific antibodies against YFP. Ponceau S staining of rubisco large subunit is shown for protein loading control. (d) Quantification of eGFP proteins in leaves shown in panel (c).

Fig. 7. Functional analysis and subcellular localization patterns of individual or combined Sw-5b domains. (a) Schematic diagrams showing a full length Sw-5b or Sw-5b domains fused with YFP. (b) Confocal images of *N. benthamiana* leaf epidermal cells expressing various YFP fusions. Images of the cells were taken at 24 hpi. N nucleus, Nu nucleolus, and C cytoplasm. Bar = 10 μm. (c) TSWV-inoculated

transgenic *N. benthamiana* plants expressing these various YFP fusions and photographed at 15 dpi.

Fig. 8. Roles of *importins* α and β in YFP-Sw-5b nucleus targeting and Sw-5b-mediated immunity to TSWV systemic infection. (a) Transient expression of YFP-Sw-5b in *N. benthamiana* leaf epidermal cells silenced for *importin* $\alpha 1$ (IMP α1 KD), *importin* $\alpha 2$ (IMP α2 KD), *importin* $\alpha 1$ and $\alpha 2$ (IMP α1 & α2 KD), *importin* β (IMP β KD) or *importin* $\alpha 1$ and $\alpha 2$ and β (IMP α1 & α2 & β KD) through VIGS. Images of the cells were captured using a confocal microscope at 26 hpi. N nucleus, C cytoplasm. Bar = 10 μm. (b) YFP-Sw-5b transgenic *N. benthamiana* plants were silenced for *importin* $\alpha 1$, *importin* $\alpha 2$, *importin* $\alpha 1$ and $\alpha 2$, *importin* β or *importin* $\alpha 1$ and $\alpha 2$ and β expression through VIGS followed by inoculation with TSWV. TSWV-inoculated YFP-Sw-5b transgenic *N. benthamiana* plants were photographed at 15 dpi. White arrowhead indicates HR trailing in systemic leaves.

Fig. 9. A working model for Sw-5b. Sw-5b furcates disease resistances by proper nucleocytoplasmic partition to block different infection steps of tomato spotted wilt tospovirus. Sw-5b switched from the autoinhibited state to an activated state upon recognition of NSm in the cytoplasm. Cytoplasm portion of Sw-5b induce cell death and defense that inhibit viral replication. The activated Sw-5b also translocated into nucleus via *importins* α and β. Nucleus-localized Sw-5b induces a defense that block viral cell-to-cell and long-distance movement. Cytoplasm- and nucleus-localized

1229 Sw-5b have additively effects on defense to inhibit viral replication, intercellular and

1230 long-distance movement during tospovirus infection.

1231

1232 **Supporting Information**

1233 **Short legends**

1234 **Fig. S1** Sw-5b recognizes TSWV NSm in cytoplasm.

1235 **Fig. S2** Analysis of virus replication monitoring system using a TSWV-based
1236 mini-genome replicon and a movement defective NSm mutant.

1237 **Fig. S3** Effects of nes-Sw-5b and nls-Sw-5b on NSm-GFP cell-to-cell movement and
1238 effects of Sw-5b and EV on NSm^{T120N}-GFP cell-to-cell movement.

1239 **Fig. S4** Effects of cytoplasmic and nuclear Sw-5b on host immunity to TSWV
1240 systemic infection.

1241 **Fig. S5** Cytoplasmic and nuclear Sw-5b activity on TSWV-GFP cell-to-cell
1242 movement in *N. benthamiana* leaves.

1243 **Fig. S6** An immunoblot showing the accumulations of various YFP-tagged proteins
1244 expressed in different transgenic *N. benthamiana* plants and RT-PCR analysis of
1245 TSWV accumulation in the systemic leaves.

1246 **Fig. S7** Bimolecular fluorescence complementation (BiFC) assay of cYFP-SD,
1247 cYFP-Sw-5b and nYFP-Importin α1 (nYFP-IMP α1), nYFP-Importin α2 (nYFP-IMP
1248 α2), nYFP-Importin β (nYFP-IMP β) interaction in *N. benthamiana* leaf epidermal
1249 cells.

1250 **Fig. S8** RT-PCR analyses of *importin a1*, *a2* and *b* expressions in the assayed plants
1251 and their effects on TSWV systemic infection.

1252 **Table S1.** List of primers used in this study.

1253 **Table S2.** Response of six different types of transgenic *Nicotiana benthamina* plants
1254 driven by 35S promoter to TSWV infection.

1255 **Table S3.** Response of six different types of transgenic *Nicotiana benthamina* plants
1256 driven by Sw-5b native promoter to TSWV infection.

1257 **Table S4.** Response of six different types of transgenic *Nicotiana benthamina* plants
1258 to TSWV infection.

1259 **Table S5.** Mass spectrum data of YFP-SD

1260 **Table S6.** Mass spectrum data of YFP-Sw-5b

1261

Cytoplasmic and nuclear Sw-5b NLR act both independently and synergistically to dictate full host defense against tospovirus infection

Hongyu Chen[1, ¶], Xin Qian[1, ¶], Xiaojiao Chen[1, ¶], Tongqing Yang[1], Mingfeng Feng[1], Jing Chen[1], Ruixiang Cheng[1], Hao Hong[1], Ying Zheng[1], Yuzhen Mei[4], Danyu Shen[1], Yi Xu[1], Min Zhu[1], Xin Shun Ding[1] and Xiaorong Tao[1, *]

[1] Key Laboratory of Plant Immunity, Department of Plant Pathology, College of Plant Protection, Nanjing Agricultural University, Nanjing 210095, P. R. China.

[2] Huaiyin Institute of Agricultural Sciences of Xuhuai Region in Jiangsu，Huaian 223001, Jiangsu, P. R. China.

[3] College of Plant Protection, Yunnan Agricultural University, Kunming 650201, Yunnan, P. R. China.

[4] State Key Laboratory of Rice Biology, Institute of Biotechnology, Zhejiang University, Hanghzou 310029, P. R. China.

[¶] These authors contributed equally to this work.

Author for correspondence:

Xiaorong Tao

Tel: (+86)-25-84399027

Email: taoxiaorong@njau.edu.cn

RUNNING HEAD

Independent role of cytoplasmic and nuclear Sw-5b in immunity

Word Count: Main body of the text, 8136

Title 18, Summary 249, Keywords 8, Introduction 1286, Materials and Methods 1562, Results 3030, Discussion 1884, Acknowledgments 35, References 3687, Figure Legends 1103, Supporting Information Legends 786

9 Figures (Colors); Supporting information: 8 Supplemental Figures, 6 Supplemental Tables

Summary

- Plant intracellular nucleotide binding-leucine-rich repeat (NLR) receptors play critical roles in mediating host immunity to pathogen attack. We use tomato Sw-5b::tospovirus as a model system to study the specific role of the compartmentalized plant NLR in dictating host defense against virus at different infection steps.
- We demonstrated here that tomato NLR Sw-5b translocates to cytoplasm and nucleus, respectively, to play different roles in inducing host resistances against *Tomato spotted wilt tospovirus* (TSWV) infection. The cytoplasmic Sw-5b functions to induce a strong cell death response to inhibit TSWV replication. This host response is, however, insufficient to block viral intercellular and long-distance movement. The nucleus-localized Sw-5b triggers a host defense that weakly inhibits viral replication but strongly impedes virus intercellular and systemic movement. Furthermore, the cytoplasmic and nuclear Sw-5b act synergistically to dictate full host defense to TSWV infection.
- We further demonstrated that the extended N-terminal *Solanaceae* domain (SD) of Sw-5b plays critical roles in cytoplasm/nucleus partitioning. Sw-5b nucleotide-binding leucine-rich repeat (NB-LRR) controls its cytoplasm localization. Strikingly, the SD but not coil-coil (CC) domain is crucial for Sw-5b receptor to translocate from cytoplasm to nucleus to trigger the immunity. The SD was found to interact with importins. Silencing both importin α and β expression disrupted Sw-5b nucleus translocation and host immunity

against TSWV systemic infection.

- Collectively, our findings suggest that Sw-5b bifurcates disease resistances by cytoplasm/nucleus partitioning to block different infection steps of TSWV. The findings also identified a new regulatory role of extra domain of a plant NLR in mediating host innate immunity.

Keywords:

NLRs, Cytoplasm, Nuclear, Plant innate immunity, Tomato spotted wilt virus, Replication, Cell-to-cell movement and Long distance movement

Introduction

Plant innate immunity plays critical roles in host defense against pathogen invasions, and is triggered by cell-surface receptors or intracellular nucleotide-binding leucine-rich repeat (NLR) receptors (Soosaar *et al.*, 2005; Dodds & Rathjen, 2010; Cui *et al.*, 2015; Li *et al.*, 2015; Jones *et al.*, 2016; Kourelis & van der Hoorn, 2018; Kapos *et al.*, 2019; van Wersch, 2020). Plant intracellular NLRs are the largest classes of resistance proteins that function to detect pathogen effectors, and to activate host immunity upon pathogen attack (Caplan, J *et al.*, 2008; Takken & Goverse, 2012; Li *et al.*, 2015; Jones *et al.*, 2016; Kourelis & van der Hoorn, 2018; Kapos *et al.*, 2019). Plant NLRs typically contain an N-terminal domain, a central nucleotide-binding domain (NB), a nucleotide-binding adaptor (ARC domain shared by Apaf-1, certain resistance proteins, and CED-4), and a C-terminal leucine-rich repeat (LRR) domain (Ea & Jones, 1998; Jones *et al.*, 2016; Ma *et al.*, 2018; Wang *et al.*, 2019a; Wang *et al.*, 2019b; Ma *et al.*, 2020). Based on the differences among the N-terminal domains, plant NLRs can be further divided into two main categories, known as the coiled-coil NLR (refers to as CNL) category and the Toll/interleukin-1 receptor NLR (TNL) category (Meyers *et al.*, 2003; Collier & Moffett, 2009; Qi & Innes, 2013). The CC- or the TIR-domain-bearing NLRs have distinct genetic requirements and can regulate different functions in the downstream of defense signaling (Collier & Moffett, 2009; Qi & Innes, 2013; Horsefield *et al.*, 2019; Jubic *et*

114 *al.*, 2019; van Wersch & Li, 2019; Wan *et al.*, 2019).

115 In addition to classical domains, non-canonical domains were frequently found to
116 integrate into certain NLRs. The additional domain, called BED, was first found in 32
117 poplar NLR proteins (Germain & Seguin, 2011). This extra BED domain was also
118 found in nine rice NLRs (Das *et al.*, 2014). The RATX1/HMA domain in the rice
119 NLRs RGA5 and Pik‐1 was found to act as integrated decoys to detect the cognate
120 pathogen effectors (Kanzaki *et al.*, 2012; Cesari *et al.*, 2013; Cesari *et al.*, 2014). The
121 WRKY domain on Arabidopsis thaliana NLR RRS1 was further found to function as
122 an integrated decoy that recognizes the effectors AvrRps4 and PopP2 (Le Roux *et al.*,
123 2015; Sarris *et al.*, 2015). Genome-wide analyses of plant NLR receptors revealed
124 that about 3.5 % of the NLRs carried specific non-canonical domains (Cesari *et al.*,
125 2014; Kroj *et al.*, 2016; Sarris *et al.*, 2016), and some of these non-canonical domains
126 were shown to be targeted by pathogen effectors during pathogen infections (Sarris *et*
127 *al.*, 2016). However, molecular functions of most non-canonical domains in plant
128 NLRs remain largely unexplored.

129 Translocations of plant NLRs into proper subcellular compartments are critical for
130 the induction of innate immunity (Cui *et al.*, 2015; van Wersch, 2020). Multiple plant
131 NLRs and immune regulators, including tobacco N, Arabidopsis snc1, RRS1/RPS4,
132 barley MLA10, and Arabidopsis EDS1, NPR1, have been shown to accumulate in
133 both cytoplasm and nucleus, and for several nucleocytoplasmic NLRs accumulation
134 in nucleus is required for triggering host resistance to pathogen infections (Deslandes
135 *et al.*, 2003; Burch-Smith *et al.*, 2007; Shen *et al.*, 2007; Wirthmueller *et al.*, 2007;

136 Tasset *et al.*, 2010; Bai *et al.*, 2012; Inoue *et al.*, 2013; Padmanabhan *et al.*, 2013).
137 Wheat Sr33, a homolog of barley MLA10, however, was reported to accumulate in
138 cytoplasm to induce host resistance against stem rust pathogen (Cesari *et al.*, 2016).
139 For potato Rx, a balanced cytoplasm and nucleus accumulation of Rx is needed to
140 induce the host immunity (Slootweg *et al.*, 2010; Tameling *et al.*, 2010). Other studies
141 have shown that *Arabidopsis* Rpm1 (Gao *et al.*, 2011), RPS2 (Axtell & Staskawicz,
142 2003), RPS5 (Qi *et al.*, 2012), rice Pit (Takemoto *et al.*, 2012), and tomato Tm-2^2
143 (Chen *et al.*, 2017; Wang *et al.*, 2020) need to associate with plasma membrane in
144 order to trigger cell death and host immunity. Latest studies have shown that the
145 activated *Arabidopsis* ZAR1 can bind to cellular membrane, leading to a membrane
146 leakage followed by cell death and host immunity (Wang *et al.*, 2019a; Wang *et al.*,
147 2019b). Flax L6 and M have been shown to accumulate in both Golgi apparatus and
148 tonoplast, and these compartmentalized localizations are necessary for the induction
149 of host resistance (Kawano *et al.*, 2014). The re-distribution of potato R3a from
150 cytosol to endosomal compartments is crucial for the induction of host resistance to
151 *Phytophthora infestans* infection (Engelhardt *et al.*, 2012). Different plant NLRs have
152 diverse subcellular localizations for their proper functions. However, how the
153 compartmentalized plant NLRs specifically dictate defense signaling remains largely
154 unknown.

155 Tomato spotted wilt tospovirus (TSWV) is one of most destructive plant NSVs,
156 infecting more than 1000 plant species, and causes crop losses more than one billion
157 US dollars annually worldwide (Kormelink *et al.*, 2011; Scholthof *et al.*, 2011; Oliver

& Whitfield, 2016). Tomato NLR Sw-5b confers strong resistance to TSWV infection and has been widely used in tomato breeding projects to produce tospovirus resistant tomato cultivars (Brommonschenkel *et al.*, 2000; Spassova M I, 2001; Turina *et al.*, 2016; Zhu *et al.*, 2019). Upon recognition of TSWV movement protein, NSm, Sw-5b can trigger a hypersensitive response (HR), which typically associated with localized cell death (Lopez *et al.*, 2011; Hallwass *et al.*, 2014; Peiro *et al.*, 2014; De Oliveira *et al.*, 2016; Zhao *et al.*, 2016; Leastro *et al.*, 2017). Tospoviruses are divided into American and Euro-Asia type based on their geographic distribution and amino acid sequence identity of viral nucleocapsid protein. We have previously shown that Sw-5b can confer a broad-spectrum resistance to American type tospoviruses, including TSWV, through recognition of a conserved 21 amino acid PAMP-like region in the viral movement protein NSm (Zhu *et al.*, 2017). Sw-5b carries an extended N-terminal *Solanaceae* domain (SD), a CC domain, a NB-ARC domain, and a LRR domain (Brommonschenkel *et al.*, 2000; Spassova M I, 2001; Lukasik-Shreepaathy *et al.*, 2012). Similar SDs have also been found in the Mi-1.2, R8, Rpi-blb2, and Hero (Milligan *et al.*, 1998; Vos *et al.*, 1998; Ernst *et al.*, 2002; van der Vossen *et al.*, 2005; Lukasik-Shreepaathy *et al.*, 2012; Vossen *et al.*, 2016). More recently, Seong and others reported that the extended CNL has been evolved initially in the ancestor of *Asterids* and *Amaranthaceae*, predated the *Solanaceae* family (Seong *et al.*, 2020). In the presence of the extended N-terminal SD, Sw-5b is in an autoinhibited state through multilayered interactions between SD, CC, NB-ARC, and LRR domains (Chen *et al.*, 2016). For activation, the extra SD also recognizes NSm.

Sw-5b adopts a two-step NSm recognition strategy through SD and then LRR domain (Li *et al.*, 2019). This two-step recognition mechanism significantly enhances the sensitivity of the detection on TSWV NSm (Li *et al.*, 2019). Although Sw-5b is known to localize in both cytoplasm and nucleus (De Oliveira *et al.*, 2016), the biological roles of the cytoplasm- and the nucleus-accumulated Sw-5b in host immunity signaling are unknown.

In this study, we investigated the subcellular distribution pattern of Sw-5b and the functions of the compartmentalized Sw-5b in the induction of host immunity to TSWV infection. We determined here that cytoplasm- and nucleus-accumulated Sw-5b functions differently in inducing host defense response to inhibit multiple tospovirus infection steps. The cytoplasmic Sw-5b can induce a strong cell death response to suppress TSWV replication, whereas the nucleus-accumulated Sw-5b can induce a strong defense against viral intercellular movement and systemic infection. The combination of cytoplasmic and nuclear Sw-5b induces a synergistic and strong plant immunity against tospovirus infection. We also found that the extended SD functions as the key regulator for this critical intracellular translocation. The SD was also found to interact with importins α and β to mediate Sw-5b nucleus translocation, and to confer the full host immunity against tospovirus infection.

Materials and Methods

Plasmid construction

p2300S-YFP-Sw-5b was from a previously described source (Chen *et al.*, 2016).

Different domains of Sw-5b were PCR-amplified from p2300S-Sw-5b (Chen *et al.*, 2016) and cloned individually behind the *YFP* gene in the p2300S vector using a two-step overlap PCR procedure as described (Li *et al.*, 2019). All the primers used in this study are listed in Table S1.

To visualize the subcellular localization patterns of various fusion proteins, a SV40 T-Ag-derived nuclear localization signal (NLS, QPKKKRKVGG) (Lanford & Butel, 1984) or a PK1 nuclear export signal (NES, NELALKLAGLDINK) (Wen *et al.*, 1995) was fused to the N-terminus of YFP-Sw-5b or the C-terminus of NSm-YFP, as described (Kong *et al.*, 2017), to produce pNES-YFP-Sw-5b, pNLS-YFP-Sw-5b, pNSm-YFP-NES, and pNSm-YFP-NLS, respectively. In addition, YFP-Sw-5b and NSm-YFP were fused individually with a mutant NLS (nls, QPKKTRKVGG) or a mutant NES (nes, NELALKAAGADANK) to produce pnes-YFP-Sw-5b, pnls-YFP-Sw-5b, pNSm-YFP-nes, and pNSm-YFP-nls. The constructs were then transformed individually into *Agrobacterium tumefaciens* strain GV3101 cells.

Transient gene expression, stable plant transformation, and virus inoculation

Nicotiana benthamiana were grown in soil in pots inside a greenhouse maintained at 25°C and a 16 h light/8 h dark photoperiod. Six-to-eight week-old *N. benthamiana* plants were used for various assays. Transient gene expression assays were performed in *N. benthamiana* leaves through agro-infiltration using Agrobacterium cultures carrying specific expressing constructs as described previously (Feng *et al.*, 2016; Ma *et al.*, 2017). Transgenic *N. benthamiana* lines expressing YFP-Sw-5b or its

224 derivatives were made using constructs with a 35S promoter or a Sw-5b native
225 promoter via a standard leaf-disc transformation method (Chen *et al.*, 2016). The
226 resulting transgenic *N. benthamiana* lines were named as NES-YFP-Sw-5b,
227 NLS-YFP-Sw-5b, nes-YFP-Sw-5b, nls-YFP-Sw-5b, YFP-Sw-5b, and EV
228 (transformed with an empty vector), respectively. Inoculation of transgenic *N.*
229 *benthamiana* plants with TSWV was done by rubbing plant leaves with TSWV-YN
230 isolate-infected crude saps as described (Zhu *et al.*, 2017). TRV-mediated VIGS in *N.*
231 *benthamiana* plants was done as described (Ma *et al.*, 2015). The agro-infiltrated or
232 the virus-inoculated plants were growning inside a growth chamber maintained at
233 25/23 °C (day/night) with a 16/8 h light and dark photoperiod.
234
235 **Particle bombardment**
236 The particle bombardment is described (Feng et al., 2016). Briefly, 60 mg Tungsten
237 M-10 microcarrier (Bio-RAD) was placed into a 1.5 ml Eppendorf tube with 1 mL
238 70% ethanol. The tube was vortexes for 3 minutes, and then stood at room
239 temperature for 15 minutes. After centrifuge at low speed for 5 seconds, the
240 supernatant was removed and the pellet was rinsed with 70% ethanol for 3 times. One
241 mL 50% sterile glycerol solution was added and divided Tungsten M-10 microcarrier
242 into 50 µl. Five µg pRTL2-YFP, pRTL2-YFP-Sw-5b or pRTL2-YFP-Sw-5bD857V
243 plasmid DNA, 50 µl of 2.5 M CaCl2, and 20 µl of 0.1 M spermidine, respectively
244 were added and mixed with microcarrier. After centrifuge at low speed for 5 seconds
245 and the supernatant removed. The pellet was resuspended in 200 µl 70% ethanol and

246 centrifugation as described above. Use 48 µl of 100% ethanol to resuspend the
247 tungsten particle::plasmid DNA complexes, and load 15 48 µl mixture onto the center
248 of carrier (Bio-RAD), air dry, and use He/1000 particle transport system (BIO-RAD)
249 to bombard tomato leaves harvested from 3- or 4-week-old of Money Marker. The
250 bombarded leaves were incubated in Petri dishes for 24 hours at 25°C followed with
251 Confocal Microscope analysis.

252

253 **Trypan blue staining**

254 *N. benthamiana* leaves were harvested at 3 days post agro-infiltration (dpai) and
255 boiled for 5 min in a 1.15:1 (v/v) mixed ethanol and trypan blue staining solution (10
256 g phenol, 10 mL glycerol, 10 mL lactic acid, and 20 mg trypan blue in 10 mL distilled
257 water). The stained leaves were then de-stained in a chloral hydrate solution (2.5 g per
258 mL distilled water) as described (Bai *et al.*, 2012).

259

260 **Electrolyte leakage assay**

261 Electrolyte leakage assay was performed as previously described (Mittler *et al.*, 1999;
262 Zhu *et al.*, 2017) with slight modifications. Briefly, five leaf discs (9 mm in diameter
263 each) were taken from the agro-infiltrated leaves per treatment and at various dpai.
264 The harvested leaf discs from a specific treatment were floated on a 10 mL distilled
265 water for 3 h at room temperature (RT), and the conductivity of each bathing water
266 was measured (referred to as value A) using a Multiparameter Meter as instructed
267 (Mettler Toledo, Zurich, Switzerland). After the first measurement, the leaf discs were

268 returned to the bathing water and incubated at 95°C for 25 min. After cooling down to
269 RT, the conductivity of each bathing sample was measured again (referred to as value
270 B). The ion leakage was expressed as the ratio determined by value A/value B × 100.
271 The mean value and standard error of each treatment were calculated using the data
272 from three biological replicates per treatment at each sampling time point.
273
274 **Confocal laser scanning microscopy**
275 Tissue samples were collected from the leaves of transiently expressing YFP-Sw-5b
276 or one of the fusion proteins at 24–36 hours post agro-infiltration (hpai). The collected
277 tissue samples were mounted in water between a glass slide and a coverslip. Images
278 of individual samples were captured under a Carl Zeiss LSM 710 confocal laser
279 scanning microscope. YFP fusions were excited at 488 nm and the emission was
280 captured at 497–520 nm. The resulting images were further processed using the Zeiss
281 710 CLSM software followed by the Adobe Photoshop software (San Jose, CA,
282 USA).
283
284 **Nucleus and cytoplasm fractionations**
285 *N. benthamiana* leaf tissues (1 g per sample), representing a specific treatment, were
286 collected at 24 hpai, frozen in liquid nitrogen, ground to fine powders, and then
287 homogenized in 2 mL (per sample) extraction buffer 1 (20 mM Tris-HCl, pH 7.5, 20
288 mM KCl, 2.5 mM $MgCl_2$, 2 mM EDTA, 25% glycerol, 250 mM sucrose, 1×Protease
289 Inhibitor Cocktail, and 5 mM DTT). The resulting lysate was filtered through 30 μm

filters to remove debris, and the filtrate was centrifuged at 2,000 × *g* for 5 minutes to pellet nuclei. The supernatant from a sample was transferred into a new tube and centrifuged at 10,000 × *g* for 10 min. The resulting supernatant was used as the cytoplasm fraction. The nuclei containing pellet was resuspended in 5 mL extraction buffer 2 (20 mM Tris-HCl, pH 7.4, 25% glycerol, 2.5 mM MgCl2, and 0.2% Triton X-100), centrifuged for 10 min at 2,000 × *g* followed by 4-6 cycles of resuspension and centrifugation as described above. The resulting pellet was resuspended again in 500 μl extraction buffer 3 (20 mM Tris-HCl, pH 7.5, 0.25 M sucrose, 10 mM MgCl2, 0.5% Triton X-100, and 5 mM β-mercaptoethanol). The nuclei fraction was carefully layered on the top of 500 mL extraction buffer 4 (20 mM Tris-HCl, pH 7.5, 1.7 M sucrose, 10 mM MgCl2, 0.5% Triton X-100, 1×Protease Inhibitor Cocktail, and 5 mM β-mercaptoethanol), and then centrifuged at 16,000 × *g* for 1 h. The resulting pellet was resuspended in 500 μL extraction buffer 1 and stored at −80°C until use or used immediately for SDS-PAGE assays. All the processes were performed on ice or at 4°C. In this study, actin and histone H3 were used as the cytoplasmic and the nuclear markers, respectively.

Western blot, co-immunoprecipitation and mass spectrometry analysis

Western blot and co-immunoprecipitation assays were performed as described (Zhu *et al.*, 2017). Briefly, agro-infiltrated leaf samples (1 g per sample) were harvested and homogenized individually in pre-chilled mortars with pestles in 2 mL extraction buffer [10% (v/v) glycerol, 25 mM Tris, pH 7.5, 1 mM EDTA, 150 mM NaCl, 10 mM

312 DTT, 2% (w/v) polyvinylpolypyrrolidone, and 1 × protease inhibitor cocktail (Sigma,
313 Shanghai, China)]. Each crude slurry was transferred into a 2 mL Eppendorf tube, and
314 spun for 2 min at full speed in a refrigerated microcentrifuge. The supernatant was
315 transferred into a clean 1.5 mL Eppendorf tube and spun for 10 min at 4°C. For
316 Western blot assays, 50 μL supernatant from a sample was mixed with 150 μL
317 Laemmli buffer, boiled for 5 min, and analyzed in SDS-PAGE gels through
318 electrophoresis. For immunoprecipitation assays, 1 mL supernatant was mixed with
319 25 μL GFP-trap agarose beads (ChromoTek, Planegg-Martinsried, Germany),
320 incubated for 2 h at 4°C on an orbital shaker, and then pelleted through low speed
321 centrifugation. The blots were probed with a 1:2,500 (v/v) diluted anti-YFP antibody
322 or other specific antibodies followed a 1:10,000 (v/v) diluted horseradish peroxidase
323 (HRP)-conjugated goat anti-rabbit or a goat anti-mouse antibody (Sigma-Aldrich, St.
324 Louis, MO, USA). The detection signal was developed using the ECL substrate kit as
325 instructed (Thermo Scientific, Hudson, NH, USA).

326 For mass spectrometry analysis, the immunoprecipitation samples of YFP-SD
327 and SD without tag were processed by The Beijing Genomics Institute (BGI) for mass
328 spectrometry analysis. The immunoprecipitation samples of YFP-Sw-5b and Sw-5b
329 without tag were processed by Applied Protein Technology in Shanghai. Database
330 searches were performed using the Mascot search engine against *N. benthamiana*.
331 (https://solgenomics.net/organism/Nicotiana_benthamiana/genome).

332

333 **RT-PCR detection of TSWV infection**

Total RNA was extracted from TSWV-inoculated *N. benthamiana* plant leaves using an RNA Purification Kit (Tiangen Biotech, Beijing, China), and then treated with RNase-free DNase I (TaKaRa, Dalian, China). First-strand cDNA was synthesized using a TSWV-specific primer (S3 Table). PCR reactions were as follows: initial denaturation at 94°C for 2 min followed by 35 cycles of 94°C for 30 s, 52°C for 30 s, and 72°C for 1 min. The final extension was 72°C for 10 min. The resulting PCR products were visualized in 1.0% (w/v) agarose gels through electrophoresis.

Results

Determination of Sw-5b subcellular localization pattern

Expression of YFP-Sw-5b in *N. benthamiana* leaves resulted in a strong HR cell death as well as Sw-5b (Chen *et al.*, 2016; Zhu *et al.*, 2017). To investigate the subcellular localization pattern of Sw-5b, we transiently expressed YFP and YFP-Sw-5b in *N. benthamiana* leaves, respectively, through agro-infiltration. Confocal Microscopy results showed that the YFP-Sw-5b fusion accumulated in both cytoplasm and nucleus in *N. benthamiana* leaf cells (Fig. 1b, middle image). This subcellular localization pattern was similar to that of YFP (Fig. 1b, left image). When a D857V mutation, which keeps Sw-5b in an autoactivated state (Chen *et al.*, 2016), was introduced into Sw-5b to produce pYFP-Sw-5b^{D857V} and expressed in *N. benthamiana* leaves, the mutant YFP-Sw-5b^{D857V} fusion also accumulated in both cell cytoplasm and nucleus (Fig. 1b, right image). We also making a construct pNativePro::YFP-Sw-5b

355 expressing YFP-Sw-5b under native Sw-5b promoter. However, the expression of
356 YFP-Sw-5b by native Sw-5b promoter is too low to detect green fluorescence signal.
357 To investigate the subcellular localization pattern of Sw-5b in tomato leaf cells,
358 we transiently expressed YFP, YFP-Sw-5b, and YFP-Sw-5b^{D857V}, respectively,
359 through particle bombardment. Confocal Microscopy results showed that these three
360 proteins exhibited the same subcellular localization pattern as that in the *N.*
361 *benthamiana* leaf cells (Fig. 1c).
362 To further confirm the above results, we harvested *N. benthamiana* leaves
363 expressing YFP-Sw-5b or YFP-Sw-5b^{D857V} and analyzed by cytoplasm and nucleus
364 fractionation assay. Leaf samples agro-infiltrated with the empty vector (p2300S)
365 were also harvested and used as controls. Analyses of total protein, cytoplasm
366 fractions, and nucleus fractions from these harvested leaves using Western blot assays
367 showed that both YFP-Sw-5b and YFP-Sw-5b^{D857V} were accumulated in the
368 cytoplasm and nucleus (Fig. 1d).
369
370 **Sw-5b recognizes TSWV NSm in the cytoplasm**
371 TSWV NSm is known to reside in cytoplasm and plasmodesmata, but not in nucleus
372 (Kormelink *et al.*, 1994; Feng *et al.*, 2016). To determine where Sw-5b can recognize
373 TSWV NSm, we fused a NES, a nes, a NLS or a nls signal peptide to the C-terminus
374 of NSm-YFP to produce NSm-YFP-NES, NSm-YFP-nes, NSm-YFP-NLS, and
375 NSm-YFP-nls, respectively. Transient expressions of these fusions in *N. benthamiana*
376 leaves showed that NSm-YFP-NES accumulated exclusively in the cytoplasm, while

377 NSm-YFP-NLS accumulated in the nucleus (Fig. S1a). As expected, NSm-YFP-nes
378 and NSm-YFP-nls showed the same accumulation pattern as that of NSm-YFP (Fig.
379 S1a). When Sw-5b was co-expressed with one of the above four fusions in *N.*
380 *benthamiana* leaves through agro-infiltration, the leaf tissues co-expressing Sw-5b
381 and NSm-YFP-NES (Sw-5b + NSm-YFP-NES), Sw-5b and NSm-YFP-nes (Sw-5b +
382 NSm-YFP-nes), or Sw-5b and NSm-YFP-nls (Sw-5b + NSm-YFP-nls) developed a
383 strong HR cell death (Fig. S1b). In contrast, the leaf tissues co-expressing Sw-5b and
384 NSm-YFP-NLS (Sw-5b + NSm-YFP-NLS) did not. Western blot assays using a YFP
385 specific antibody confirmed that all the assayed proteins were expressed in the
386 infiltrated tissues (Fig. S1c), indicating that Sw-5b recognizes NSm in the cytoplasm.
387
388 **Sw-5b activity in cell death induction is enhanced in the cytoplasm but**
389 **suppressed in the nucleus**
390 To investigate the roles of the cytoplasmic and nuclear Sw-5b in the induction of cell
391 death and host immunity, we produced constructs to express YFP-Sw-5b,
392 NLS-YFP-Sw-5b, nls-YFP-Sw-5b, NES-YFP-Sw-5b, and nes-YFP-Sw-5b,
393 respectively, and then tested their abilities to elicit cell death and host immunity to
394 tospovirus infection. Transient expressions of these fusions in *N. benthamiana* leaves
395 showed that NES-YFP-Sw-5b accumulated exclusively in the cytoplasm, while
396 NLS-YFP-Sw-5b accumulated only in the nucleus (Fig. 2a). In addition,
397 nes-YFP-Sw-5b and nls-YFP-Sw-5b showed the same accumulation pattern as that
398 shown by YFP-Sw-5b. We then tested cell death induction through co-expressions of

399 NSm and YFP-Sw-5b (NSm + YFP-Sw-5b), NSm and NES-YFP-Sw-5b (NSm +
400 NES-YFP-Sw-5b), NSm and nes-YFP-Sw-5b (NSm + nes-YFP-Sw-5b), NSm and
401 NLS-YFP-Sw-5b (NSm + NLS-YFP-Sw-5b), or NSm and nls-YFP-Sw-5b (NSm +
402 nls-YFP-Sw-5b) in *N. benthamiana* leaves through agro-infiltration. Results of this
403 study showed that the NSm + NES-YFP-Sw-5b-induced cell death was stronger than
404 that induced by NSm + nes-YFP-Sw-5b or NSm + nls-YFP-Sw-5b co-expression (Fig.
405 2b). In addition, the cell death induced by NSm + NLS-YFP-Sw-5b co-expression
406 was suppressed (Fig. 2b). Western blot results showed that the stronger cell death
407 caused by NSm + NES-YFP-Sw-5b co-expression was not due to a greater
408 accumulation of NES-YFP-Sw-5b in the leaves (Fig. 2c). The ion leakage assay
409 results (Fig. 2d) agreed with the phenotype observation results, and indicated that
410 co-expression of NSm + NES-YFP-Sw-5b in leaves lead to a greater ion leakage
411 compared with that induced by the co-expression of NSm + nes-YFP-Sw-5b at 24 and
412 48 hours post agro-infiltration (hpai). The ion leakage caused by the co-expression of
413 NSm + NLS-YFP-Sw-5b was significantly weaker than that caused by the
414 co-expression of NSm + nls-YFP-Sw-5b (Fig. 2d).
415
416 **Cytoplasmic Sw-5b induces a strong host defense against tospovirus replication**
417 Virus infection in plant starts with virus replication in the initially infected cells
418 followed by spreading into adjacent cells for further infection. To monitor tospovirus
419 replication in plant cells, we recently developed a TSWV mini-replicon-based reverse
420 genetic system (Feng et al., 2020). In this study, co-expression of TSWV

421 mini-replicon $SR_{(+)eGFP}$, $L_{(+)opt}$ (with a codon usage optimized RdRp), VSRs and NSm
422 resulted in a cell-to-cell movement of $SR_{(+)eGFP}$. In contrast, co-expression of $SR_{(+)eGFP}$,
423 $L_{(+)opt}$, VSRs, and $NSm^{H93A\&H94A}$ mutant, a defective movement protein but can be
424 recognized by Sw-5b to cause a strong HR (Li *et al.*, 2009; Zhao *et al.*, 2016), in cells
425 resulted in the expression of $SR_{(+)eGFP}$ in only single cells (Fig. S2), thus dissecting the
426 viral replication from viral cell-to-cell movement. We then co-expressed $SR_{(+)eGFP}$,
427 $L_{(+)opt}$, VSRs, $NSm^{H93A\&H94A}$ mutant and one of the five proteins (i.e., Sw-5b,
428 NES-Sw-5b, nes-Sw-5b, NLS-Sw-5b, nls-Sw-5b) in *N. benthamiana* leaves. Leaves
429 co-expressing $SR_{(+)eGFP}$, $L_{(+)opt}$, VSRs, $NSm^{H93A\&H94A}$ mutant and p2300 (empty vector,
430 EV) were used as controls. The results showed that in the presence of Sw-5b or one of
431 its derivatives, the expression of $SR_{(+)eGFP}$ was strongly suppressed compared with
432 that expressed in the presence of EV (Fig. 3a). It is noteworthy that the expression of
433 $SR_{(+)eGFP}$ was less inhibited in the presence of NLS-Sw-5b (Fig. 3a). Western blot
434 result indicated that the GFP accumulation of $SR_{(+)eGFP}$ was strongly inhibited in the
435 presence of Sw-5b, NES-Sw-5b, nes-Sw-5b or nls-Sw-5b compared with that
436 expressed in the presence of NLS-Sw-5b or EV (Fig. 3b). This finding indicates that
437 the cytoplasmic Sw-5b can inhibit $SR_{(+)eGFP}$ expression, possibly through induction of
438 a host defense against TSWV replication.
439
440 **Sw-5b induces a host defense against viral NSm intercellular movement**
441 In our previous study, we used pmCherry-HDEL//NSm-GFP vector (Fig. 4a) to
442 investigate TSWV NSm cell-to-cell movement (Feng *et al.*, 2016). The expressed

443 mCherry-HDEL binds ER membrane in the initial cells but NSm-eGFP traffics
444 between cells. To investigate whether the Sw-5b-induced host defense can affect
445 TSWV NSm cell-to-cell movement, we co-expressed mCherry-HDEL, NSm-GFP,
446 and Sw-5b or mCherry-HDEL, NSm-GFP, and EV in *N. benthamiana* leaves through
447 agro-infiltration. Under the fluorescence microscope, both NSm-GFP and
448 mCherry-HDEL were found in single cells in the presence of Sw-5b. In the presence
449 of EV, however, NSm-GFP moved into multiple cells, while mCherry-HDEL
450 accumulated in the initial cells (Fig. 4b, upper two panels). The result suggested that
451 Sw-5b elicited a defense that strongly inhibited cell-to-cell movement of viral NSm.
452 To make sure this inhibition to viral NSm cell-to-cell movement is not caused by
453 overexpression of Sw-5b, we also used the NSm^{T120N} mutant, from the resistance -
454 breaking (RB) TSWV isolates, which cannot be recognized by Sw-5b (Zhao et al.,
455 2016). The assays showed that in the presence of either Sw-5b or EV, NSm^{T120N}-GFP
456 moved into multiple cells, while mCherry-HDEL retained in the initial cells (Fig S3a).
457

458 **Sw-5b in the nucleus but not in the cytoplasm triggers a defense against NSm**
459 **cell-to-cell movement**

460 To determine the effects of the cytoplasmic and nuclear Sw-5b on host defense against
461 TSWV NSm intercellular movement, we co-expressed mCherry-HDEL and
462 NSm-GFP with NES-Sw-5b, nes-Sw-5b, NLS-Sw-5b, or nls-Sw-5b in *N.*
463 *benthamiana* leaves via agro-infiltration. The results showed that in the presence of
464 NLS-Sw-5b, the cell-to-cell movement of NSm-GFP was inhibited (Fig. 4b). Similar

results were also obtained in the leaves co-expressing mCherry-HDEL and NSm-GFP with nls-YFP-Sw-5b or nes-YFP-Sw-5b (Fig S3b). In the presence of NES-YFP-Sw-5b, however, NSm-GFP did move into surrounding cells. (Fig. 4b). This finding indicates that the Sw-5b in the nucleus but not in the cytoplasm induced a host defense that inhibited TSWV NSm cell-to-cell movement.

Nuclear Sw-5b confers host immunity to TSWV systemic infection

To dissect the host immunity induced by the cytoplasmic and the nuclear Sw-5b, we generated transgenic *N. benthamiana* lines expressing YFP-Sw-5b, NES-YFP-Sw-5b, nes-YFP-Sw-5b, NLS-YFP-Sw-5b, and nls-YFP-Sw-5b, respectively (Tables S1 and S2). After inoculation of these transgenic lines with TSWV-YN isolate, the EV (control) transgenic plants developed typical viral symptoms including stunt, leaf curl and mosaic at 7 to 15 days post inoculation (dpi). The NES-YFP-Sw-5b transgenic plants developed a strong HR trailing in the systemic leaves by 7 to 15 days post inoculation (dpi) (Fig. 5a and Fig. S4a), suggesting that NES-YFP-Sw-5b transgenic plant did not block TSWV systemic infection and caused virus infection-related systemic HR. In contrast, no systemic virus infection symptoms were observed in the YFP-Sw-5b and the nes-YFP-Sw-5b transgenic plants. The RT-PCR agreed with the symptom observation results and showed that TSWV-YN genomic RNA was accumulated in the systemic leaves of the TSWV-YN-inoculated NES-YFP-Sw-5b or the EV transgenic plants, but not in the systemic leaves of the TSWV-YN-inoculated YFP-Sw-5b or nes-YFP-Sw-5b transgenic plants (Fig. 5c and Fig. S4b). Also in this

study, the TSWV-YN-inoculated NLS-YFP-Sw-5b or nls-YFP-Sw-5b transgenic plants did not show virus like symptoms in their systemic leaves by 7-15 dpi (Fig. 5a, and Fig. S4a). The RT-PCR result confirmed that TSWV-N genomic RNA had not accumulated in the systemic leaves of the NLS-YFP-Sw-5b or the nls-YFP-Sw-5b transgenic plants (Fig. 5c, and Fig. S4b), indicating that the nuclear Sw-5b is responsible for the host immunity against TSWV systemic infection.

The cytoplasmic and the nuclear Sw-5b act synergistically to confer a strong immunity to TSWV infection in *N. benthamiana*

To investigate whether cytoplasm-targeted and nucleus-targeted Sw-5b have joint effects on the defense against TSWV infection, we constructed a $M_{(-)opt}$-$pSR_{(+)eGFP}$ vector by inserting a cassette expressing optimized TSWV M genomic sequence (Feng *et al.*, 2020) into the $pSR_{(+)eGFP}$ mini-replicon to express NSm, N, and eGFP simultaneously in the same cells (Fig. 6a). The construct $M_{(-)opt}$-$pSR_{(+)eGFP}$ couples the functions for both viral replication and viral cell-to-cell movement, mimicking the virus infection in plant leaves. After co-expressing this vector, the $L_{(+)opt}$ and the EV in *N. benthamiana* leaves through agro-infiltration, the eGFP fluorescence was observed in many cells, due to the presence of the NSm movement protein and the $RdRp_{opt}$ (Fig. 6b, upper left image). When $M_{(-)opt}$-$SR_{(+)eGFP}$, $L_{(+)opt}$ and Sw-5b were co-expressed in *N. benthamiana* leaves, the eGFP fluorescence was hardly detected and some were observed only in single leaf cells (Fig. 6b upper right image, Fig. S5a and b). When $M_{(-)opt}$-$SR_{(+)eGFP}$, $L_{(+)opt}$ and NES-Sw-5b were co-expressed in *N. benthamiana* leaves,

509 the eGFP fluorescence was observed in clusters of a few cells (Fig. 6b, Fig. S5a),
510 indicating that limited cell-to-cell movement had occurred in these leaves (Fig. S5b).
511 When $M_{(-)opt}$-$SR_{(+)eGFP}$, $L_{(+)opt}$ and NLS-Sw-5b were co-expressed in leaves, a few of
512 eGFP fluorescence were detected but they were in single cells only. When leaves
513 co-expressing $M_{(-)opt}$-$SR_{(+)eGFP}$, $L_{(+)opt}$ and NES-Sw-5b + NLS-Sw-5b, the eGFP
514 fluorescence was also hardly detected and some were observed only in single leaf
515 cells. Western blot results showed that more eGFP had accumulated in the leaves
516 co-expressing $M_{(-)opt}$-$SR_{(+)eGFP}$, $L_{(+)opt}$, and EV, followed by the leaves co-expressing
517 $M_{(-)opt}$-$SR_{(+)eGFP}$, $L_{(+)opt}$, and NLS-Sw-5b, and then the leaves co-expressing
518 $M_{(-)opt}$-$SR_{(+)eGFP}$, $L_{(+)opt}$, and NES-Sw-5b. Much less eGFP had accumulated in the
519 leaves co-expressing $M_{(-)opt}$-$SR_{(+)eGFP}$, $L_{(+)opt}$, and NLS-Sw-5b + NES-Sw-5b, and in
520 the leaves co-expressing $M_{(-)opt}$-$SR_{(+)eGFP}$, $L_{(+)opt}$, and Sw-5b (Fig. 6c and d). The
521 accumulation of eGFP was lower in the leaves co-expressing NES-Sw-5b +
522 NLS-Sw-5b than that in the leaves co-expressing NES-Sw-5b or NLS-Sw-5b (Fig. 6c
523 and d), indicating that NES-Sw-5b and NLS-Sw-5b have additive role in mediating
524 host immunity against different TSWV infection steps.
525
526 **The Sw-5b NB-ARC-LRR control its cytoplasm localization whereas the**
527 **extended N-terminal SD domain is crucial for targeting Sw-5b into nucleus, and**
528 **for inducing host systemic immunity**
529 Sw-5b has an extended N-terminal SD domain, a CC domain, a NB-ARC domain, and
530 a C-terminal LRR domain (Chen *et al.*, 2016). To determine which domain(s) of

Sw-5b is/are responsible for nucleoplasm/nucleolus targeting and for plant immunity, we tested these domains using various deletion mutants and YFP fusion proteins (Fig. 7a). We reported previously that the Sw-5b NB-ARC-LRR region was able to induce HR cell death in plant in the presence of NSm (Chen *et al.*, 2016). In this study, we fused YFP to the N-terminus of NB-ARC-LRR (Fig. 7a). Transient expression of YFP-NB-ARC-LRR (112 kDa) in *N. benthamiana* leaf cells resulted in a localization of the fusion protein in cytoplasm exclusively (Fig. 7b).

A previous study had shown that the CC domain of potato NLR receptor Rx was required for targeting this protein to nucleus (Slootweg *et al.*, 2010). To determine the function of Sw-5b CC domain in intracellular trafficking, we inserted the CC domain between the YFP and NB-ARC-LRR to generate an YFP-CC-NB-ARC-LRR construct or fused the CC domain to YFP to produce an YFP-CC construct. Transient expression of these two fusion proteins individually in *N. benthamiana* leaves, and examined the leaves under a confocal microscope, we determined that the YFP-CC fusion protein accumulated in both cytoplasm and nucleus of the cells while the YFP-CC-NB-ARC-LRR fusion protein was in the cytoplasm only (Fig. 7b). This result indicated that addition of the CC domain to YFP-NB-ARC-LRR was not sufficient to traffic the fusion protein into the nucleus.

An extended N-terminal SD domain is known to be present at the upstream of the Sw-5b CC domain. In this study, we first generated an YFP-SD and an YFP-SD-CC constructs, and transiently expressed them individually in *N. benthamiana* leaf cells. Confocal Microscopy showed that both YFP-SD and YFP-SD-CC fusion proteins

553 accumulated in the cytoplasm and nucleus (Fig. 7b). We then inserted a SD between
554 the YFP and CC-NB-ARC-LRR to produce an YFP-SD-CC-NB-ARC-LRR
555 construction. Transient expression of this construct in *N. benthamiana* leaf cells
556 showed that this fusion protein accumulated in the cytoplasm and nucleus (Fig. 7b).

557 We next generated stable transgenic *N. benthamiana* plants expressing
558 YFP-NB-ARC-LRR, YFP-CC-NB-ARC-LRR and YFP-SD-CC-NB-ARC-LRR.
559 Upon inoculation transgenic *N. benthamiana* plants expressing YFP-NB-ARC-LRR
560 with TSWV, large HR foci were observed in the TSWV-inoculated leaves and later,
561 HR trailing was seen in the systemic leaves of most assayed plants (Fig. 7c; Table S2
562 and S3). RT-PCR results confirmed the presence of TSWV genomic RNA in these
563 systemic leaves (Fig. S6b). We also inoculate *N. benthamiana* plants expressing
564 YFP-CC-NB-ARC-LRR with TSWV. By 7 dpi, no systemic resistance to TSWV
565 infection was observed in these plants (Fig. 6a and B, Table S4). RT-PCR results
566 showed that systemic infection of TSWV did occur in the TSWV-inoculated
567 YFP-CC-NB-ARC-LRR transgenic plants (Fig. S6b). In contrast, transgenic plants
568 expressing YFP-SD-CC-NB-ARC-LRR fusion exhibited a systemic immunity to
569 TSWV infection (Fig. 7c, Fig. S6b).

570 These data indicated that Sw-5b NB-ARC-LRR control its cytoplasm localization,
571 CC domain of Sw-5b alone was not sufficient to transport the NB-ARC-LRR into
572 nucleus and the extended SD domain is required for targeting Sw-5b to the nucleus,
573 and for inducing host immunity.

574

The extended SD domain interacted with *importin α1*, *α2* and *β*

To identify the cellular machinery needed for transporting Sw-5b into nucleus, we co-expressed YFP-SD and YFP-Sw-5b in *N. benthamiana* leaves followed by a co-immunoprecipitation (co-IP) and Mass Spectrometry. The results identified *N. benthamiana* importin α as one of candidate proteins interacted with YFP-SD and YFP-Sw-5b (Table S5 and S6). The co-IP and Mass Spectrometry also identified nuclear pore complex protein TPRb and nuclear pore complex protein Nup160a interacted with YFP-Sw-5b (Table S6). *Importins* play important roles in translocating proteins from cytoplasm into nucleus (Kanneganti *et al.*, 2007). We used BiFC analysis to confirm the interaction between YFP-SD with *N. benthamiana* importin homologs α1, α2 and *β*. The result showed that co-expression of cYFP-SD with nYFP-IMP α1, nYFP-IMP α2 or nYFP-IMP *β* produced a strong YFP fluorescence signal in nucleus. Co-expression of cYFP-Sw-5b with nYFP-IMP α1, nYFP-IMP α2 or nYFP-IMP *β* also detected a strong YFP fluorescence signal in nucleus (Fig. S7). In contrast, co-expression of controls cYFP-SD and nYFP, cYFP-Sw-5b and nYFP, cYFP and nYFP-IMP α1, cYFP and nYFP-IMP α2 or cYFP and nYFP-IMP *β* did not show fluorescence signal in *N. benthamiana* leaf cells (Fig. S7).

Silencing *importin α1*, *α2* and *β* expression abolished Sw-5b nucleus accumulation and host resistance to TSWV systemic infection

To determine the functions of importin α1, α2 and β in Sw-5b nucleus localization, we

597 silenced *importin α1, α2, β, α1* and *α2,* and *α1* and *α2* and *β* expressions, respectively,
598 in *N. benthamiana* leaves using a tobacco rattle virus (TRV)-based virus-induced gene
599 silencing (VIGS) vector, and then transiently expressed YFP-Sw-5b in these plants.
600 Analyses of these plants through RT-PCR using gene specific primers showed that
601 silencing of these *importin* genes in *N. benthamiana* leaves were successful (Fig.
602 S8a). However, silencing individual *importin* gene or both *importin α1* and *α2* was
603 not enough to block the nucleus accumulation of YFP-Sw-5b (Fig. 8a). In contrast,
604 after *importin α1*, *α2* and *β* were all silenced through VIGS, the nucleus accumulation
605 of YFP-Sw-5b was inhibited (Fig. 8a, the middle image in the bottom panel).

606 To investigate the effects of nuclear import defected Sw-5b on host immunity to
607 TSWV systemic infection, we silenced these *importin* genes in the Sw-5b transgenic
608 *N. benthamiana* plants as described above, and then inoculated them with TSWV. The
609 results showed that the plants silenced for *importin α1*, *α2*, and *β* gene, individually,
610 did not show TSWV systemic infection (Fig. 8b and Fig. S8b). In addition, the
611 transgenic plants silenced for both *importin α1* and *α2* genes also did not show
612 TSWV systemic infection (Fig. 8b and Fig. S8b). In contrast, after silencing *importin*
613 *α1*, *α2* and *β* together, the plants developed clear TSWV symptoms in systemic
614 leaves followed by HR (Fig. 8b, white arrow and Fig. S8b), indicating that the nucleus
615 accumulation of Sw-5b is indispensable for the induction of host immunity against
616 TSWV systemic infection.

617

618 **Discussion**

In this report, we provide evidence to show that the cytoplasm-accumulated and the nucleus-accumulated Sw-5b, a tomato immune receptor, play different roles in inducing host defense against TSWV infection in plant. The cytoplasmic Sw-5b functions to induce a strong cell death response to inhibit TSWV replication. This host response is, however, insufficient to block virus intercellular and long-distance movement. The nuclear-localized Sw-5b triggers a host defense that weakly inhibit viral replication but strongly inhibit tospovirus intercellular and systemic movement. These findings suggest that tomato Sw-5b NLR induces different types of defense responses by cytoplasm and nucleus partitioning to combat virus at different infection steps. Furthermore, the cytoplasmic and the nuclear Sw-5b act synergistically to confer a strong host immunity to TSWV infection in plant. We also demonstrated that the extra SD domain functioned as a critical intracellular translocation modulator, allowing Sw-5b receptor to translocate from cytoplasm to nucleus to trigger the immunity. The Sw-5b NB-LRR controls its cytoplasm localization. Unlike Rx CC domain, Sw-5b CC domain is not sufficient to translocate NB-LRR into nucleus. Strikingly, the SD is crucial for Sw-5b to translocate from cytoplasm for nucleus. This SD-mediated receptor translocation is dependent on importins α and β.

Successful virus infection in plant requires several steps including viral replication in the initially infected cells followed by cell-to-cell and long-distance movement (Heinlein, 2015; Wang, 2015). After entering into plant cells, virus first encode multiple proteins needed for its replication. Once the initial replication is established, virus will encode specific protein(s), known as movement proteins (MPs), to traffic

641 viral genome or virions into adjacent cells through plasmodesmata in cell walls, and
642 then long-distantly into other parts of the plant to cause a systemic infection (Rao,
643 2002; Lucas, 2006; Taliansky *et al.*, 2008). To date, multiple plant NLRs, conferring
644 host resistance against plant viruses have been identified (Soosaar *et al.*, 2005; Meier
645 *et al.*, 2019), but how these plant NLRs induce host resistance against virus infection
646 remain largely unknown.

647 In this study, we have determined that the forced cytoplasm accumulation of
648 Sw-5b can induce a stronger cell death than that caused by the accumulation of Sw-5b
649 in both cytoplasm and nucleus. While, the cell death induced by the forced nucleus
650 accumulation of Sw-5b was significantly weakened. We then analyzed
651 Sw-5b-mediated immunity against TSWV replication using a TSWV mini-replicon
652 system and a movement defective NSm mutant. Our results showed that the forced
653 cytoplasm accumulation of Sw-5b can induce a strong host defense against virus
654 replication in cells. This finding implies that cytoplasm is one of the main source of
655 defense signaling against TSWV replication. The defense signaling generated in
656 nucleus can only induce a weak defense against TSWV replication. Therefore, the
657 nuclear localized Sw-5b is only partially responsible for the induction of host defense
658 against TSWV replication. It is also possible that this nuclear localized
659 Sw-5b-induced weak host response is caused by a trace of NLS-YFP-Sw-5b
660 maintained in the cytoplasm that maybe below the detection limit of Confocal
661 Microscope. It has been shown to accumulate in both cytoplasm and nucleus, and the
662 forced cytoplasm accumulation of Barley MLA10 enhance cell death signaling (Bai *et*

663 *al.*, 2012). We speculate that, for both MLA10 and Sw-5b, the cytoplasm
664 accumulation is crucial for the initiation and/or amplification of the cell death
665 signaling. The CC and the TIR domain of several plant NLRs have been shown to
666 trigger cell death (Swiderski *et al.*, 2009; Krasileva *et al.*, 2010; Bernoux *et al.*, 2011;
667 Collier *et al.*, 2011; Maekawa *et al.*, 2011; Bai *et al.*, 2012; Chen *et al.*, 2017; Wang
668 *et al.*, 2020). Analyses of the three dimensional structures of Arabidopsis ZAR1
669 resistosome have also shown that its CC domain can form pentamer structures that
670 was able to target into host cell membranes, leading to ion leakage and cell death
671 (Wang *et al.*, 2019a; Wang *et al.*, 2019b). We speculate that cell death likely cause the
672 toxicity on viral replicase or other proteins associated with virus replication in cells.

673 Plant virus encodes specific movement protein(s) to traffic viral genome between
674 cells and then leaves to cause systemic infection (Rao, 2002; Lucas, 2006; Taliansky
675 *et al.*, 2008). We reported previously that TSWV NSm alone can move between plant
676 cells (Feng *et al.*, 2016). In this study, we investigated the effect of the
677 Sw-5b-mediated host defense on TSWV intercellular movement. Through this study,
678 we have determined that after the recognition of NSm, Sw-5b receptor induced a
679 strong reaction to block NSm intercellular trafficking. Previous reports have some
680 indications on the role of plant NLRs in viral movement. Nevertheless it has no direct
681 evidence showing that plant NLRs induce resistance against viral movement. Deom
682 and colleagues had shown that the 9.4-kDa fluorescein isothiocyanate-labeled dextran
683 was unable to move between cells in the transgenic tobacco *N* leaves expressing
684 tobacco mosaic virus (TMV) movement protein at 24°C, an HR-permissive

685 temperature (Deom *et al.*, 1991). However, that study did not involve a TMV Avr
686 protein. In a different report, TMV-GFP showed a limited cell-to-cell movement in
687 leaves of tobacco cv. Sumsan NN at 33°C, an HR-nonpermissive temperature (Canto
688 & Palukaitis, 2002). Li and colleagues found that after treatment of SMV-inoculated
689 Jidou 7 resistant plants with a callose synthase inhibitor, the plants showed enlarged
690 HR lesions (Li *et al.*, 2012). The soybean *Rsv3* induced extreme resistance. However,
691 after this extremely resistant soybean line was treated with a callose synthase inhibitor,
692 the plants developed HR lesions upon SMV-G5H inoculation (Seo *et al.*, 2014). These
693 reports indicate that plant NLRs likely involves the defense against viral movement.
694 Here we provide the direct evidence that Sw-5b NLR can induce a strong defense
695 response to impede NSm intercellular trafficking. More importantly, we have
696 determined that the induction of host immunity to TSWV intercellular movement
697 requires the accumulation of Sw-5b in nucleus. Although the cytoplasmic Sw-5b can
698 induce a strong cell death response, it cannot prevent TSWV NSm cell-to-cell
699 movement. Consequently, we propose that nucleus is a key compartment to generate
700 defense signaling to block TSWV cell-to-cell movement.

701 In this study, although the NES-YFP-Sw-5b transgenic *N. benthamiana* plants
702 showed an HR, they were unable to stop TSWV systemic infection. We also showed
703 that Sw-5b YFP-NB-ARC-LRR (112 kDa) accumulates in cytoplasm exclusively (Fig.
704 7b), however, transgenic *N. benthamiana* plants expressing YFP-NB-ARC-LRR show
705 strong systemic HR trailing caused by TSWV infection. Based on these findings, we
706 conclude that HR cell death alone is not sufficient to block TSWV long-distance

707 movement. In our study, the NLS-YFP-Sw-5b transgenic plants were resistant to
708 TSWV systemic infection. After silencing the expressions of *importin α1*, *α2* and *β*
709 simultaneously to inhibit the nucleus accumulation of Sw-5b, however, the resistance
710 to TSWV systemic infection was abolished. These findings indicate that the
711 Sw-5b-mediated resistance signaling against viral systemic infection is generated in
712 nucleus. Some plant NLRs are known to interact with specific transcription factors in
713 nucleus upon recognition of pathogen effectors (Cui *et al.*, 2015; Kapos *et al.*, 2019).
714 The immune regulator EDS1 has also been shown to accumulate in nucleus to
715 reprogram RNA transcription (Garcia *et al.*, 2010; Heidrich *et al.*, 2011; Cui *et al.*,
716 2015; Lapin *et al.*, 2020). How Sw-5b regulates host immunity in nucleus requires
717 further investigations.

718 Several plant immune receptors and immune regulators, including, e.g. potato Rx
719 (Slootweg *et al.*, 2010; Tameling *et al.*, 2010), tobacco N (Burch-Smith *et al.*, 2007;
720 Caplan, JL *et al.*, 2008), barley MLA10 (Shen *et al.*, 2007), Arabidopsis
721 RRS1-R/RPS4, and snc1 (Deslandes *et al.*, 2003; Wirthmueller *et al.*, 2007; Cheng *et*
722 *al.*, 2009), as well as Arabidopsis NPR1 (Katagiri & Tsuda, 2010), and EDS1 (Lapin
723 *et al.*, 2020) have been found to be nucleocytoplasmic. For some of them, nuclear
724 accumulation of NLRs are required for the induction of plant immunity to pathogen
725 attacks. Moreover, the MLA10-YFP-NES fusion was found to induce a strong cell
726 death response, but not a strong host resistance to powdery mildew fungus infection.
727 In contrast, the MLA10-YFP-NLS fusion inhibited its activity to induce a cell death
728 response, but caused a host immunity to this pathogen (Bai *et al.*, 2012). In many

729 plant-pathogen interactions, cell death responses can be uncoupled from disease
730 resistance (Bendahmane *et al.*, 1999; Gassmann, 2005; Coll *et al.*, 2010; Heidrich *et*
731 *al.*, 2011). This separation raises questions about how host resistance prevents
732 pathogen invasion and what are the roles of cell death during pathogen infection. It is
733 unclear whether the MLA10-YFP-NES-induced cell death has some inhibitory effects
734 on powdery mildew fungus infection. In this study, we determined that cytoplasm-
735 and nuclear-accumulation of Sw-5b have different functions. The
736 cytoplasm-accumulated Sw-5b induces a strong defense against virus replication,
737 whereas the nuclear-accumulated Sw-5b induced an inhibition of virus cell-to-cell and
738 long distance movement. Both cytoplasmic and nuclear Sw-5b are needed to confer a
739 synergistic and full defense against tospovirus infection.

740 We have also determined that Sw-5b NB-ARC-LRR and SD domains are
741 important to regulate the proper subcellular localization of Sw-5b and the proper
742 nucleoplasmic distribution of Sw-5b is needed to elicit full immune responses to
743 inhibit different TSWV infection steps. Sw-5b NB-ARC-LRR controls its cytoplasm
744 localization. The CC domain of the Sw-5b is not sufficient to target the receptor into
745 nuclear. Importantly, the extended SD of Sw-5b is absolutely required for the nucleus
746 translocation. Because non-canonical domains are frequently found in other NLRs
747 and are quite diversified, our findings have broad implications to investigate the
748 potential new functions of non-canonical domains that integrated in the plant NLRs to
749 regulate the plant immunity against pathogen invasions.

750 Through co-IP, Mass Spectrometry and BiFC analysis, we found that the extended

751 SD domain and Sw-5b interacted with host importin machineries to translocate the
752 Sw-5b receptor from cytoplasm into nucleus to mediate local and systemic resistance
753 to tospovirus. Recent studies have shown that nuclearporin MOS3, MOS6 and nuclear
754 pore complex component MOS7/Nup88 proteins played important roles in regulating
755 Arabidopsis innate immunity (Palma *et al.*, 2005; Zhang & Li, 2005; Cheng *et al.*,
756 2009). We found that when *importin α1*, *importin α2* and *importin β* gene were all
757 silenced through VIGS, the nucleus targeting of Sw-5b were completely blocked, and
758 consequently, the Sw-5b-mediated systemic immunity to tospovirus infection was
759 compromised. Importin α and β are known to form a nucleus import complex.
760 Binding with importin β could activate importin α to form a binding surface for NLS
761 proteins (Stewart, 2007). Hence, disruption of either importin α or importin β would
762 block the nucleus import of NLS proteins. Because silencing *importin α* or
763 *importin β* gene expression through VIGS did not disrupt the nuclear targeting of
764 Sw-5b, we speculate that a non-canonical nuclear import pathway may take part in
765 importing Sw-5b into nucleus.

766 Based on the above results, we have created a working model for the Sw-5b
767 NLR-induced host resistance against TSWV replication, and intercellular and
768 long-distance movement in plant (Fig. 9). Upon recognition of NSm in cytoplasm,
769 Sw-5b switched from an autoinhibited state to an activated state. The activated Sw-5b
770 accumulated in cytoplasm and also translocate into nucleus via importins α and β .
771 The cytoplasm-accumulated and the nucleus-accumulated Sw-5b play different roles
772 in inducing host immunity against TSWV infection. The cytoplasmic Sw-5b functions

773 to induce a cell death response to inhibit TSWV replication, while the nuclear Sw-5b
774 functions to induce a weak host defense against TSWV replication, but a strong
775 defense against TSWV cell-to-cell and long-distance movement. The concerted
776 defense signaling generated in the cytoplasm and nucleus resulted in a strong host
777 resistance to tospovirus infection.
778
779
780 **Acknowledgments**
781 This work was supported by the National Natural Science Foundation of China
782 (31630062, 31925032 and 31870143), the Fundamental Research Funds for the
783 Central Universities (JCQY201904 and KYXK202012), Youth Science and
784 Technology Innovation Program to XT.
785
786 **Author contributions**
787 HC XQ, XC and XT, designed the research; HC, XQ and XC, TY, MF, JC, RC, HH,
788 YZ, YM, DS, YX, MZ performed the experiments; HC, XSD and XT interpreted the
789 result and wrote the paper.
790
791 **ORCID**
792 Hongyu Chen, 0000-0001-8142-0653
793 Yi Xu, 0000-0002-1913-4530
794 Min Zhu, 0000-0002-9354-4300

Xiaorong Tao, 0000-0003-1259-366X

Competing interests

The authors declare that nocompeting interests exist.

Data availability

All data produced in this study are presented in this manuscript or as the supporting files

References

Axtell MJ, Staskawicz BJ. 2003. Initiation of RPS2-specified disease resistance in Arabidopsis is coupled to the AvrRpt2-directed elimination of RIN4. *Cell* **112**(3): 369-377.

Bai S, Liu J, Chang C, Zhang L, Maekawa T, Wang Q, Xiao W, Liu Y, Chai J, Takken FL, Schulze-Lefert P, Shen QH. 2012. Structure-function analysis of barley NLR immune receptor MLA10 reveals its cell compartment specific activity in cell death and disease resistance. *PLoS Pathog* **8**(6): e1002752.

Bendahmane A, Kanyuka K, Baulcombe DC. 1999. The Rx gene from potato controls separate virus resistance and cell death responses. *Plant Cell* **11**(5): 781-792.

Bernoux M, Ve T, Williams S, Warren C, Hatters D, Valkov E, Zhang X, Ellis JG, Kobe B, Dodds PN. 2011. Structural and functional analysis of a plant resistance protein TIR domain reveals interfaces for self-association, signaling, and autoregulation. *Cell Host Microbe* **9**(3): 200-211.

Brommonschenkel SH, Frary A, Frary A, Tanksley SD. 2000. The broad-spectrum tospovirus resistance gene Sw-5 of tomato is a homolog of the root-knot nematode resistance gene Mi. *Mol Plant Microbe Interact* **13**(10): 1130-1138.

Burch-Smith TM, Schiff M, Caplan JL, Tsao J, Czymmek K, Dinesh-Kumar SP. 2007. A novel role for the TIR domain in association with pathogen-derived elicitors. *PLoS Biol* **5**(3): e68.

Canto T, Palukaitis P. 2002. Novel N gene-associated, temperature-independent resistance to the movement of tobacco mosaic virus vectors neutralized by a cucumber mosaic virus RNA1 transgene. *J Virol* **76**(24): 12908-12916.

Caplan J, Padmanabhan M, Dinesh-Kumar SP. 2008. Plant NB-LRR Immune Receptors: From Recognition to Transcriptional Reprogramming. *Cell Host Microbe* **3**(3): 126-135.

827 **Caplan JL, Mamillapalli P, Burch-Smith TM, Czymmek K, Dinesh-Kumar SP. 2008.**
828 Chloroplastic protein NRIP1 mediates innate immune receptor recognition of a viral effector.
829 *Cell* **132**(3): 449-462.
830 **Cesari S, Bernoux M, Moncuquet P, Kroj T, Dodds PN. 2014.** A novel conserved mechanism for
831 plant NLR protein pairs: the "integrated decoy" hypothesis. *Front Plant Sci* **5**: 606.
832 **Cesari S, Moore J, Chen C, Webb D, Periyannan S, Mago R, Bernoux M, Lagudah ES, Dodds**
833 **PN. 2016.** Cytosolic activation of cell death and stem rust resistance by cereal MLA-family
834 CC-NLR proteins. *Proc Natl Acad Sci U S A* **113**(36): 10204-10209.
835 **Cesari S, Thilliez G, Ribot C, Chalvon V, Michel C, Jauneau A, Rivas S, Alaux L, Kanzaki H,**
836 **Okuyama Y, Morel JB, Fournier E, Tharreau D, Terauchi R, Kroj T. 2013.** The rice
837 resistance protein pair RGA4/RGA5 recognizes the Magnaporthe oryzae effectors AVR-Pia
838 and AVR1-CO39 by direct binding. *Plant Cell* **25**(4): 1463-1481.
839 **Chen T, Liu D, Niu X, Wang J, Qian L, Han L, Liu N, Zhao J, Hong Y, Liu Y. 2017.** Antiviral
840 Resistance Protein Tm-2(2) Functions on the Plasma Membrane. *Plant Physiol* **173**(4):
841 2399-2410.
842 **Chen X, Zhu M, Jiang L, Zhao W, Li J, Wu J, Li C, Bai B, Lu G, Chen H, Moffett P, Tao X. 2016.**
843 A multilayered regulatory mechanism for the autoinhibition and activation of a plant
844 CC-NB-LRR resistance protein with an extra N-terminal domain. *New Phytol* **212**(1):
845 161-175.
846 **Cheng YT, Germain H, Wiermer M, Bi D, Xu F, Garcia AV, Wirthmueller L, Despres C, Parker**
847 **JE, Zhang Y, Li X. 2009.** Nuclear pore complex component MOS7/Nup88 is required for
848 innate immunity and nuclear accumulation of defense regulators in Arabidopsis. *Plant Cell*
849 **21**(8): 2503-2516.
850 **Coll NS, Vercammen D, Smidler A, Clover C, Van Breusegem F, Dangl JL, Epple P. 2010.**
851 Arabidopsis type I metacaspases control cell death. *Science* **330**(6009): 1393-1397.
852 **Collier SM, Hamel LP, Moffett P. 2011.** Cell death mediated by the N-terminal domains of a unique
853 and highly conserved class of NB-LRR protein. *Mol Plant Microbe Interact* **24**(8): 918-931.
854 **Collier SM, Moffett P. 2009.** NB-LRRs work a "bait and switch" on pathogens. *Trends Plant Sci*
855 **14**(10): 521-529.
856 **Cui H, Tsuda K, Parker JE. 2015.** Effector-triggered immunity: from pathogen perception to robust
857 defense. *Annu Rev Plant Biol* **66**: 487-511.
858 **Das B, Sengupta S, Prasad M, Ghose TK. 2014.** Genetic diversity of the conserved motifs of six
859 bacterial leaf blight resistance genes in a set of rice landraces. *BMC Genet* **15**: 82.
860 **De Oliveira AS, Koolhaas I, Boiteux LS, Caldararu OF, Petrescu AJ, Oliveira Resende R,**
861 **Kormelink R. 2016.** Cell death triggering and effector recognition by Sw-5 SD-CNL proteins
862 from resistant and susceptible tomato isolines to Tomato spotted wilt virus. *Mol Plant Pathol*
863 **17**(9): 1442-1454.
864 **Deom CM, Wolf S, Holt CA, Lucas WJ, Beachy RN. 1991.** Altered function of the tobacco mosaic
865 virus movement protein in a hypersensitive host. *Virology* **180**(1): 251-256.
866 **Deslandes L, Olivier J, Peeters N, Feng DX, Khounlotham M, Boucher C, Somssich I, Genin S,**
867 **Marco Y. 2003.** Physical interaction between RRS1-R, a protein conferring resistance to
868 bacterial wilt, and PopP2, a type III effector targeted to the plant nucleus. *Proc Natl Acad Sci*
869 *U S A* **100**(13): 8024-8029.
870 **Dodds PN, Rathjen JP. 2010.** Plant immunity: towards an integrated view of plant-pathogen

interactions. *Nat Rev Genet* **11**(8): 539-548.

Ea VDB, Jones JD. 1998. Plant disease-resistance proteins and the gene-for-gene concept. *Trends in Biochemical Sciences* **23**(12): 454-456(453).

Engelhardt S, Boevink PC, Armstrong MR, Ramos MB, Hein I, Birch PR. 2012. Relocalization of late blight resistance protein R3a to endosomal compartments is associated with effector recognition and required for the immune response. *Plant Cell* **24**(12): 5142-5158.

Ernst K, Kumar A, Kriseleit D, Kloos DU, Phillips MS, Ganal MW. 2002. The broad-spectrum potato cyst nematode resistance gene (Hero) from tomato is the only member of a large gene family of NBS-LRR genes with an unusual amino acid repeat in the LRR region. *Plant J* **31**(2): 127-136.

Feng M, Cheng R, Chen M, Guo R, Li L, Feng Z, Wu J, Xie L, Hong J, Zhang Z, Kormelink R, Tao X. 2020. Rescue of tomato spotted wilt virus entirely from complementary DNA clones. *Proc Natl Acad Sci U S A* **117**(2): 1181-1190.

Feng Z, Xue F, Xu M, Chen X, Zhao W, Garcia-Murria MJ, Mingarro I, Liu Y, Huang Y, Jiang L, Zhu M, Tao X. 2016. The ER-Membrane Transport System Is Critical for Intercellular Trafficking of the NSm Movement Protein and Tomato Spotted Wilt Tospovirus. *PLoS Pathog* **12**(2): e1005443.

Gao Z, Chung EH, Eitas TK, Dangl JL. 2011. Plant intracellular innate immune receptor Resistance to Pseudomonas syringae pv. maculicola 1 (RPM1) is activated at, and functions on, the plasma membrane. *Proc Natl Acad Sci U S A* **108**(18): 7619-7624.

Garcia AV, Blanvillain-Baufume S, Huibers RP, Wiermer M, Li G, Gobbato E, Rietz S, Parker JE. 2010. Balanced nuclear and cytoplasmic activities of EDS1 are required for a complete plant innate immune response. *PLoS Pathog* **6**: e1000970.

Gassmann W. 2005. Natural variation in the Arabidopsis response to the avirulence gene hopPsyA uncouples the hypersensitive response from disease resistance. *Mol Plant Microbe Interact* **18**(10): 1054-1060.

Germain H, Seguin A. 2011. Innate immunity: has poplar made its BED? *New Phytol* **189**(3): 678-687.

Hallwass M, de Oliveira AS, de Campos Dianese E, Lohuis D, Boiteux LS, Inoue-Nagata AK, Resende RO, Kormelink R. 2014. The Tomato spotted wilt virus cell-to-cell movement protein (NSM) triggers a hypersensitive response in Sw-5-containing resistant tomato lines and in Nicotiana benthamiana transformed with the functional Sw-5b resistance gene copy. *Mol Plant Pathol* **15**(9): 871-880.

Heidrich K, Wirthmueller L, Tasset C, Pouzet C, Deslandes L, Parker JE. 2011. Arabidopsis EDS1 connects pathogen effector recognition to cell compartment-specific immune responses. *Science* **334**(6061): 1401-1404.

Heinlein M. 2015. Plant virus replication and movement. *Virology* **479-480**: 657-671.

Horsefield S, Burdett H, Zhang X, Manik MK, Shi Y, Chen J, Qi T, Gilley J, Lai JS, Rank MX, Casey LW, Gu W, Ericsson DJ, Foley G, Hughes RO, Bosanac T, von Itzstein M, Rathjen JP, Nanson JD, Boden M, Dry IB, Williams SJ, Staskawicz BJ, Coleman MP, Ve T, Dodds PN, Kobe B. 2019. NAD(+) cleavage activity by animal and plant TIR domains in cell death pathways. *Science* **365**(6455): 793-799.

Inoue H, Hayashi N, Matsushita A, Xinqiong L, Nakayama A, Sugano S, Jiang CJ, Takatsuji H. 2013. Blast resistance of CC-NB-LRR protein Pb1 is mediated by WRKY45 through

protein-protein interaction. *Proc Natl Acad Sci U S A* **110**(23): 9577-9582.

Jones JD, Vance RE, Dangl JL. 2016. Intracellular innate immune surveillance devices in plants and animals. *Science* **354**(6316).

Jubic LM, Saile S, Furzer OJ, El Kasmi F, Dangl JL. 2019. Help wanted: helper NLRs and plant immune responses. *Curr Opin Plant Biol* **50**: 82-94.

Kanneganti TD, Bai X, Tsai CW, Win J, Meulia T, Goodin M, Kamoun S, Hogenhout SA. 2007. A functional genetic assay for nuclear trafficking in plants. *Plant J* **50**(1): 149-158.

Kanzaki H, Yoshida K, Saitoh H, Fujisaki K, Hirabuchi A, Alaux L, Fournier E, Tharreau D, Terauchi R. 2012. Arms race co-evolution of Magnaporthe oryzae AVR-Pik and rice Pik genes driven by their physical interactions. *Plant J* **72**(6): 894-907.

Kapos P, Devendrakumar KT, Li X. 2019. Plant NLRs: From discovery to application. *Plant Sci* **279**: 3-18.

Katagiri F, Tsuda K. 2010. Understanding the plant immune system. *Mol Plant Microbe Interact* **23**(12): 1531-1536.

Kawano Y, Fujiwara T, Yao A, Housen Y, Hayashi K, Shimamoto K. 2014. Palmitoylation-dependent membrane localization of the rice resistance protein pit is critical for the activation of the small GTPase OsRac1. *J Biol Chem* **289**(27): 19079-19088.

Kong L, Qiu X, Kang J, Wang Y, Chen H, Huang J, Qiu M, Zhao Y, Kong G, Ma Z, Wang Y, Ye W, Dong S, Ma W, Wang Y. 2017. A Phytophthora Effector Manipulates Host Histone Acetylation and Reprograms Defense Gene Expression to Promote Infection. *Curr Biol* **27**(7): 981-991.

Kormelink R, Garcia ML, Goodin M, Sasaya T, Haenni AL. 2011. Negative-strand RNA viruses: the plant-infecting counterparts. *Virus Res* **162**(1-2): 184-202.

Kormelink R, Storms M, Van Lent J, Peters D, Goldbach R. 1994. Expression and subcellular location of the NSM protein of tomato spotted wilt virus (TSWV), a putative viral movement protein. *Virology* **200**(1): 56-65.

Kourelis J, van der Hoorn RAL. 2018. Defended to the Nines: 25 Years of Resistance Gene Cloning Identifies Nine Mechanisms for R Protein Function. *Plant Cell* **30**(2): 285-299.

Krasileva KV, Dahlbeck D, Staskawicz BJ. 2010. Activation of an Arabidopsis resistance protein is specified by the in planta association of its leucine-rich repeat domain with the cognate oomycete effector. *Plant Cell* **22**(7): 2444-2458.

Kroj T, Chanclud E, Michel-Romiti C, Grand X, Morel JB. 2016. Integration of decoy domains derived from protein targets of pathogen effectors into plant immune receptors is widespread. *New Phytol* **210**(2): 618-626.

Lanford RE, Butel JS. 1984. Construction and characterization of an SV40 mutant defective in nuclear transport of T antigen. *Cell* **37**(3): 801-813.

Lapin D, Bhandari DD, Parker JE. 2020. Origins and Immunity Networking Functions of EDS1 Family Proteins. *Annu Rev Phytopathol* **58**: 253-276.

Le Roux C, Huet G, Jauneau A, Camborde L, Tremousaygue D, Kraut A, Zhou B, Levaillant M, Adachi H, Yoshioka H, Raffaele S, Berthome R, Coute Y, Parker JE, Deslandes L. 2015. A receptor pair with an integrated decoy converts pathogen disabling of transcription factors to immunity. *Cell* **161**(5): 1074-1088.

Leastro MO, Pallas V, Resende RO, Sanchez-Navarro JA. 2017. The functional analysis of distinct tospovirus movement proteins (NSM) reveals different capabilities in tubule formation,

cell-to-cell and systemic virus movement among the tospovirus species. *Virus Res* **227**: 57-68.

Li J, Huang H, Zhu M, Huang S, Zhang W, Dinesh-Kumar SP, Tao X. 2019. A Plant Immune Receptor Adopts a Two-Step Recognition Mechanism to Enhance Viral Effector Perception. *Mol Plant* **12**(2): 248-262.

Li W, Lewandowski DJ, Hilf ME, Adkins S. 2009. Identification of domains of the Tomato spotted wilt virus NSm protein involved in tubule formation, movement and symptomatology. *Virology* **390**(1): 110-121.

Li W, Zhao Y, Liu C, Yao G, Wu S, Hou C, Zhang M, Wang D. 2012. Callose deposition at plasmodesmata is a critical factor in restricting the cell-to-cell movement of Soybean mosaic virus. *Plant Cell Rep* **31**(5): 905-916.

Li X, Kapos P, Zhang Y. 2015. NLRs in plants. *Curr Opin Immunol* **32**: 114-121.

Lopez C, Aramburu J, Galipienso L, Soler S, Nuez F, Rubio L. 2011. Evolutionary analysis of tomato Sw-5 resistance-breaking isolates of Tomato spotted wilt virus. *J Gen Virol* **92**(Pt 1): 210-215.

Lucas WJ. 2006. Plant viral movement proteins: agents for cell-to-cell trafficking of viral genomes. *Virology* **344**(1): 169-184.

Lukasik-Shreepaathy E, Slootweg E, Richter H, Goverse A, Cornelissen BJ, Takken FL. 2012. Dual regulatory roles of the extended N terminus for activation of the tomato MI-1.2 resistance protein. *Mol Plant Microbe Interact* **25**(8): 1045-1057.

Ma S, Lapin D, Liu L, Sun Y, Song W, Zhang X, Logemann E, Yu D, Wang J, Jirschitzka J, Han Z, Schulze-Lefert P, Parker JE, Chai J. 2020. Direct pathogen-induced assembly of an NLR immune receptor complex to form a holoenzyme. *Science* **370**(6521).

Ma Y, Guo H, Hu L, Martinez PP, Moschou PN, Cevik V, Ding P, Duxbury Z, Sarris PF, Jones JDG. 2018. Distinct modes of derepression of an Arabidopsis immune receptor complex by two different bacterial effectors. *Proc Natl Acad Sci U S A* **115**(41): 10218-10227.

Ma Z, Song T, Zhu L, Ye W, Wang Y, Shao Y, Dong S, Zhang Z, Dou D, Zheng X, Tyler BM, Wang Y. 2015. A Phytophthora sojae Glycoside Hydrolase 12 Protein Is a Major Virulence Factor during Soybean Infection and Is Recognized as a PAMP. *Plant Cell* **27**(7): 2057-2072.

Ma Z, Zhu L, Song T, Wang Y, Zhang Q, Xia Y, Qiu M, Lin Y, Li H, Kong L, Fang Y, Ye W, Wang Y, Dong S, Zheng X, Tyler BM, Wang Y. 2017. A paralogous decoy protects Phytophthora sojae apoplastic effector PsXEG1 from a host inhibitor. *Science* **355**(6326): 710-714.

Maekawa T, Cheng W, Spiridon LN, Toller A, Lukasik E, Saijo Y, Liu P, Shen QH, Micluta MA, Somssich IE, Takken FLW, Petrescu AJ, Chai J, Schulze-Lefert P. 2011. Coiled-coil domain-dependent homodimerization of intracellular barley immune receptors defines a minimal functional module for triggering cell death. *Cell Host Microbe* **9**(3): 187-199.

Meier N, Hatch C, Nagalakshmi U, Dinesh-Kumar SP. 2019. Perspectives on intracellular perception of plant viruses. *Mol Plant Pathol* **20**(9): 1185-1190.

Meyers BC, Kozik A, Griego A, Kuang H, Michelmore RW. 2003. Genome-wide analysis of NBS-LRR-encoding genes in Arabidopsis. *Plant Cell* **15**(4): 809-834.

Milligan SB, Bodeau J, Yaghoobi J, Kaloshian I, Zabel P, Williamson VM. 1998. The root knot nematode resistance gene Mi from tomato is a member of the leucine zipper, nucleotide binding, leucine-rich repeat family of plant genes. *Plant Cell* **10**(8): 1307-1319.

Mittler R, Herr EH, Orvar BL, van Camp W, Willekens H, Inze D, Ellis BE. 1999. Transgenic

tobacco plants with reduced capability to detoxify reactive oxygen intermediates are hyperresponsive to pathogen infection. *Proc Natl Acad Sci U S A* **96**(24): 14165-14170.

Oliver JE, Whitfield AE. 2016. The Genus Tospovirus: Emerging Bunyaviruses that Threaten Food Security. *Annu Rev Virol* **3**(1): 101-124.

Padmanabhan MS, Ma S, Burch-Smith TM, Czymmek K, Huijser P, Dinesh-Kumar SP. 2013. Novel positive regulatory role for the SPL6 transcription factor in the N TIR-NB-LRR receptor-mediated plant innate immunity. *PLoS Pathog* **9**(3): e1003235.

Palma K, Zhang Y, Li X. 2005. An importin alpha homolog, MOS6, plays an important role in plant innate immunity. *Curr Biol* **15**(12): 1129-1135.

Peiro A, Canizares MC, Rubio L, Lopez C, Moriones E, Aramburu J, Sanchez-Navarro J. 2014. The movement protein (NSm) of Tomato spotted wilt virus is the avirulence determinant in the tomato Sw-5 gene-based resistance. *Mol Plant Pathol* **15**(8): 802-813.

Qi D, DeYoung BJ, Innes RW. 2012. Structure-function analysis of the coiled-coil and leucine-rich repeat domains of the RPS5 disease resistance protein. *Plant Physiol* **158**(4): 1819-1832.

Qi D, Innes RW. 2013. Recent Advances in Plant NLR Structure, Function, Localization, and Signaling. *Front Immunol* **4**: 348.

Rao ALNC, Y. G，Khan, J. A，Dijkstra, J. 2002. Molecular biology of plant virus movement. *Plant Viruses As Molecular Pathogens*.

Sarris PF, Cevik V, Dagdas G, Jones JD, Krasileva KV. 2016. Comparative analysis of plant immune receptor architectures uncovers host proteins likely targeted by pathogens. *BMC Biol* **14**: 8.

Sarris PF, Duxbury Z, Huh SU, Ma Y, Segonzac C, Sklenar J, Derbyshire P, Cevik V, Rallapalli G, Saucet SB, Wirthmueller L, Menke FL, Sohn KH, Jones JD. 2015. A Plant Immune Receptor Detects Pathogen Effectors that Target WRKY Transcription Factors. *Cell* **161**(5): 1089-1100.

Scholthof KB, Adkins S, Czosnek H, Palukaitis P, Jacquot E, Hohn T, Hohn B, Saunders K, Candresse T, Ahlquist P, Hemenway C, Foster GD. 2011. Top 10 plant viruses in molecular plant pathology. *Mol Plant Pathol* **12**(9): 938-954.

Seo JK, Kwon SJ, Cho WK, Choi HS, Kim KH. 2014. Type 2C protein phosphatase is a key regulator of antiviral extreme resistance limiting virus spread. *Sci Rep* **4**: 5905.

Seong K, Seo E, Witek K, Li M, Staskawicz B. 2020. Evolution of NLR resistance genes with noncanonical N-terminal domains in wild tomato species. *New Phytol* **227**(5): 1530-1543.

Shen QH, Saijo Y, Mauch S, Biskup C, Bieri S, Keller B, Seki H, Ulker B, Somssich IE, Schulze-Lefert P. 2007. Nuclear activity of MLA immune receptors links isolate-specific and basal disease-resistance responses. *Science* **315**(5815): 1098-1103.

Slootweg E, Roosien J, Spiridon LN, Petrescu AJ, Tameling W, Joosten M, Pomp R, van Schaik C, Dees R, Borst JW, Smant G, Schots A, Bakker J, Goverse A. 2010. Nucleocytoplasmic distribution is required for activation of resistance by the potato NB-LRR receptor Rx1 and is balanced by its functional domains. *Plant Cell* **22**(12): 4195-4215.

Soosaar JL, Burch-Smith TM, Dinesh-Kumar SP. 2005. Mechanisms of plant resistance to viruses. *Nat Rev Microbiol* **3**(10): 789-798.

Spassova M I PTW, Folkertsma R T, et al. 2001. The tomato gene Sw-5 is a member of the coiled coil, nucleotide binding, leucine-rich repeat class of plant resistance genes and confers resistance to TSWV in tobacco. *Molecular Breeding.* **7(2)**: 151.

Stewart M. 2007. Molecular mechanism of the nuclear protein import cycle. *Nat Rev Mol Cell Biol* **8**(3): 195-208.

Swiderski MR, Birker D, Jones JD. 2009. The TIR domain of TIR-NB-LRR resistance proteins is a signaling domain involved in cell death induction. *Mol Plant Microbe Interact* **22**(2): 157-165.

Takemoto D, Rafiqi M, Hurley U, Lawrence GJ, Bernoux M, Hardham AR, Ellis JG, Dodds PN, Jones DA. 2012. N-terminal motifs in some plant disease resistance proteins function in membrane attachment and contribute to disease resistance. *Mol Plant Microbe Interact* **25**(3): 379-392.

Takken FLW, Goverse A. 2012. How to build a pathogen detector: structural basis of NB-LRR function. *Current Opinion in Plant Biology* **15**(4): 375-384.

Taliansky M, Torrance L, Kalinina NO. 2008. Role of plant virus movement proteins. *Methods Mol Biol* **451**: 33-54.

Tameling WI, Nooijen C, Ludwig N, Boter M, Slootweg E, Goverse A, Shirasu K, Joosten MH. 2010. RanGAP2 mediates nucleocytoplasmic partitioning of the NB-LRR immune receptor Rx in the Solanaceae, thereby dictating Rx function. *Plant Cell* **22**(12): 4176-4194.

Tasset C, Bernoux M, Jauneau A, Pouzet C, Briere C, Kieffer-Jacquinod S, Rivas S, Marco Y, Deslandes L. 2010. Autoacetylation of the Ralstonia solanacearum effector PopP2 targets a lysine residue essential for RRS1-R-mediated immunity in Arabidopsis. *PLoS Pathog* **6**(11): e1001202.

Turina M, Kormelink R, Resende RO. 2016. Resistance to Tospoviruses in Vegetable Crops: Epidemiological and Molecular Aspects. *Annu Rev Phytopathol* **54**: 347-371.

van der Vossen EA, Gros J, Sikkema A, Muskens M, Wouters D, Wolters P, Pereira A, Allefs S. 2005. The Rpi-blb2 gene from Solanum bulbocastanum is an Mi-1 gene homolog conferring broad-spectrum late blight resistance in potato. *Plant J* **44**(2): 208-222.

van Wersch S, Li X. 2019. Stronger When Together: Clustering of Plant NLR Disease resistance Genes. *Trends Plant Sci* **24**(8): 688-699.

van Wersch S, Tian, L., Hoy, R., Li, X. . 2020. Plant NLRs: The whistleblowers of plant immunity. *Plant Commun*: doi: https://doi.org/10.1016/j.xplc.2019.100016.

Vos P, Simons G, Jesse T, Wijbrandi J, Heinen L, Hogers R, Frijters A, Groenendijk J, Diergaarde P, Reijans M, Fierens-Onstenk J, de Both M, Peleman J, Liharska T, Hontelez J, Zabeau M. 1998. The tomato Mi-1 gene confers resistance to both root-knot nematodes and potato aphids. *Nat Biotechnol* **16**(13): 1365-1369.

Vossen JH, van Arkel G, Bergervoet M, Jo KR, Jacobsen E, Visser RG. 2016. The Solanum demissum R8 late blight resistance gene is an Sw-5 homologue that has been deployed worldwide in late blight resistant varieties. *Theor Appl Genet* **129**(9): 1785-1796.

Wan L, Essuman K, Anderson RG, Sasaki Y, Monteiro F, Chung EH, Osborne Nishimura E, DiAntonio A, Milbrandt J, Dangl JL, Nishimura MT. 2019. TIR domains of plant immune receptors are NAD(+)-cleaving enzymes that promote cell death. *Science* **365**(6455): 799-803.

Wang A. 2015. Dissecting the molecular network of virus-plant interactions: the complex roles of host factors. *Annu Rev Phytopathol* **53**: 45-66.

Wang J, Chen T, Han M, Qian L, Li J, Wu M, Han T, Cao J, Nagalakshmi U, Rathjen JP, Hong Y, Liu Y. 2020. Plant NLR immune receptor Tm-22 activation requires NB-ARC domain-mediated self-association of CC domain. *PLoS Pathog* **16**(4): e1008475.

Wang J, Hu M, Wang J, Qi J, Han Z, Wang G, Qi Y, Wang HW, Zhou JM, Chai J. 2019a. Reconstitution and structure of a plant NLR resistosome conferring immunity. *Science* **364**(6435).

Wang J, Wang J, Hu M, Wu S, Qi J, Wang G, Han Z, Qi Y, Gao N, Wang HW, Zhou JM, Chai J. 2019b. Ligand-triggered allosteric ADP release primes a plant NLR complex. *Science* **364**(6435).

Wen W, Meinkoth JL, Tsien RY, Taylor SS. 1995. Identification of a signal for rapid export of proteins from the nucleus. *Cell* **82**(3): 463-473.

Wirthmueller L, Zhang Y, Jones JD, Parker JE. 2007. Nuclear accumulation of the Arabidopsis immune receptor RPS4 is necessary for triggering EDS1-dependent defense. *Curr Biol* **17**(23): 2023-2029.

Zhang Y, Li X. 2005. A putative nucleoporin 96 Is required for both basal defense and constitutive resistance responses mediated by suppressor of npr1-1,constitutive 1. *Plant Cell* **17**(4): 1306-1316.

Zhao W, Jiang L, Feng Z, Chen X, Huang Y, Xue F, Huang C, Liu Y, Li F, Liu Y, Tao X. 2016. Plasmodesmata targeting and intercellular trafficking of Tomato spotted wilt tospovirus movement protein NSm is independent of its function in HR induction. *J Gen Virol* **97**(8): 1990-1997.

Zhu M, Jiang L, Bai B, Zhao W, Chen X, Li J, Liu Y, Chen Z, Wang B, Wang C, Wu Q, Shen Q, Dinesh-Kumar SP, Tao X. 2017. The Intracellular Immune Receptor Sw-5b Confers Broad-Spectrum Resistance to Tospoviruses through Recognition of a Conserved 21-Amino Acid Viral Effector Epitope. *Plant Cell* **29**(9): 2214-2232.

Zhu M, van Grinsven IL, Kormelink R, Tao X. 2019. Paving the Way to Tospovirus Infection: Multilined Interplays with Plant Innate Immunity. *Annu Rev Phytopathol* **57**: 41-62.

FIGURE LEGENDS

Fig. 1. Subcellular localization of Sw-5b in *Nicotiana benthamiana* and tomato leaf cells. (a) Schematic diagrams of Sw-5b. (b) Subcellular localizations of free YFP (left), YFP-Sw-5b (middle) and autoactive YFP-Sw-5b^{D857V} mutant (right) in *N. benthamiana* leaf cells at 24 hours post agro-infiltration (hpi). (c) Subcellular localization of free YFP (left), YFP-Sw-5b (middle) and autoactive YFP-Sw-5b^{D857V} mutant (right) in tomato leaf cells at 24 hpi. N nucleus, and C cytoplasm inside the cell are indicated. Bar = 10 μm. (d) Nucleocytoplasmic partitioning analysis of YFP-Sw-5b and autoactive YFP-Sw-5b^{D857V}. Total lysate (T) from p2300S empty vector (EV), YFP-Sw-5b or YFP-Sw-5b^{D857V} expressing leaves were fractionated into cytoplasm and nucleus, and analyzed by immunoblots using antibodies against YFP. The actin and histone were used as a cytoplasm marker and nucleus marker, respectively, in the fractionation analysis. Ponceau S staining was also used as cytoplasm marker.

Fig. 2. Effect of Sw-5b subcellular localization pattern on HR induction. (a) Confocal images of *N. benthamiana* leaf cells transiently expressing NES-YFP-Sw-5b, nes-YFP-Sw-5b, NLS-YFP-Sw-5b or nls-YFP-Sw-5b fusion. The images were taken at 24–36 hpi. N nucleus and C cytoplasm (c). Bar = 10 μm. (b) Induction of HR in *N. benthamiana* leaf tissues co-expressing NSm and one of the five Sw-5b fusion proteins. The infiltrated *N. benthamiana* leaf was photographed at 3 dpi (left image). Induction of HR in the infiltrated tissues were visualized using a trypan blue staining

method (right image). (c) Immunoblot analysis of NES-YFP-Sw-5b, nes-YFP-Sw-5b, NLS-YFP-Sw-5b, and nls-YFP-Sw-5b expressions in the infiltrated *N. benthamiana* leaf tissues. These fusion proteins were enriched using the GFP-Trap beads prior to SDS-PAGE, and the blot was probed using an YFP specific antibody. Ponceau-S staining was used to estimate sample loadings. (d) Time course analysis of ion leakage in Nicotiana benthamiana leaves co-expressing NSm with one of the five Sw-5b fusion proteins. Measurements were performed at 4 h intervals starting from 24 to 48 hpi. Error bars (SEs) were calculated using the results from three biological replicates per treatment collected at each time point.

Fig. 3. The effect of cytoplasm- and nucleus-targeted Sw-5b on viral replication. (a) Schematic representation of binary constructs to express TSWV $SR_{(-)eGFP}$ mini-genome replicon, TSWV L RNA segment containing an optimized RdRp and $NSm^{H93A\&H94A}$ mutant that defected in viral movement. Minus sign (-) and 5′ to 3′ designation represent the negative (genomic)-strand of tospovirus RNA. 35S: a double 35S promoter; HH: hammerhead ribozyme; RZ: hepatitis delta virus (HDV) ribozyme; NOS: nopaline synthase terminator; 35S Ter: a 35S transcription terminator. (b) Accumulation of eGFP fluorescence in *N. benthamiana* leaves co-expressing p2300S empty vector (EV), Sw-5b, NES-Sw-5b, nes-Sw-5b, NLS-Sw-5b, or nls-Sw-5b with TSWV $SR_{(-)eGFP}$, L, and $NSm^{H93A\&H94A}$ at 4 days post infiltration (dpi) viewed with a fluorescence microscope. Bar represents 400 μm. (c) Immunoblot analysis of expression of eGFP proteins in leaves shown in panel (b) using specific

1163 antibodies against YFP. Ponceau S staining of rubisco large subunit is shown for
1164 protein loading control.
1165
1166 **Fig. 4.** Effect of subcellular localization of Sw-5b on cell-to-cell movement of NSm
1167 in leaf epidermis of *N. benthamiana.* (a) Schematic diagram of the binary construct to
1168 co-express mCherry-HDEL and NSm-GFP. (b) Cell-to-cell movement analysis of
1169 NSm-GFP in *N. benthamiana* leaves co-expressing p2300S empty vector (EV), Sw-5b,
1170 NES-Sw-5b, NLS-Sw-5b, or nls-Sw-5b with the construct harboring both
1171 mCherry-HDEL and NSm-GFP. *Agrobacterium* containing the construct to co-express
1172 mCherry-HDEL and NSm-GFP was diluted 500 times for expression in a single
1173 epidermal cell. All other *Agrobacterium* were infiltrated at the concentration of OD_{600}
1174 = 0.2. Bar, 50 μm.
1175
1176 **Fig. 5.** Analysis of cytoplasm- and nucleus-targeted Sw-5b-mediated host immunity
1177 to TSWV systemic infection. (a) TSWV systemic infection in transgenic *N.*
1178 *benthamiana* plants expressing NES-YFP-Sw-5b, nes-YFP-Sw-5b, NLS-YFP-Sw-5b,
1179 nls-YFP-Sw-5b, YFP-Sw-5b or p2300S empty vector (EV) driven by 35S promoter.
1180 TSWV-inoculated plants were photographed at 15 dpi. White arrow indicates the
1181 systemic leaves showing HR trailing. White arrowhead indicates the systemic leaves
1182 showing mosaic. (b) Immunoblot analysis of NES-YFP-Sw-5b, nes-YFP-Sw-5b,
1183 NLS-YFP-Sw-5b, nls-YFP-Sw-5b and YFP-Sw-5b expressions in different transgenic
1184 *N. benthamiana* plants. EV plants transformed with an empty vector and were used as

a negative control. (c) RT-PCR analysis of TSWV accumulation in the systemic leaves of different transgenic *N. benthamiana* plants at 15 dpi.

Fig. 6. Joint effects of cytoplasm- and nucleus-targeted Sw-5b on defenses against tospovirus infection in *Nicotiana benthamiana* leaves. (a) Schematic representation of binary constructs to express TSWV $SR_{(+)eGFP}$-$M_{(-)op}$ and TSWV L RNA segment containing an optimized RdRp. 35S: a double 35S promoter; HH: hammerhead ribozyme; RZ: hepatitis delta virus (HDV) ribozyme; NOS: nopaline synthase terminator. (b) Accumulation of eGFP fluorescence in *N. benthamiana* leaves co-expressing p2300S empty vector (EV), Sw-5b, NES-Sw-5b, NLS-Sw-5b, or NES-Sw-5b+NLS-Sw-5b with TSWV $SR_{(+)eGFP}$-$M_{(-)op}$ at 4 days post infiltration (dpi) viewed with a fluorescence microscope. Bar represents 400 μm. (c) Immunoblot analysis of expression of eGFP proteins in leaves shown in panel (b) using specific antibodies against YFP. Ponceau S staining of rubisco large subunit is shown for protein loading control. (d) Quantification of eGFP proteins in leaves shown in panel (c).

Fig. 7. Functional analysis and subcellular localization patterns of individual or combined Sw-5b domains. (a) Schematic diagrams showing a full length Sw-5b or Sw-5b domains fused with YFP. (b) Confocal images of *N. benthamiana* leaf epidermal cells expressing various YFP fusions. Images of the cells were taken at 24 hpi. N nucleus, Nu nucleolus, and C cytoplasm. Bar = 10 μm. (c) TSWV-inoculated

transgenic *N. benthamiana* plants expressing these various YFP fusions and photographed at 15 dpi.

Fig. 8. Roles of *importins* α and β in YFP-Sw-5b nucleus targeting and Sw-5b-mediated immunity to TSWV systemic infection. (a) Transient expression of YFP-Sw-5b in *N. benthamiana* leaf epidermal cells silenced for *importin* $\alpha 1$ (IMP α1 KD), *importin* $\alpha 2$ (IMP α2 KD), *importin* $\alpha 1$ and $\alpha 2$ (IMP α1 & α2 KD), *importin* β (IMP β KD) or *importin* $\alpha 1$ and $\alpha 2$ and β (IMP α1 & α2 & β KD) through VIGS. Images of the cells were captured using a confocal microscope at 26 hpi. N nucleus, C cytoplasm. Bar = 10 μm. (b) YFP-Sw-5b transgenic *N. benthamiana* plants were silenced for *importin* $\alpha 1$, *importin* $\alpha 2$, *importin* $\alpha 1$ and $\alpha 2$, *importin* β or *importin* $\alpha 1$ and $\alpha 2$ and β expression through VIGS followed by inoculation with TSWV. TSWV-inoculated YFP-Sw-5b transgenic *N. benthamiana* plants were photographed at 15 dpi. White arrowhead indicates HR trailing in systemic leaves.

Fig. 9. A working model for Sw-5b. Sw-5b furcates disease resistances by proper nucleocytoplasmic partition to block different infection steps of tomato spotted wilt tospovirus. Sw-5b switched from the autoinhibited state to an activated state upon recognition of NSm in the cytoplasm. Cytoplasm portion of Sw-5b induce cell death and defense that inhibit viral replication. The activated Sw-5b also translocated into nucleus via *importins* α and β. Nucleus-localized Sw-5b induces a defense that block viral cell-to-cell and long-distance movement. Cytoplasm- and nucleus-localized

1229 Sw-5b have additively effects on defense to inhibit viral replication, intercellular and

1230 long-distance movement during tospovirus infection.

1231

1232 **Supporting Information**

1233 **Short legends**

1234 **Fig. S1** Sw-5b recognizes TSWV NSm in cytoplasm.

1235 **Fig. S2** Analysis of virus replication monitoring system using a TSWV-based
1236 mini-genome replicon and a movement defective NSm mutant.

1237 **Fig. S3** Effects of nes-Sw-5b and nls-Sw-5b on NSm-GFP cell-to-cell movement and
1238 effects of Sw-5b and EV on NSm^{T120N}-GFP cell-to-cell movement.

1239 **Fig. S4** Effects of cytoplasmic and nuclear Sw-5b on host immunity to TSWV
1240 systemic infection.

1241 **Fig. S5** Cytoplasmic and nuclear Sw-5b activity on TSWV-GFP cell-to-cell
1242 movement in *N. benthamiana* leaves.

1243 **Fig. S6** An immunoblot showing the accumulations of various YFP-tagged proteins
1244 expressed in different transgenic *N. benthamiana* plants and RT-PCR analysis of
1245 TSWV accumulation in the systemic leaves.

1246 **Fig. S7** Bimolecular fluorescence complementation (BiFC) assay of cYFP-SD,
1247 cYFP-Sw-5b and nYFP-Importin α1 (nYFP-IMP α1), nYFP-Importin α2 (nYFP-IMP
1248 α2), nYFP-Importin β (nYFP-IMP β) interaction in *N. benthamiana* leaf epidermal
1249 cells.

1250 **Fig. S8** RT-PCR analyses of *importin a1*, *a2* and *b* expressions in the assayed plants
1251 and their effects on TSWV systemic infection.

1252 **Table S1.** List of primers used in this study.

1253 **Table S2.** Response of six different types of transgenic *Nicotiana benthamina* plants
1254 driven by 35S promoter to TSWV infection.

1255 **Table S3.** Response of six different types of transgenic *Nicotiana benthamina* plants
1256 driven by Sw-5b native promoter to TSWV infection.

1257 **Table S4.** Response of six different types of transgenic *Nicotiana benthamina* plants
1258 to TSWV infection.

1259 **Table S5.** Mass spectrum data of YFP-SD

1260 **Table S6.** Mass spectrum data of YFP-Sw-5b

1261

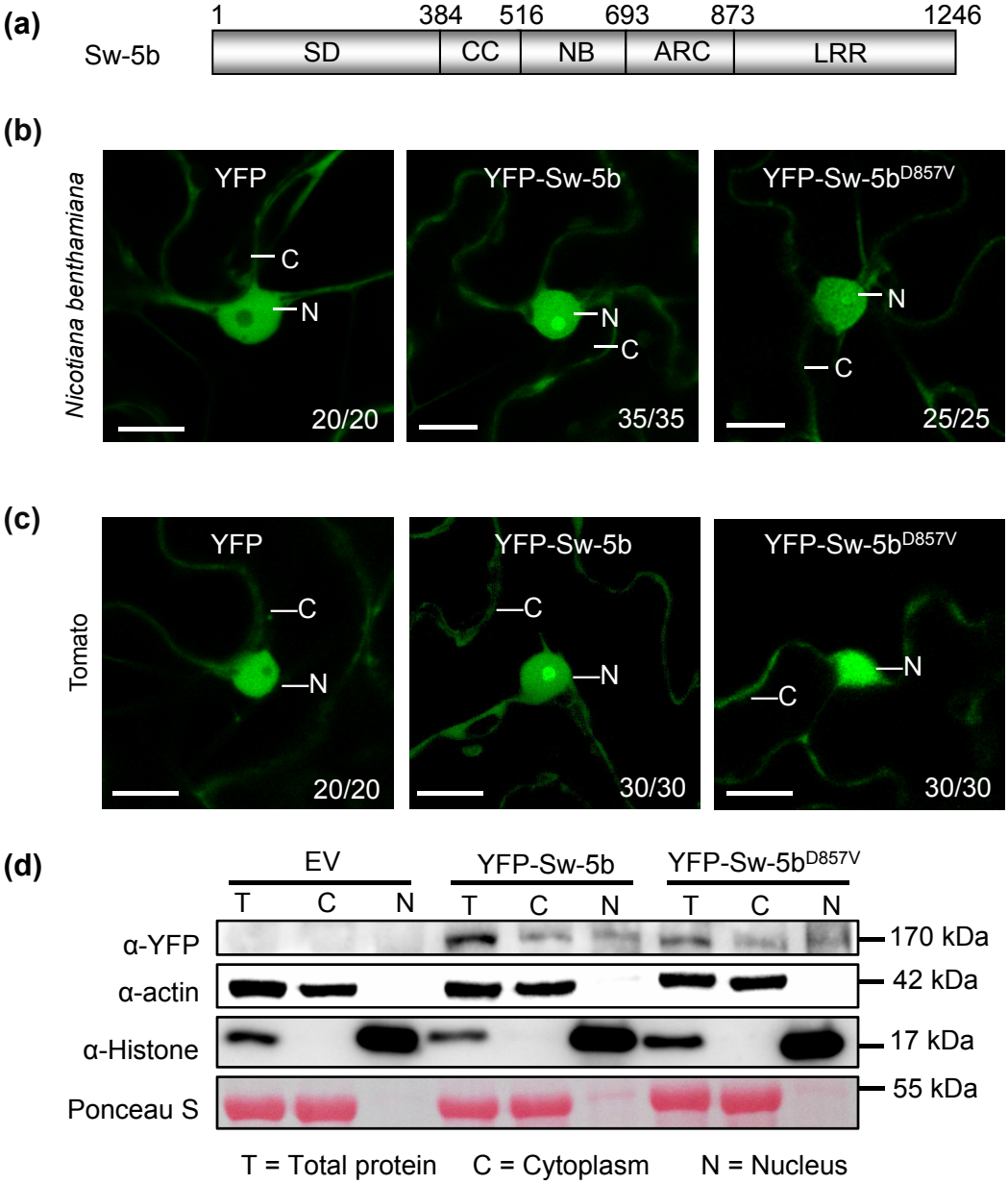

Fig. 1. Subcellular localization of Sw-5b in *Nicotiana benthamiana* and tomato leaf cells. (a) Schematic diagram of Sw-5b. (b) Subcellular localizations of free YFP (left), YFP-Sw-5b (middle) and autoactive YFP-Sw-5b^{D857V} mutant (right) in *N. benthamiana* leaf cells at 24 hours post agro-infiltration (hpi). (c) Subcellular localization of free YFP (left), YFP-Sw-5b (middle) and autoactive YFP-Sw-5b^{D857V} mutant (right) in tomato leaf cells at 24 hpi. N nucleus, and C cytoplasm inside the cell are indicated. Bar = 10 μm. (d) Nucleocytoplasmic partitioning analysis of YFP-Sw-5b and autoactive YFP-Sw-5b^{D857V}. Total lysate (T) from p2300S empty vector (EV), YFP-Sw-5b or YFP-Sw-5b^{D857V} expressing leaves were fractionated into cytoplasm and nucleus, and analyzed by immunoblots using antibodies against YFP. The actin and histone were used as a cytoplasm marker and nucleus marker, respectively, in the fractionation analysis. Ponceau S staining was also used as cytoplasm marker.

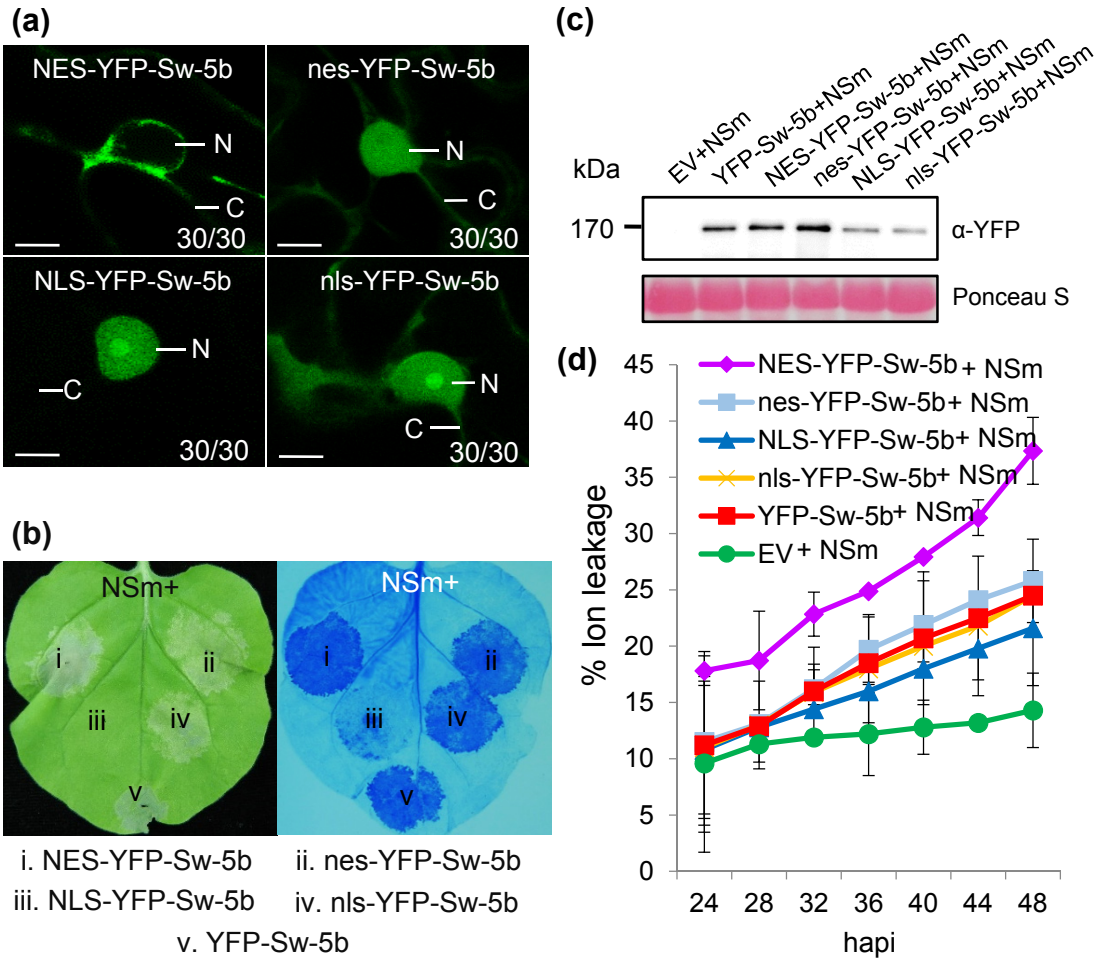

Fig. 2. Effect of Sw-5b subcellular localization pattern on HR induction. (a) Confocal images of *N. benthamiana* leaf cells transiently expressing NES-YFP-Sw-5b, nes-YFP-Sw-5b, NLS-YFP-Sw-5b or nls-YFP-Sw-5b fusion. The images were taken at 24–36 hpi. N nucleus and C cytoplasm (c). Bar = 10 µm. (b) Induction of HR in *N. benthamiana* leaf tissues co-expressing NSm and one of the five Sw-5b fusion proteins. The infiltrated *N. benthamiana* leaf was photographed at 3 dpi (left image). Induction of HR in the infiltrated tissues were visualized using a trypan blue staining method (right image). (c) Immunoblot analysis of NES-YFP-Sw-5b, nes-YFP-Sw-5b, NLS-YFP-Sw-5b, and nls-YFP-Sw-5b expressions in the infiltrated *N. benthamiana* leaf tissues. These fusion proteins were enriched using the GFP-Trap beads prior to SDS-PAGE, and the blot was probed using an YFP specific antibody. Ponceau-S staining was used to estimate sample loadings. (d) Time course analysis of ion leakage in Nicotiana benthamiana leaves co-expressing NSm with one of the five Sw-5b fusion proteins. Measurements were performed at 4 h intervals starting from 24 to 48 hpi. Error bars (SEs) were calculated using the results from three biological replicates per treatment collected at each time point.

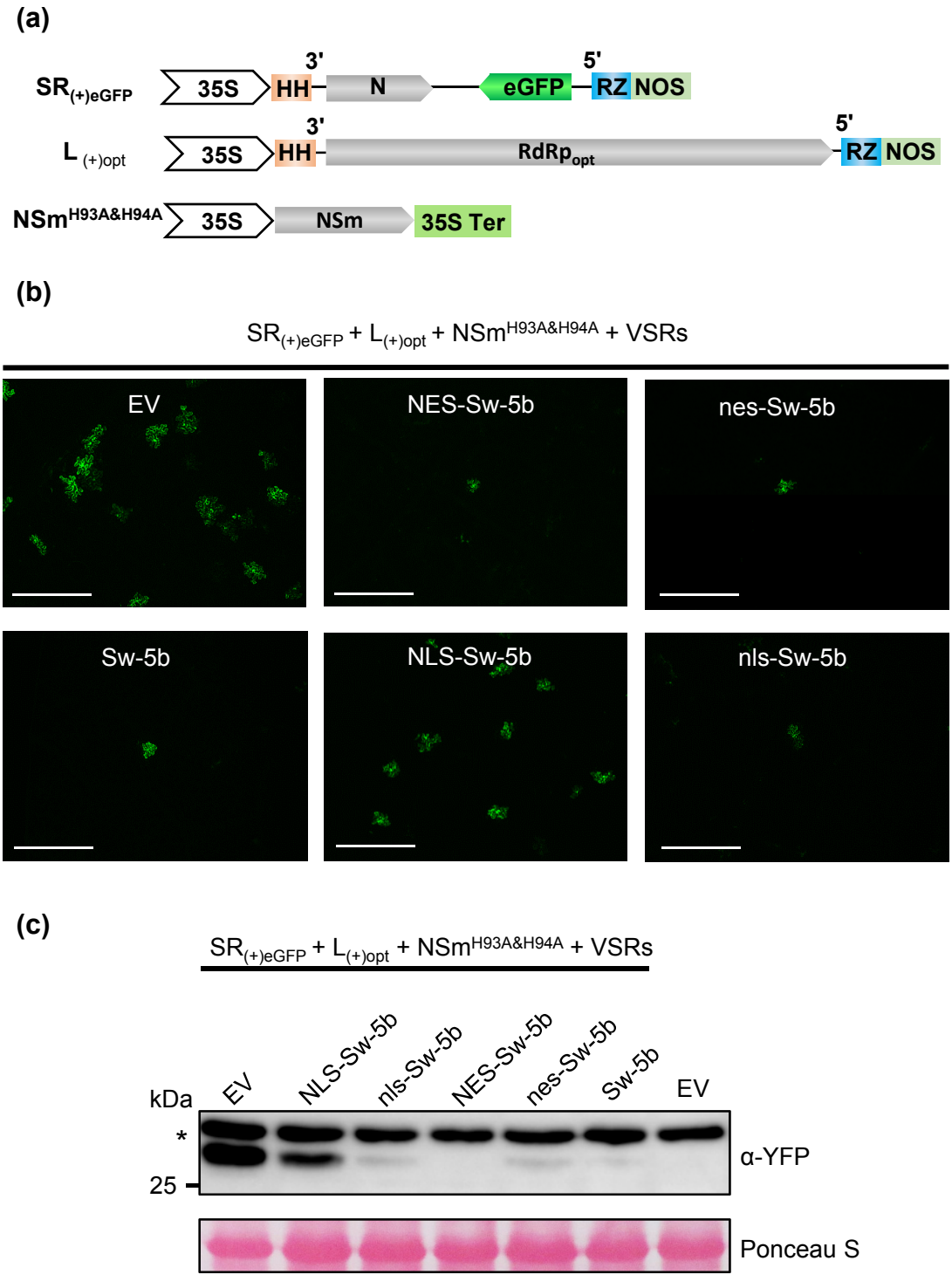

Fig. 3. The effect of cytoplasm- and nucleus-targeted Sw-5b on viral replication. (a) Schematic representation of binary constructs to express TSWV $SR_{(-)eGFP}$ mini-genome replicon, TSWV L RNA segment containing an optimized RdRp and $NSm^{H93A\&H94A}$ mutant that defected in viral movement. Minus sign (-) and 5′ to 3′ designation represent the negative (genomic)-strand of tospovirus RNA. 35S: a double 35S promoter; HH: hammerhead ribozyme; RZ: hepatitis delta virus (HDV) ribozyme; NOS: nopaline synthase terminator; 35S Ter: a 35S transcription terminator. (b) Accumulation of eGFP fluorescence in *N. benthamiana* leaves co-expressing p2300S empty vector (EV), Sw-5b, NES-Sw-5b, nes-Sw-5b, NLS-Sw-5b, or nls-Sw-5b with TSWV $SR_{(-)eGFP}$, L, and $NSm^{H93A\&H94A}$ at 4 days post infiltration (dpi) viewed with a fluorescence microscope. Bar represents 400 μm. (c) Immunoblot analysis of expression of eGFP proteins in leaves shown in panel (b) using specific antibodies against YFP. Ponceau S staining of rubisco large subunit is shown for protein loading control.

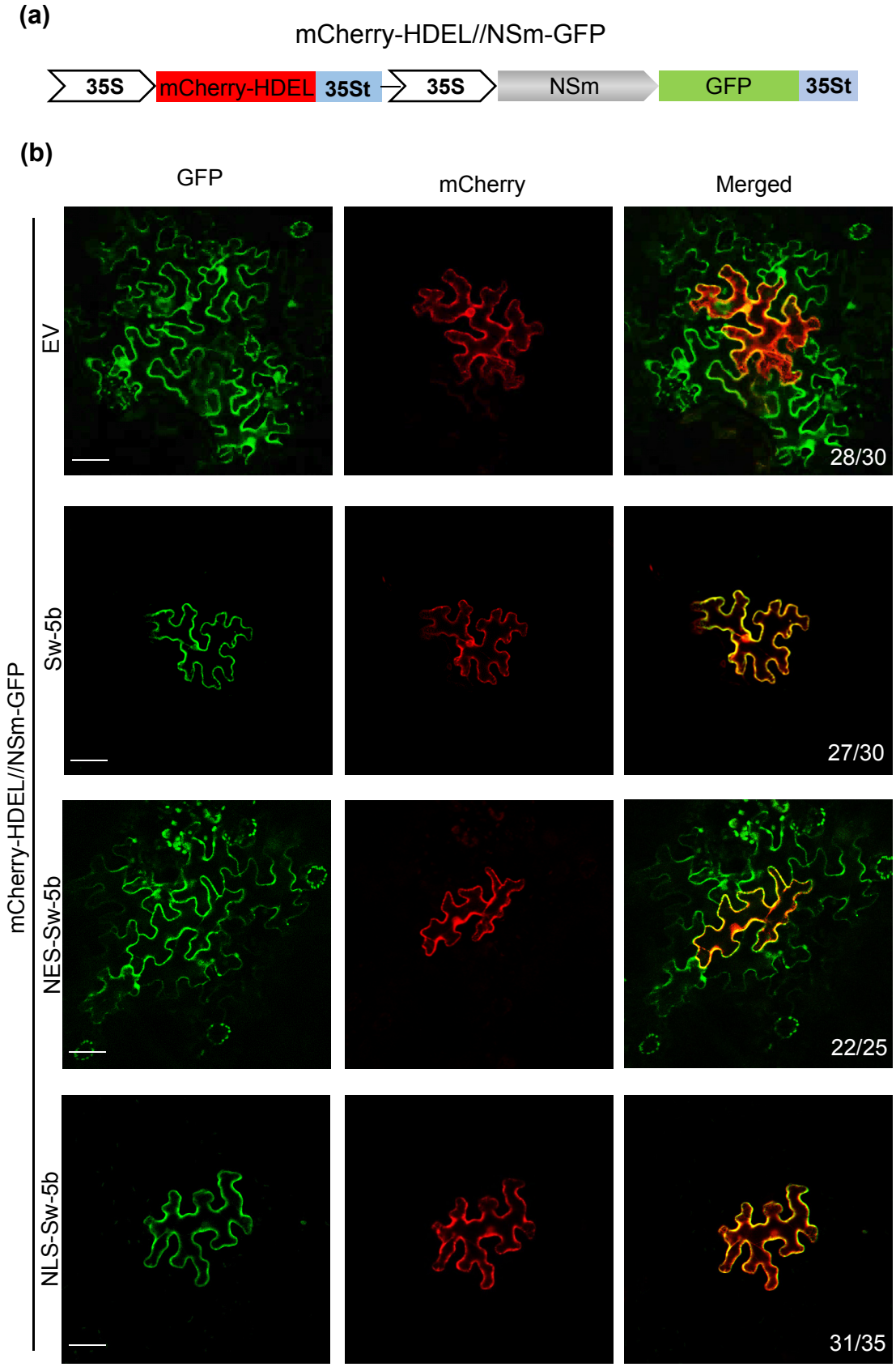

Fig. 4. Effect of subcellular localization of Sw-5b on cell-to-cell movement of NSm in leaf epidermis of *N. benthamiana.* (a) Schematic diagram of the binary construct to co-express mCherry-HDEL and NSm-GFP. (b) Cell-to-cell movement analysis of NSm-GFP in *N. benthamiana* leaves co-expressing p2300S empty vector (EV), Sw-5b, NES-Sw-5b, NLS-Sw-5b, or nls-Sw-5b with the construct harboring both mCherry-HDEL and NSm-GFP. *Agrobacterium* containing the construct to co-express mCherry-HDEL and NSm-GFP was diluted 500 times for expression in a single epidermal cell. All other *Agrobacterium* were infiltrated at the concentration of OD_{600} = 0.2. Bar = 50 μm.

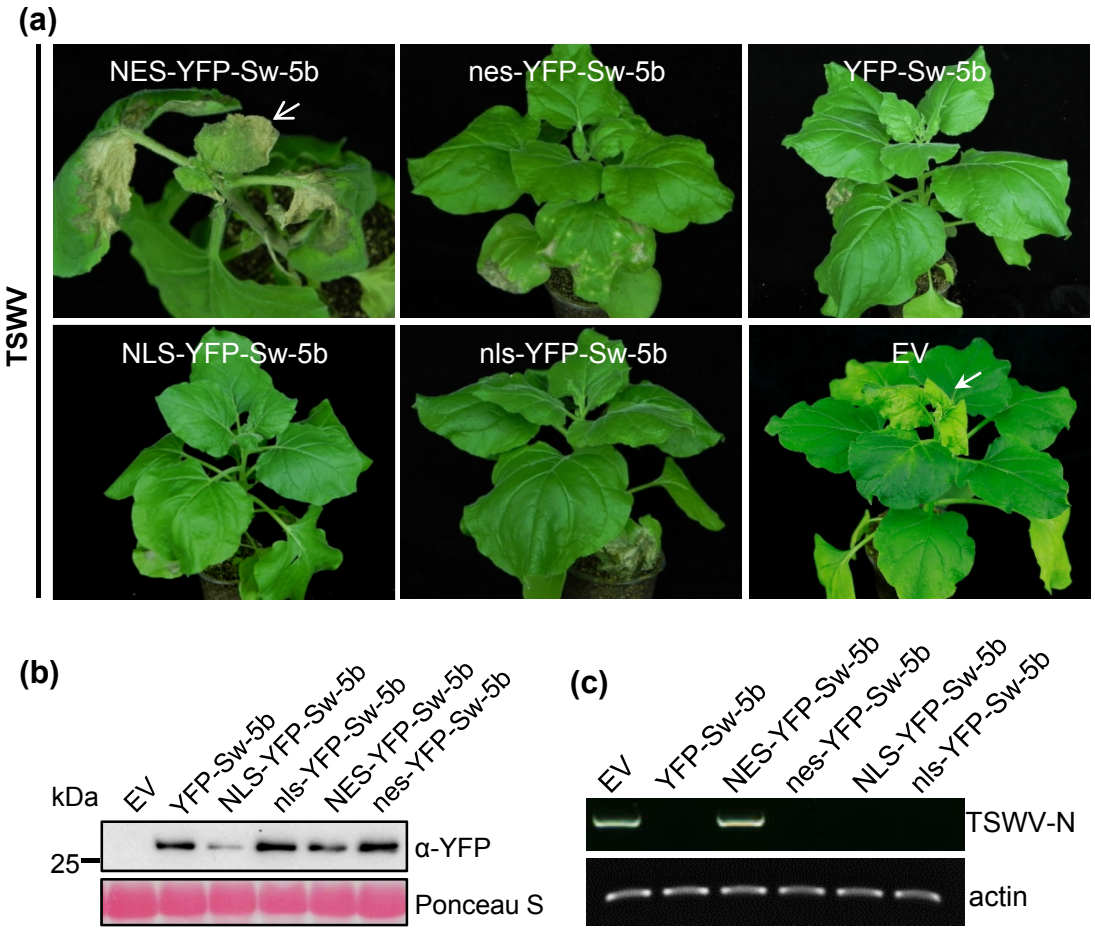

Fig. 5. Analysis of cytoplasm- and nucleus-targeted Sw-5b-mediated host immunity to TSWV systemic infection. (a) TSWV systemic infection in transgenic *N. benthamiana* plants expressing NES-YFP-Sw-5b, nes-YFP-Sw-5b, NLS-YFP-Sw-5b, nls-YFP-Sw-5b, YFP-Sw-5b or p2300S empty vector (EV) driven by 35S promoter. TSWV-inoculated plants were photographed at 15 dpi. White arrow indicates the systemic leaves showing HR trailing. White arrowhead indicates the systemic leaves showing mosaic. (b) Immunoblot analysis of NES-YFP-Sw-5b, nes-YFP-Sw-5b, NLS-YFP-Sw-5b, nls-YFP-Sw-5b and YFP-Sw-5b expressions in different transgenic *N. benthamiana* plants. EV plants transformed with an empty vector and were used as a negative control. (c) RT-PCR analysis of TSWV accumulation in the systemic leaves of different transgenic *N. benthamiana* plants at 15 dpi.

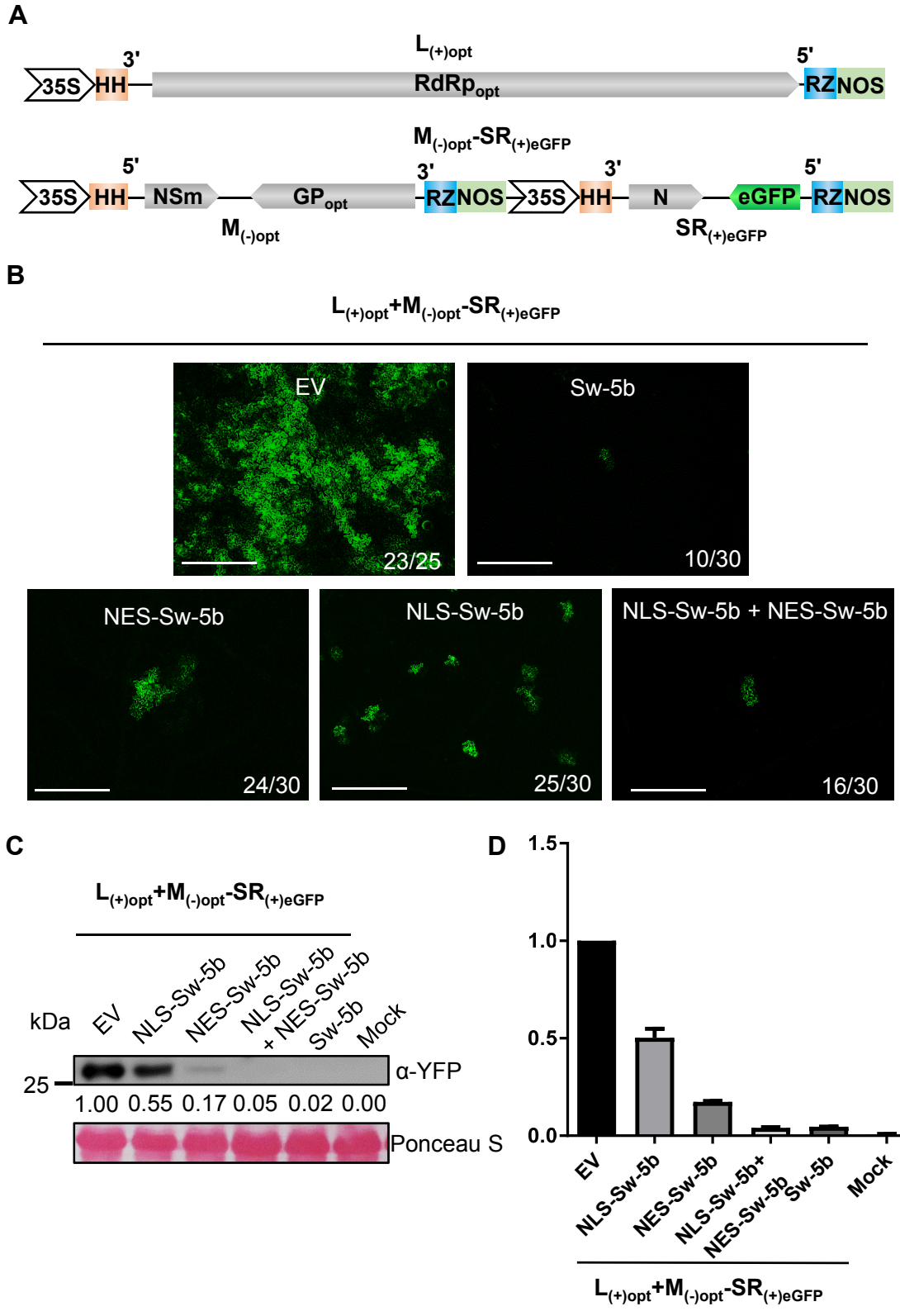

Fig. 6. Joint effects of cytoplasm- and nucleus-targeted Sw-5b on defenses against tospovirus infection in *Nicotiana benthamiana* leaves. (a) Schematic representation of binary constructs to express TSWV $SR_{(+)eGFP}$-$M_{(-)op}$ and TSWV L RNA segment containing an optimized RdRp. 35S: a double 35S promoter; HH: hammerhead ribozyme; RZ: hepatitis delta virus (HDV) ribozyme; NOS: nopaline synthase terminator. (b) Accumulation of eGFP fluorescence in *N. benthamiana* leaves co-expressing p2300S empty vector (EV), Sw-5b, NES-Sw-5b, NLS-Sw-5b, or NES-Sw-5b+NLS-Sw-5b with TSWV $SR_{(+)eGFP}$-$M_{(-)op}$ at 4 days post infiltration (dpi) viewed with a fluorescence microscope. Bar represents 400 μm. (c) Immunoblot analysis of expression of eGFP proteins in leaves shown in panel (b) using specific antibodies against YFP. Ponceau S staining of rubisco large subunit is shown for protein loading control. (d) Quantification of eGFP proteins in leaves shown in panel (c).

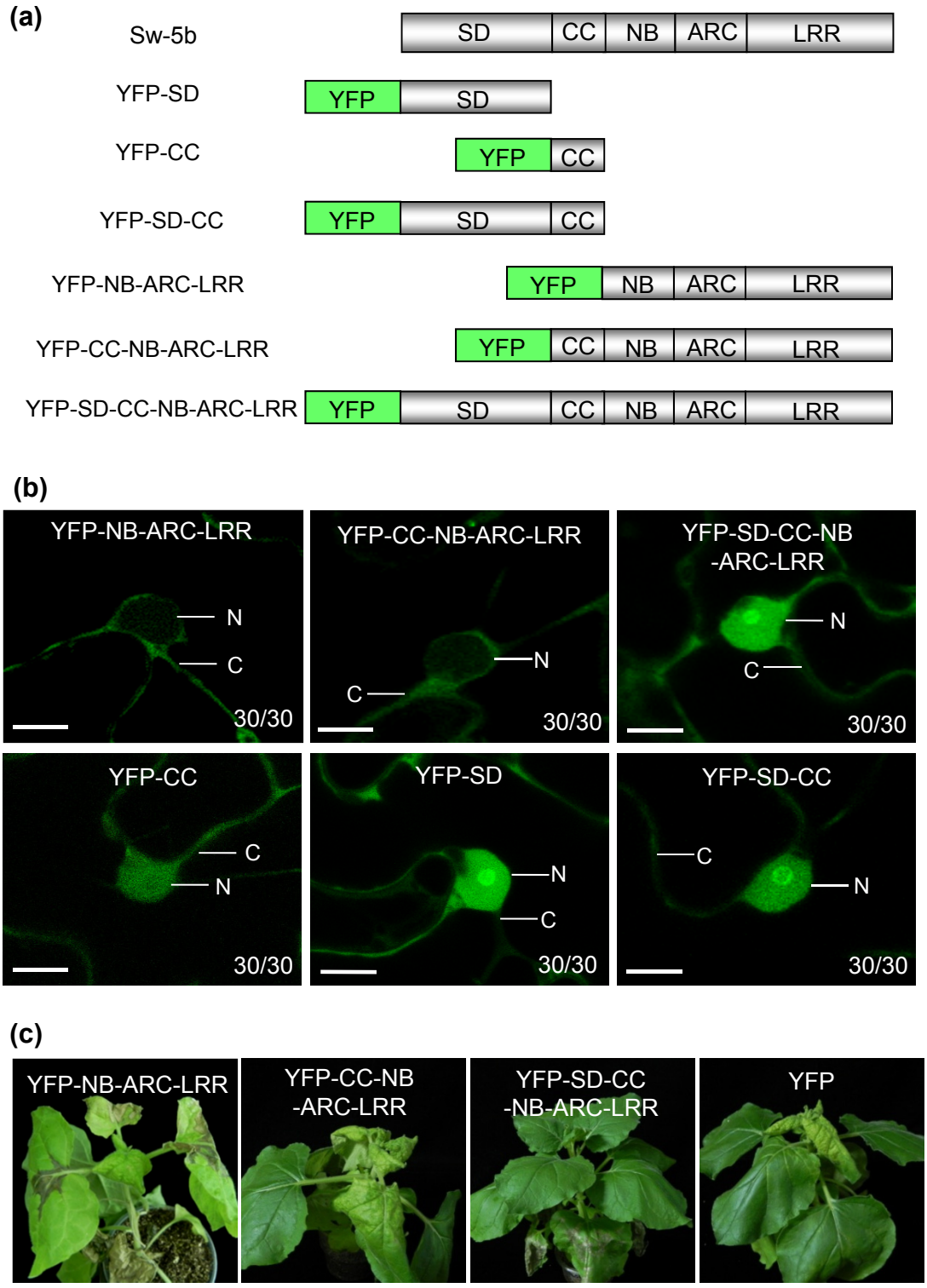

Fig. 7. Functional analysis and subcellular localization patterns of individual or combined Sw-5b domains. (a) Schematic diagram showing a full length Sw-5b or Sw-5b domains fused with YFP. (b) Confocal images of *N. benthamiana* leaf epidermal cells expressing various YFP fusions. Images of the cells were taken at 24 hpi. N nucleus, and C cytoplasm. Bar = 10 μm. (c) TSWV-inoculated transgenic *N. benthamiana* plants expressing these various YFP fusions and photographed at 15 dpi.

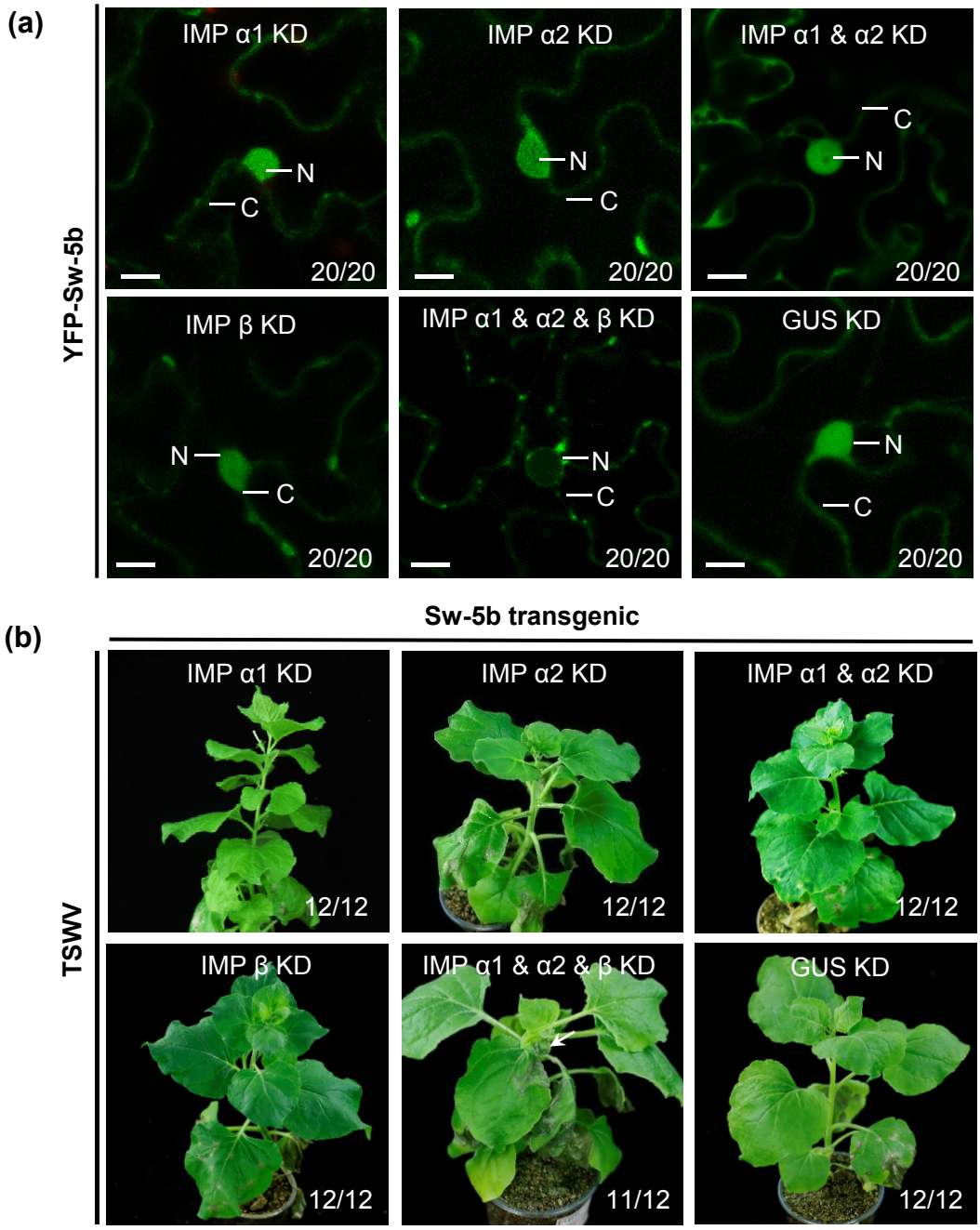

Fig. 8. Roles of *importins α* and *β* in YFP-Sw-5b nucleus targeting and Sw-5b-mediated immunity to TSWV systemic infection. (a) Transient expression of YFP-Sw-5b in *N. benthamiana* leaf epidermal cells silenced for *importin α1* (IMP α1 KD)*, importinα2* (IMP α2 KD), *importin* α*1* and α*2* (IMP α1 & α2 KD), *importin β* (IMP β KD) or *importin* α*1* and *β2* and *β* (IMP α1 & α2 & β KD) through VIGS. Images of the cells were captured using a confocal microscope at 26 hpi. N nucleus, C cytoplasm. Bar = 10 mm. (b) YFP-Sw-5b transgenic *N. benthamiana* plants were silenced for *importin a1, importin* α*2*, *importin* α*1* and α*2*, *importin β* or *importin* α*1* and α*2* and *β* expression through VIGS followed by inoculation with TSWV. TSWV-inoculated YFP-Sw-5b transgenic *N. benthamiana* plants were photographed at 15 dpi. White arrowhead indicates HR trailing in systemic leaves.

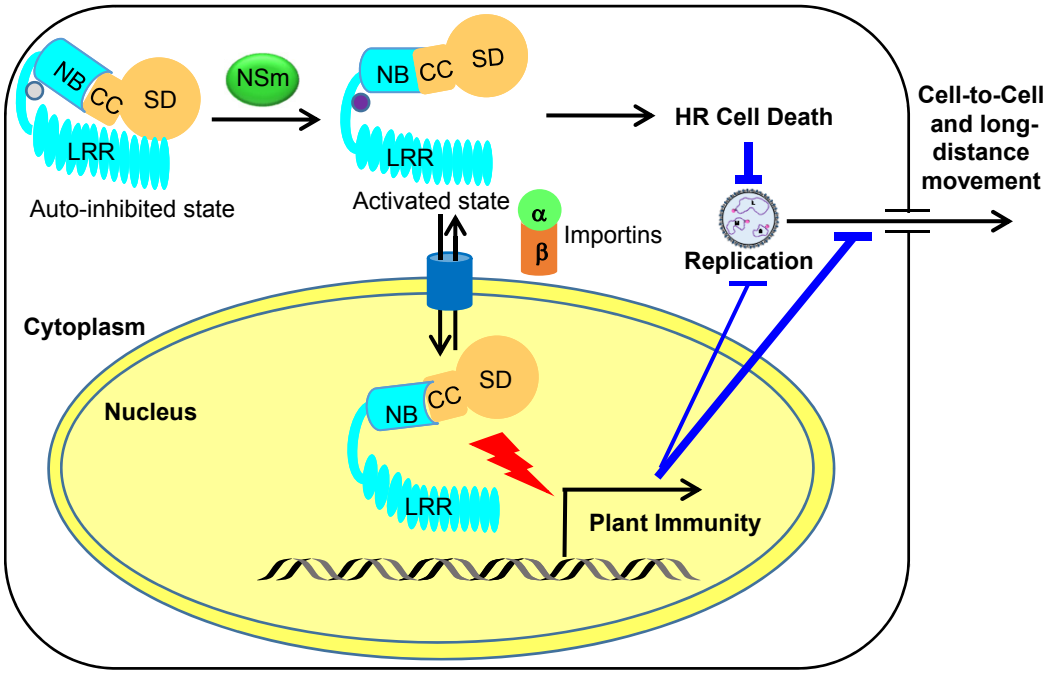

Fig. 9. A working model for Sw-5b. Sw-5b furcates disease resistances by proper nucleocytoplasmic partition to block different infection steps of tomato spotted wilt tospovirus. Sw-5b switched from the autoinhibited state to an activated state upon recognition of NSm in the cytoplasm. Cytoplasm portion of Sw-5b induce cell death and defense that inhibit viral replication. The activated Sw-5b also translocated into nucleus via *importins a* and *b* . Nucleus-localized Sw-5b induces a defense that block viral cell-to-cell and long-distance movement. Cytoplasm- and nucleus-localized Sw-5b have additively effects on defense to inhibit viral replication, intercellular and long-distance movement during tospovirus infection.

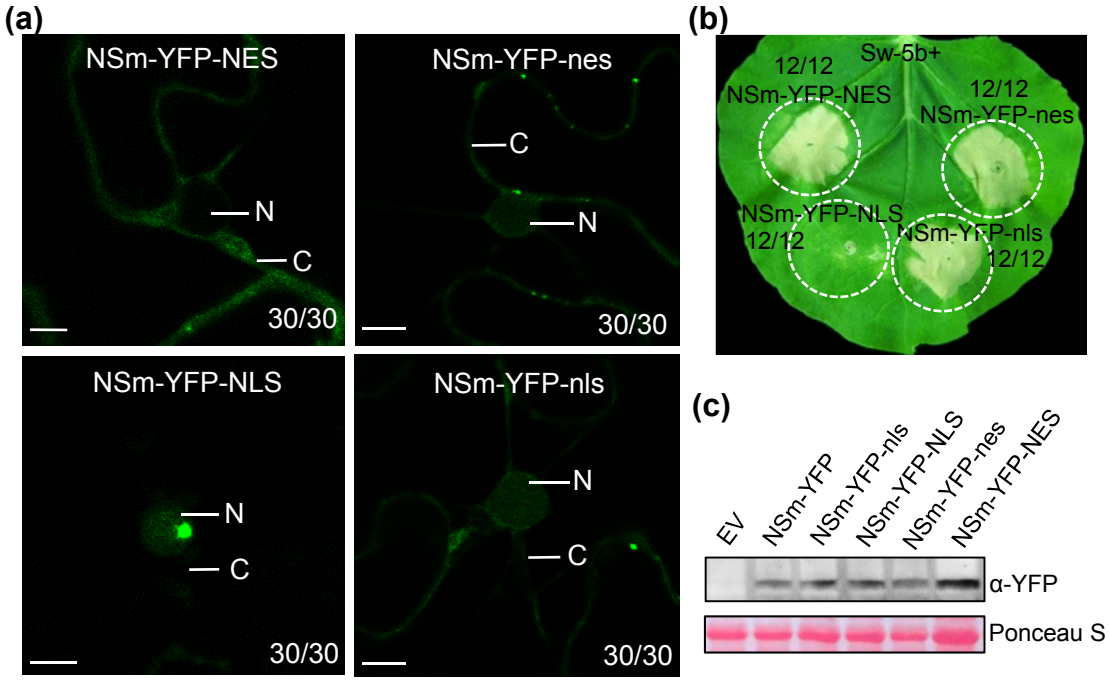

Fig. S1 Sw-5b recognizes TSWV NSm in cytoplasm. (a) Transient expressions of NSm-YFP-NES, NSm-YFP-nes, NSm-YFP-NLS, and NSm-YFP-nls, respectively, in *N. benthamiana* leaves through agro-infiltration. Epidermal cells expressing various fusion proteins were imaged under a confocal microscope at 24 hpai. The numbers in each image indicate the number of cells showing this subcellular localization pattern and the total number of cells examined per treatment. N, nucleus; C, cytoplasm. Bar = 10 μm. (b) Various fusion proteins described in (a) were, individually, co-expressed with Sw-5b in *N. benthamiana* leaves. A representative leaf was photographed at 5 dpai. (c) Western blot analysis of various NSm fusion protein expressions in the assayed *N. benthamiana* leaves using a YFP specific antibody. Leaf areas co-expressing Sw-5b and EV were used as negative controls. The Ponceau S stained Rubisco large subunit gel was used to show sample loadings.

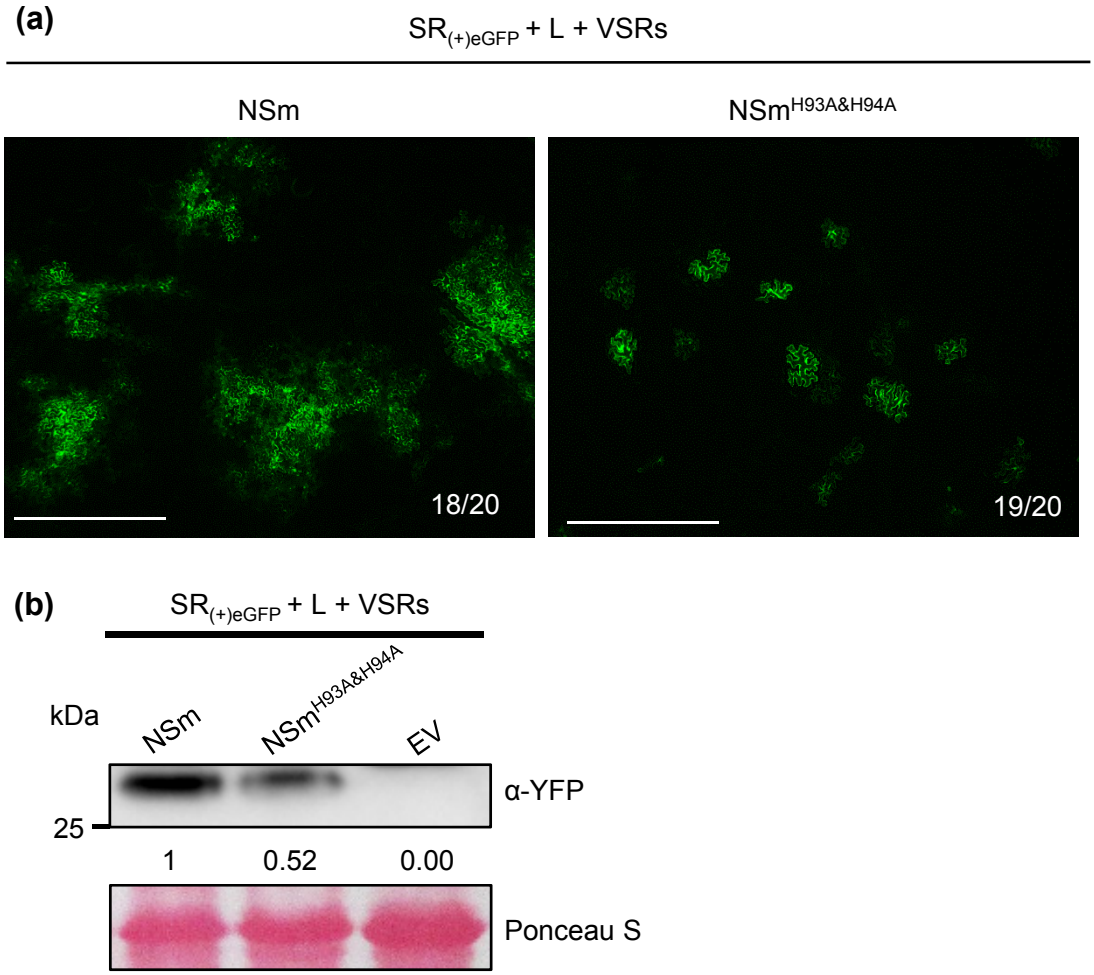

Fig. S2 Analysis of virus replication monitoring system using a TSWV-based mini-genome replicon and a movement defective NSm mutant. (a) $SR_{(+)eGFP}$, $L_{(+)opt}$, VSRs and NSm or $NSm^{H93A\&H94A}$ mutant were transiently co-expressed in *N. benthamiana* leaves through agro-infiltration. The infiltrated leaves were examined and imaged under a confocal microscope at 4 dpai. The numbers in each image indicate the number of cells showing similar expression pattern and the total number of cells examined per treatment. Bar = 400 μm. (b) Western blot analysis of eGFP accumulation in assayed leaves using a YFP specific antibody. Leaves co-expressing $SR_{(+)eGFP}$, $L_{(+)opt}$, VSRs and EV were used as negative controls. The Ponceau S stained Rubisco large subunit gel was used to show sample loadings.

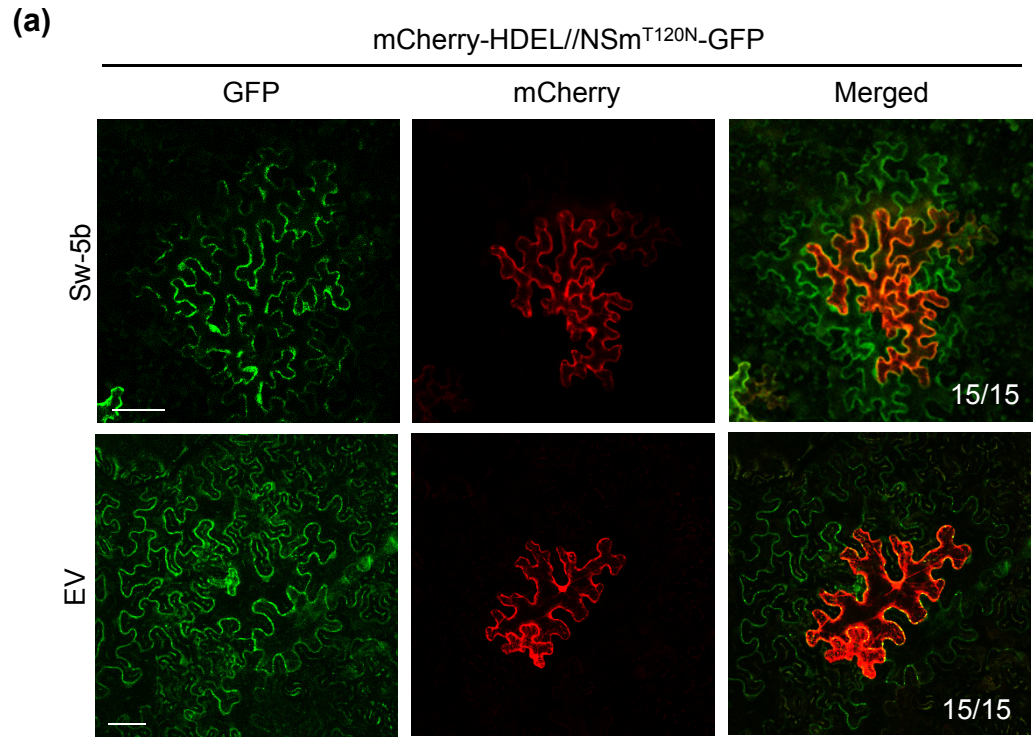

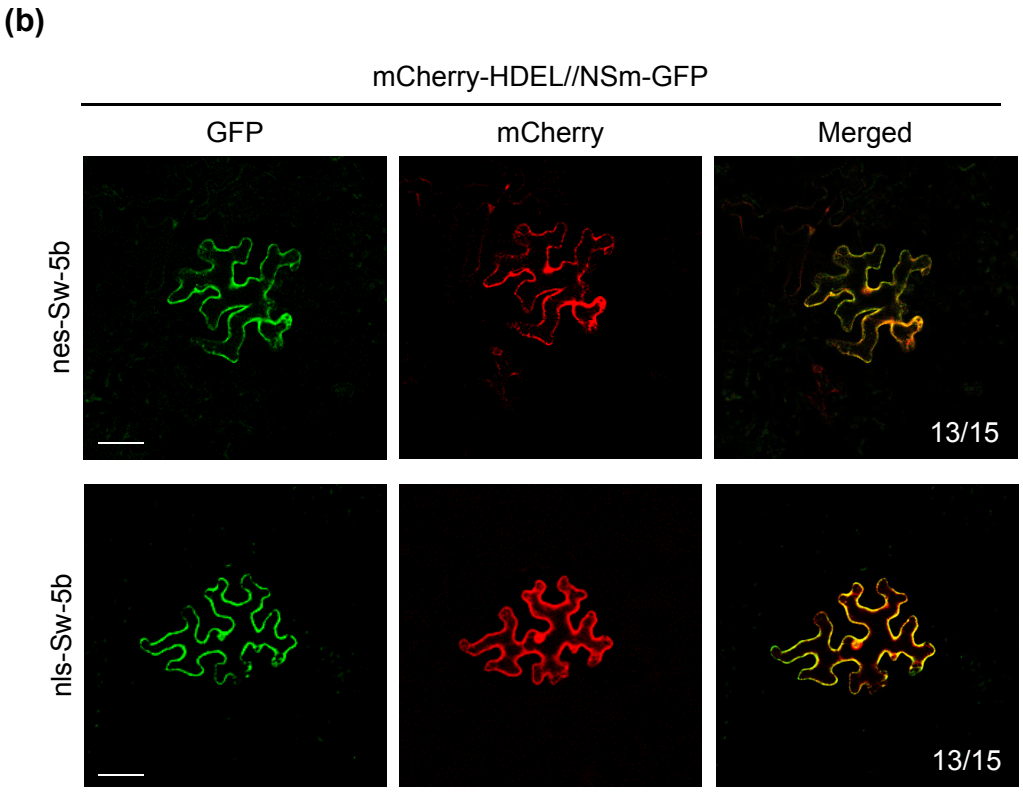

Fig. S3 Effects of nes-Sw-5b and nls-Sw-5b on NSm-GFP cell-to-cell movement and effects of Sw-5b and EV on NSm^{T120N}-GFP cell-to-cell movement. (a) Sw-5b and EV were, respectively, co-expressed with mCherry-HDEL//NSm^{T120N}-GFP in *N. benthamiana* leaves through agro-infiltration. (b) nes-Sw-5b and nls-Sw-5b were, respectively, co-expressed with mCherry-HDEL//NSm-GFP in *N. benthamiana* leaves through agro-infiltration. The Agrobacterium culture carrying pmCherry-HDEL//NSm-GFP or pmCherry-HDEL//NSm^{T120N}-GFP was first adjusted to OD_{600} = 0.2 and then further diluted 500 times prior to use. All other Agrobacterium cultures were adjusted to OD_{600} = 0.2 prior to use. The numbers in each image indicate the number of cells showing similar expression pattern and the total number of cells examined per treatment. Bar = 50 μm.

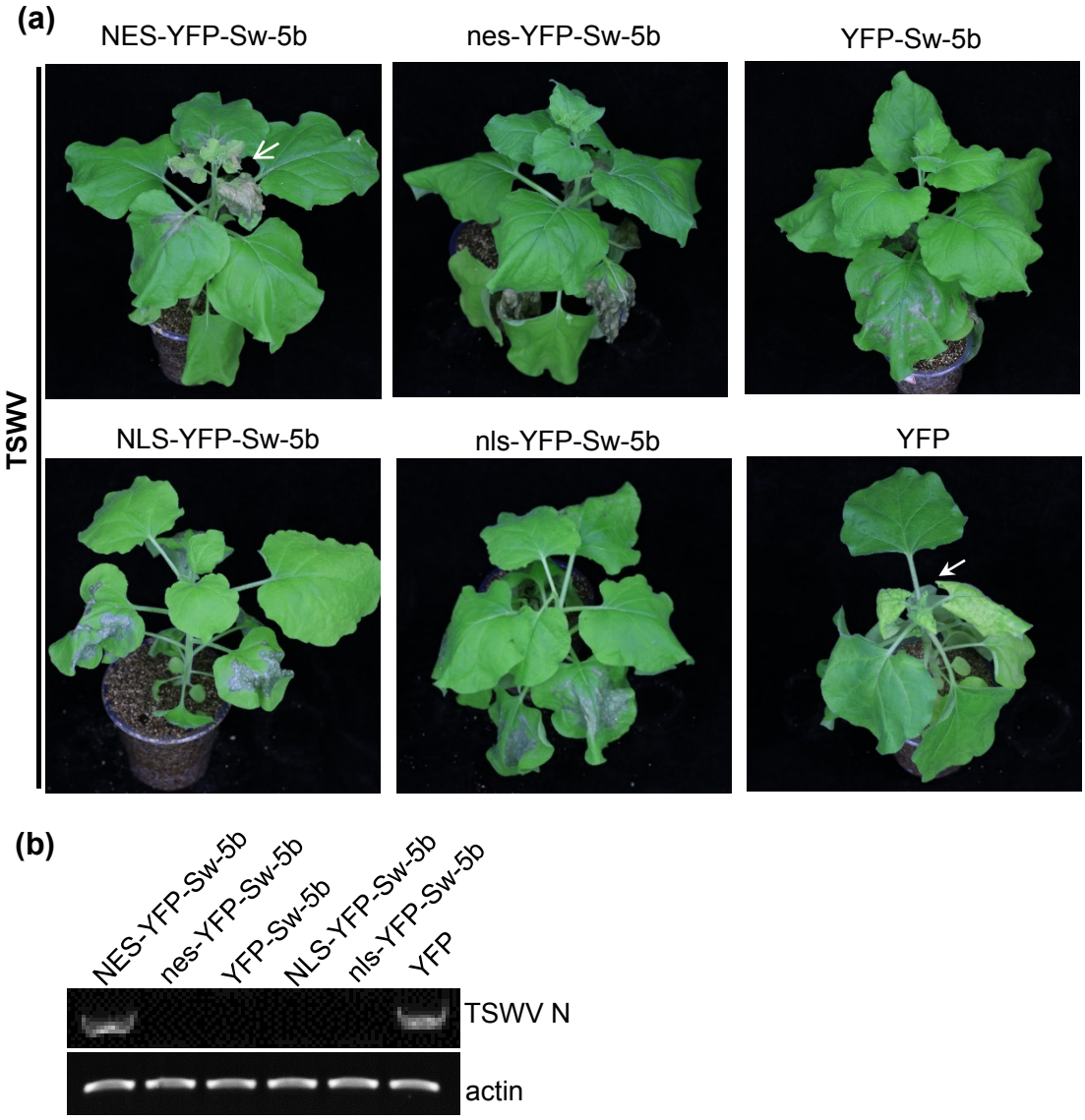

Fig. S4 Effects of cytoplasmic and nuclear Sw-5b on host immunity to TSWV systemic infection. (a) Transgenic *N. benthamiana* lines expressing NES-YFP-Sw-5b, nes-YFP-Sw-5b, NLS-YFP-Sw-5b, nls-YFP-Sw-5b or YFP-Sw-5b, driven by the Sw-5b promoter, were used in this study. The EV transgenic plants were used as controls. The transgenic plants were inoculated with TSWV and photographed at 15 dpi. White arrow indicate the systemic leaves showing HR trailing. White arrowhead indicates the systemic leaves showing mosaic symptoms. (b) RT-PCR detection of TSWV infection in the systemic leaves of the assayed *N. benthamiana* plants at 15 dpi.

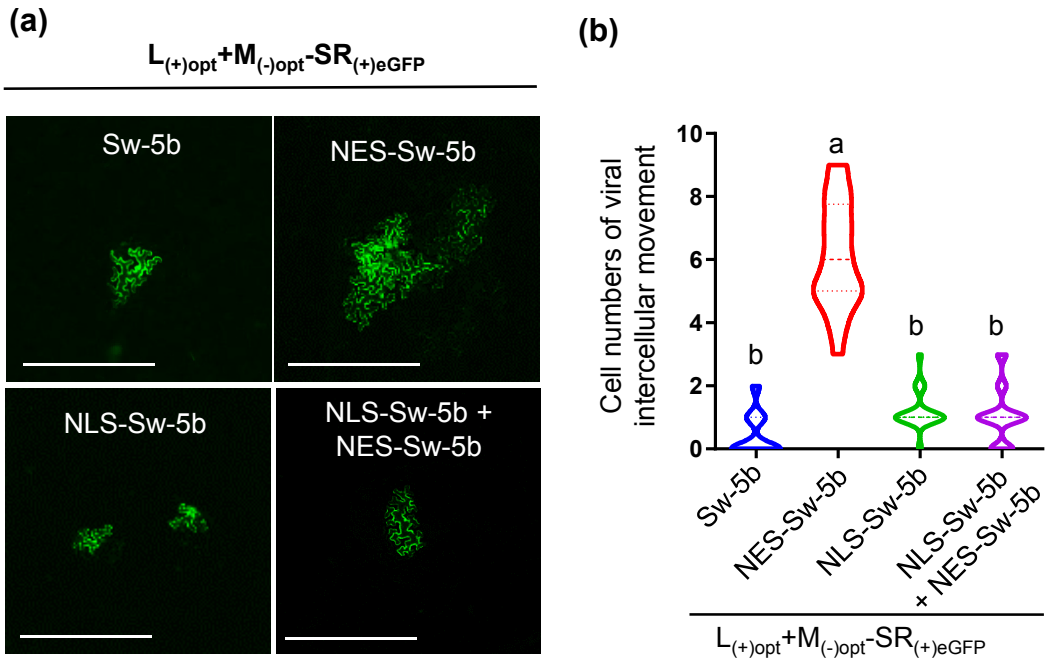

Fig. S5 Cytoplasmic and nuclear Sw-5b activity on TSWV-GFP cell-to-cell movement in *N. benthamiana* leaves. (a) $pL_{(+)opt}$ and $pSR_{(+)eGFP}$-$M_{(-)opt}$ were co-inoculated with TSWV-GFP into *Nicotiana benthamiana* leaves through agro-infiltration. The inoculated leaves were examined and imaged under a confocal microscope at 4 dpai. Bar = 400 μm. (b) Statistic analysis of TSWV-GFP cell-to-cell movement in the assayed *N. benthamiana* leaves from Figure 7B. A total of 9 assayed leaves were used for each treatment.

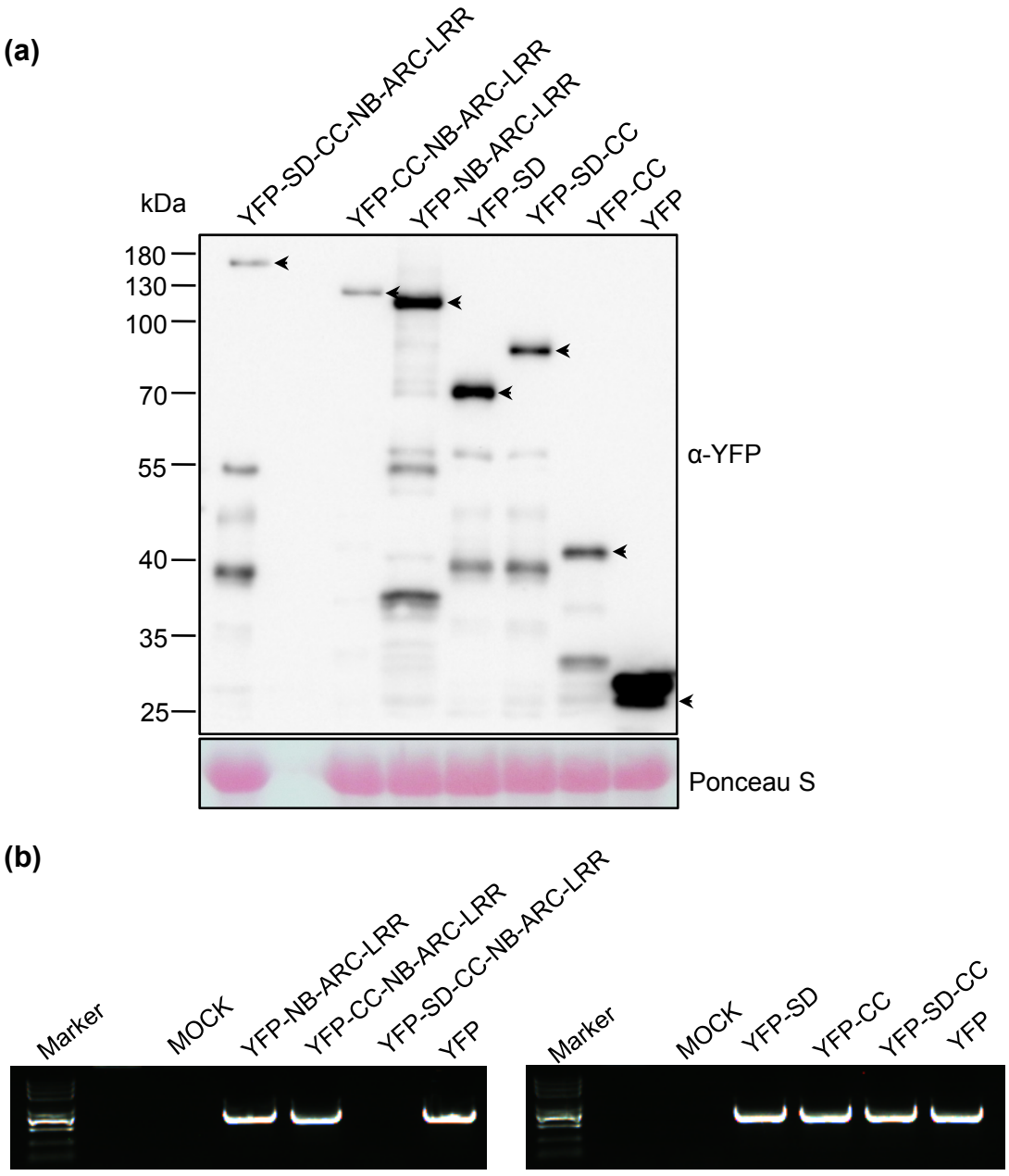

Fig. S6 An immunoblot showing the accumulations of various YFP-tagged proteins expressed in different transgenic *N. benthamiana* plants and RT-PCR analysis of TSWV accumulation in the systemic leaves. (a) The fusion proteins were detected using an YFP specific antibody. Arrows indicate the positions of the expressed fusion proteins. Ponceau S stained Rubisco large subunits were used to estimate sample loadings. (b) RT-PCR analysis of TSWV accumulation in the systemic leaves of different transgenic *N. benthamiana* plants at 15 dpi.

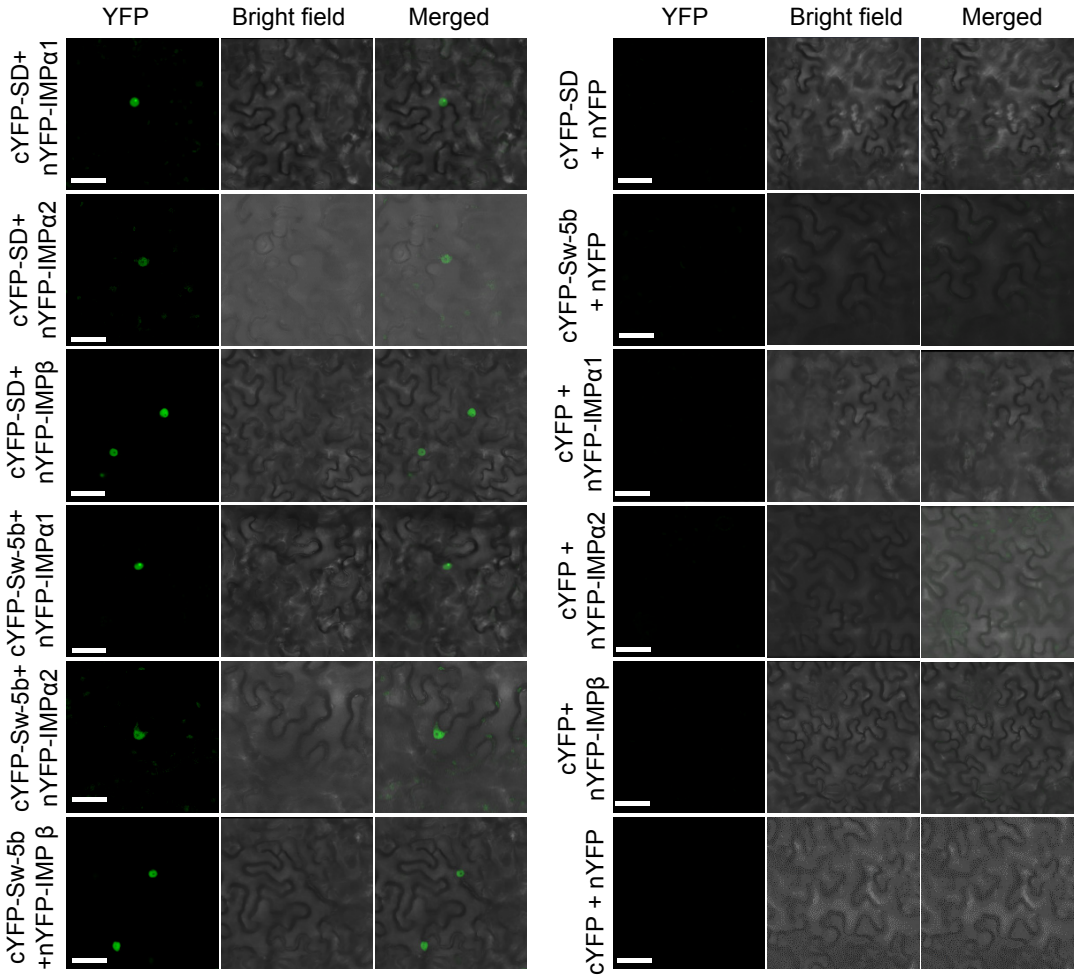

Fig. S7 Bimolecular fluorescence complementation (BiFC) assay of cYFP-SD, cYFP-Sw-5b and nYFP-Importin α1 (nYFP-IMP α1), nYFP-Importin α2 (nYFP-IMP α2), nYFP-Importin β (nYFP-IMP β) interaction in N. benthamiana leaf epidermal cells. Confocal images were taken at 26 hour post agro-infiltration. Leaf epidermal cells co-expressing cYFP-SD and nYFP, cYFP-Sw-5b and nYFP or cYFP and nYFP-IMP α1, nYFP-IMP α2, nYFP-IMP β were used as controls. Bar = 50 μm.

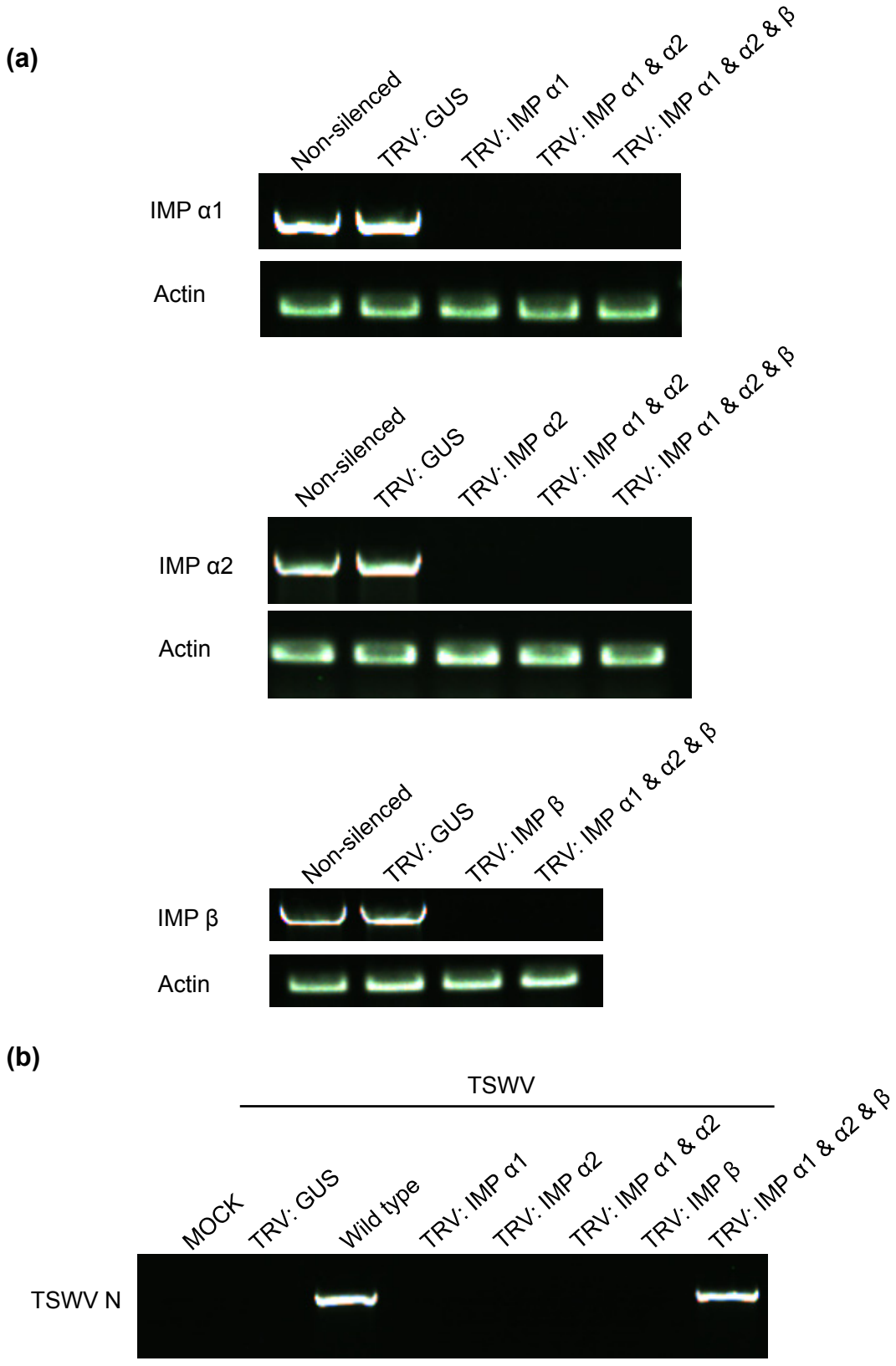

Fig. S8 RT-PCR analyses of *importin* α*1*, α*2* and *β* expressions in the assayed plants and their effects on TSWV systemic infection. (a) Expressions of *importin* α*1,* α*2*, and *β* in Sw-5b transgenic *N. benthamiana* plants were silenced individually or together using a TRV-based VIGS vector. The gene silencing results were determined through semi-quantitative RT-PCR using gene specific primers. PCR products obtained after 25 cycles of PCR reaction were visualized in 1% agrose gel through electrophoresis. (b) RT-PCR detection of TSWV systemic infection in the assayed plants. The resulting PCR products were visualized in 1% agrose gel through electrophoresis.